Bio-Design and Manufacturing (2025) 8:169–242
https://doi.org/10.1631/bdm.2400309

REVIEW

3D printing for tissue/organ regeneration in China

Chaofan He[1,2] · Jiankang He[3] · Chengtie Wu[4] · Changshun Ruan[5,6] · Qi Gu[7,8] · Yongqiang Hao[9] · Yang Wu[10] · Shuo Bai[11,12] · Xiaoxiao Han[13] · Liliang Ouyang[14,15] · Jun Yin[1] · Hongzhao Zhou[1] · Zhuo Xiong[14] · Maobin Xie[16,17] · Lei Shao[18] · Jing Nie[19] · Liang Ma[1] · Cijun Shuai[20] · Changchun Zhou[21] · Xin Zhao[22] · Xuetao Shi[23] · Mengfei Yu[24,25] · Jiayin Fu[26] · Peng Wen[27] · Huixia Xuan[28,29] · Yuan Pang[14] · Yan'en Wang[30] · Yuan Sun[1,2] · Ziqi Gao[1] · Abdellah Aazmi[1] · Jingbo Zhang[1] · Tianhong Qiao[1,2] · Qixiang Yang[1,2] · Ke Yao[1,2] · Mao Mao[3] · Jianxin Hao[4] · Pinpin Wang[5,6] · Jirong Yang[5,6] · Huawei Qu[5,6] · Xinhuan Wang[7,8] · Xin Liu[7,8] · Shen Ji[7,8] · Shasha Liu[9] · Jingke Fu[9] · Bingxian Lu[10] · Mohan Wu[10] · Feng Chen[13] · Zihao Zheng[16,17] · Boqing Zhang[21] · Muyuan Chai[23] · Chaoying Zhang[24,25] · Mouyuan Sun[24,25] · Bo Peng[27] · Huayong Yang[1] · Yong He[1,2,31]

Received: 5 August 2024 / Accepted: 12 October 2024 / Published online: 5 March 2025

Abstract

As surgical procedures transition from conventional resection to advanced tissue-regeneration technologies, human disease therapy has witnessed a great leap forward. In particular, three-dimensional (3D) bioprinting stands as a landmark in this setting, by promising the precise integration of biomaterials, cells, and bioactive molecules, thus opening up a novel avenue for tissue/organ regeneration. Curated by the editorial board of *Bio-Design and Manufacturing*, this review brings together a cohort of leading young scientists in China to dissect the core functionalities and evolutionary trajectory of 3D bioprinting, by elucidating the intricate challenges encountered in the manufacturing of transplantable organs. We further delve into the translational pathway from scientific research to clinical application, emphasizing the imperativeness of establishing a regulatory framework and rigorously enforcing quality-control measures. Finally, this review outlines the strategic landscape and innovative achievements of China in this field and provides a comprehensive roadmap for researchers worldwide to propel this field collectively to even greater heights.

Graphical abstract

Keywords 3D printing · Bioprinting · Tissue engineering · Regenerative medicine

Extended author information available on the last page of the article

1 Introduction

In the 16th century, the French surgeon Ambroise Paré summarized the five fundamental duties of surgery: to remove what is superfluous, to restore what has been dislocated, to separate what has grown together, to reunite what has been divided, and to redress the defects of nature [1]. For centuries, surgery has relied on the creation of incisions and wounds [2] to achieve therapeutic goals, such as amputations [3] and appendectomies [4], which aim to eliminate diseased or necrotic tissues, thereby preventing the spread of infection and associated complications.

With advancements in life sciences, the concept of prosthesis implantation for tissue repair emerged [5]; however, nonbioactive prosthetic materials have been limited to applications to rigid tissues, such as teeth or bone. Attempts at the transplantation of plastic artificial tracheas have also been reported [6]; however, these endeavors were met with severe complications among patients. Consequently, the utilization of bioactive materials to promote tissue regeneration has emerged as a novel paradigm in surgical practice [7]. Currently, numerous surgical procedures utilize tissue-engineered scaffolds [8–10] to successfully repair damaged tissues and promote regeneration. With the rapid advancement of biomedical, material, and engineering sciences, surgical interventions are becoming increasingly efficient, precise, and comprehensive. This field is continuously evolving with the introduction of novel tools, techniques, and approaches.

The advent of biofabrication [11], specifically of the three-dimensional (3D) bioprinting technology [12], has revolutionized the field of tissue regeneration [13]. This technology enables the seamless transition from biological models to biomimetic constructs, thus providing a novel avenue for the in vitro reconstruction of functional tissues and organs [14]. At its core lies the precise assembly of biomaterials, cells, and bioactive molecules to mimic the physiological properties, structural features, and functional characteristics of natural biological tissues [15]. Because of its unique advantages, this technology has found widespread applications in tissue engineering [16], regenerative medicine, and drug screening [17], and is considered the most promising solution for the in vitro reconstruction of functional tissues and organs [15] (Fig. 1a).

With the rapid advancement of technology, 3D bioprinting is steadily progressing toward greater biomimicry and bioactivity. The evolution of its building blocks has been transitioning from non-bioactive materials to biocompatible and degradable materials and even the direct use of cells or organoids [18], thereby vastly expanding the boundaries of biofabrication. Moreover, 3D bioprinting for tissue regeneration, as a frontier within this field, revolves around the utilization of degradable materials and cell-laden bioinks. This process can be delineated into four sequential stages, as follows. Stage 1: fabrication of acellular bioscaffolds [19], leveraging physicochemical factors to accelerate tissue repair; Stage 2: fabrication of cell-laden scaffolds [20], enabling a more accurate simulation of biological activities and functions; Stage 3: partial reconstruction of specific biological tissues while realizing their fundamental biological functions, such as artificial tracheas; Stage 4: reconstruction of organs, such as artificial hearts and livers, and achievement of their complete biological functions (Fig. 1b). Furthermore, this technological evolution encompasses an "assist" stage, which harnesses organ-on-a-chip or organoid-based in vitro tissue models to mimic biological functions [21], thereby facilitating a deeper understanding of physiological processes and optimizing tissue regeneration strategies.

Bioprinting for tissue regeneration is currently transitioning from Stage 2 to Stage 3, which is a leap that necessitates in-depth research into the multifunctional, high-precision, and self-organizing properties of biological tissues. The different tissues/organs of the human body each possess unique biological functions and physiological characteristics. For instance, the musculoskeletal system emphasizes tissue strength and flexibility [22], the nervous system prioritizes the accurate and rapid transmission of electrical signals [23], and the circulatory system focuses on permeability and sealing properties [24]. Therefore, in addition to pursuing a unified top-level design, we need to undertake personalized designs that cater to the unique characteristics of specific tissues to meet their particular needs. This necessitates close collaboration across the entire chain, from clinicians to engineers to material scientists, to collectively advance the bioprinting technology.

It should be clarified that this review aims to explore the advancements of 3D printing in the field of tissue regeneration. Therefore, the scope covered here is limited to the 3D printing of biodegradable materials and cell-laden bioinks that can facilitate tissue regeneration; non-biodegradable materials are not included in the scope of the present discussion. The main contents encompass the applicability and development trends of biomaterials, the challenges and strategies related to tissue/organ regeneration, and the key considerations for translating 3D-printed products from scientific research to clinical applications. Furthermore, this review specifically emphasizes the research landscape of this field in China, because China is one of the largest and fastest-growing markets in this context. This review will also introduce the latest achievements of Chinese research teams. Furthermore, it will explore application cases and development prospects of 3D printing in the field of tissue regeneration for each of the nine physiological systems (musculoskeletal, digestive, respiratory, urinary, reproductive, endocrine, immune, nervous, and circulatory systems) of the human body, thus providing a comprehensive overview of this rapidly evolving field.

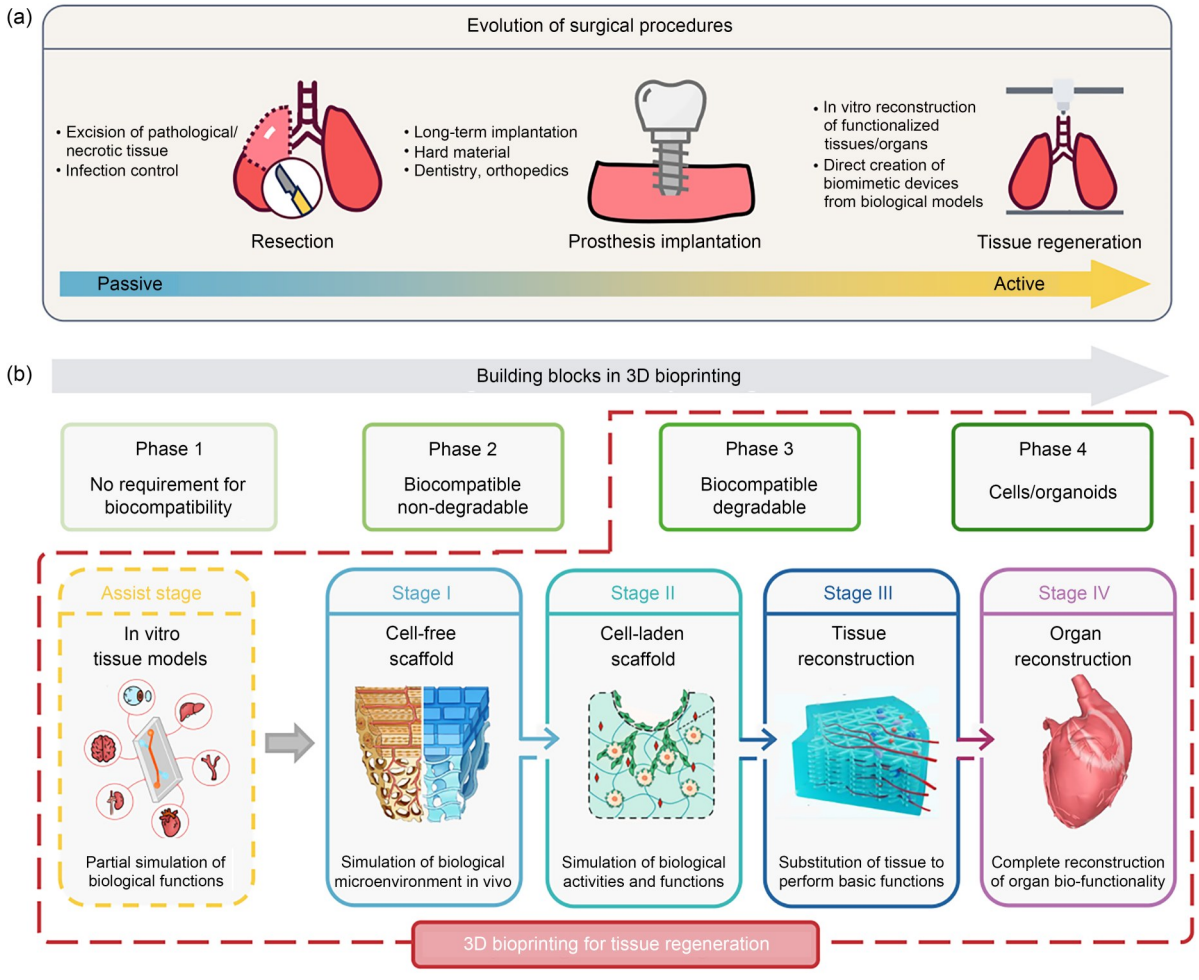

Fig. 1 Three-dimensional bioprinting in tissue/organ regeneration: (a) evolution of surgical procedures; (b) roadmap of the bioprinting technology used for tissue regeneration. Part (b, second panel) was adapted from [25], Copyright 2023, with permission from Wiley. Part (b, third panel) was adapted from [26], Copyright 2022, with permission from the authors, licensed under CC BY 4.0. Part (b, fourth panel) was adapted from [27], Copyright 2023, with permission from the authors and exclusive licensee American Association for the Advancement of Science. Part (b, fifth panel) was adapted from [28], Copyright 2023, with permission from Wiley

2 Biomaterials for 3D bioprinting

2.1 Key elements

The development of biomaterials that are suitable for 3D bioprinting has always been a pivotal element of this technology [29, 30]. Their primary requirement is exceptional bioactivity, ideally mimicking the extracellular matrix (ECM) environment in vivo to promote the proliferation of cells, establish cell-to-cell connections, and ultimately achieve functionalization. This property is often referred to as "biocompatibility" [31]. In addition, rapid shaping, high flowability, and a controllable crosslinking degree are essential properties for this purpose. Rapid shaping can significantly shorten the printing time, thereby avoiding potential damage to cells caused by prolonged manipulation; high flowability ensures the integrity and uniformity of the printed structure; and an appropriate crosslinking density is crucial for maintaining the stability of the cellular microenvironment: an insufficient crosslinking density can lead to structural deformation, whereas excessive crosslinking density can restrict cell growth. This property is typically measured by "printability" [32]. Finally, different tissues have different hardnesses, elasticities, and toughnesses, and the mechanical microenvironment has a significant impact on cell behavior. Therefore, simulating the "mechanical properties" [33] of natural tissues [34] is also a factor that needs to be considered. In 3D bioprinting, biomaterials always face the challenge of balancing biocompatibility, printability, and mechanical properties (Fig. 2a).

2.2 Classification

The biomaterials that are commonly employed in 3D bioprinting can be broadly categorized into three main classes: ionic-curing, thermal-curing, and photo-curing biomaterials.

Ionic-curing biomaterials solidify through ionic crosslinking reactions, such as alginate-based hydrogels, which are commonly used in droplet-based 3D printing [35]. Thermal-curing biomaterials rely on heating or cooling for the transition of the ink from a fluid state to a solid state, such as gelatin-based hydrogels, which are widely used in extrusion-based 3D printing [36]. Photo-curing biomaterials are activated by irradiating the photoinitiator in the ink with a light source of a specific wavelength to trigger ink solidification, such as gelatin methacryloyl (GelMA) hydrogels, which are suitable for light-based 3D printing [37] (Figs. 2b and 2c). From a manufacturing perspective, the use of light to trigger material solidification offers the most precise and convenient method. This has rendered photocurable biomaterials a subject of intense interest among researchers in recent years.

Furthermore, based on whether they contain live cells, the inks used for bioprinting can be classified into biomaterial inks and bioinks [38]. Biomaterial inks are defined as "aqueous formulations of polymers or hydrogel precursors containing biofactors, capable of cell seeding after printing but not directly containing cells." Conversely, bioinks are defined as "a formulation of cells suitable for processing by an automated biofabrication technology that may also contain biologically active components and biomaterials" [38]. Bioinks have stringent biocompatibility requirements because cells grow directly within them [30], often limiting their printability. Conversely, biomaterial inks exhibit better printability because of post-printing cell seeding onto the scaffold surface, which relaxes the biocompatibility requirements.

Living cells within bioinks are crucial for constructing functional tissues and primarily encompass stem cells, endothelial cells, and tissue-specific cells [39]. Stem cells possess high versatility, which allows them to differentiate into various cell types. Endothelial cells facilitate rapid vascularization, thus ensuring a nutrient supply to the printed tissue. Tissue-specific cells can interact with the surrounding environment for specific tissue-repair scenarios, thereby mimicking the behavior of natural tissues. In addition, biofactors, such as the transforming growth factor-β (TGF-β), vascular endothelial growth factor (VEGF), and epidermal growth factor, are often incorporated into bioinks to promote specific cellular behaviors and accelerate tissue regeneration. Because of these components, bioinks resemble natural tissues more closely, which significantly enhances their ability to construct functional tissues.

2.3 Prospects

The development of bioinks has significantly propelled the innovation of the 3D bioprinting technology, further stimulating its immense potential for constructing in vitro models and developing implantable structures for tissue repair. Currently, their clinical applications primarily focus on utilizing nondegradable materials, such as metals and bioceramics, for tissue replacement or repair. However, research on the promotion of tissue regeneration using biodegradable materials or bioinks remains in the scientific exploration stage. This is primarily due to the significant differences in requirements

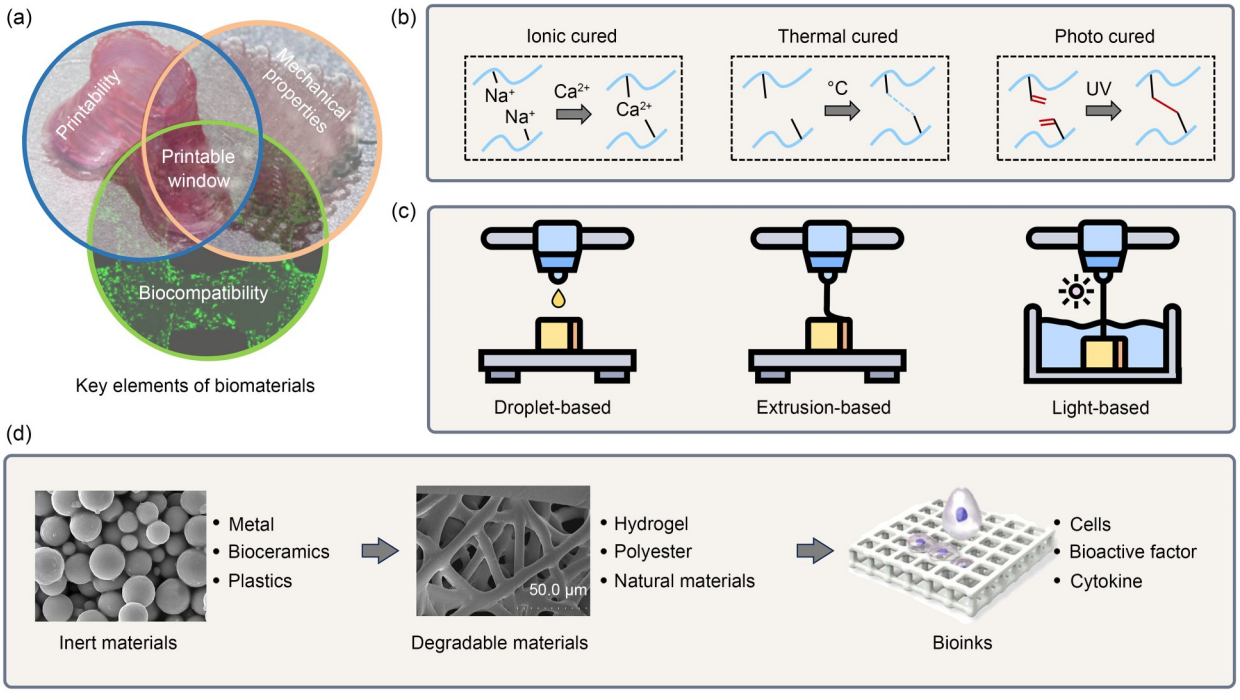

Fig. 2 Biomaterials for 3D bioprinting: (a) key elements; (b) classification of biomaterials; (c) classification of printing methods; (d) development trend. Part (d, third panel) was adapted from [38], Copyright 2018, with permission from the authors, licensed under CC BY 3.0

between hard tissue engineering (e.g., bone and cartilage) and soft tissue engineering (e.g., muscles and nerves). Soft tissue engineering necessitates a delicate balance among material elasticity, flexibility, and structural integrity, which poses a tough technical challenge (Fig. 2d).

3 From tissue engineering to organ engineering

3.1 Status

In natural tissues, the intricate structural patterns, precise transmission of biochemical signals, and close coordination among cell populations collectively drive the spontaneous integration of biological tissues, thereby efficiently executing various life activities. This complexity poses an extreme challenge in the recreation of functional biological tissues/organs in vitro. Currently, tissue engineering focuses primarily on the tissue-repair stage, promoting the regeneration and repair of surrounding tissues by implanting ECM and/or cells within the body. However, these implanted tissue-engineered scaffolds often have limited biological function, primarily relying on physical and chemical factors (such as their surface structure) and growth factors to induce the growth, differentiation, and migration of surrounding cells.

3.2 Challenges

In the pursuit of the fabrication of "transplantable organs," we face three core challenges: precise fabrication, stable transplantation, and long-term survival. Natural tissues exhibit cross-scale heterostructures, among which the nanoscale ECM transmits biochemical and physical stimuli, thus profoundly impacting cell biology; the microscale surface textures promote cell growth, migration, and differentiation through contact guidance effects, thereby facilitating the rapid functionalization of the engineered tissues; and complete tissues/organs regulate the biochemical interactions among different cell populations at the macroscale, forming the structural basis for achieving biological function.

3.2.1 Precise fabrication

Throughout natural selection and evolution, the composition, structure, synthesis process, perception mode, and functional properties of natural organisms have been continuously optimized and enhanced. They achieve maximum strength with minimal material consumption, construct complex special structures using the simplest materials, and realize multiple biological functions with the lowest energy expenditure. Although the current 3D bioprinting techniques can simulate biomimetic structures at a certain scale, they still fall short in precisely replicating the material composition, multilevel structures, and geometric shapes (Fig. 3a).

Therefore, instead of pursuing the direct reconstruction of perfect transplantable organs in vitro (which is extremely difficult in practical operations), leveraging the self-organizing, self-healing, self-adapting, and self-regulating capabilities of living organisms is a more feasible approach. By combining in vitro construction with in vivo optimization strategies, we can first fabricate artificial tissues/organs in vitro that meet the basic biological function, mechanical properties, and geometric shape requirements. These engineered structures can then serve as guiding scaffolds for the tissue-regeneration processes. Subsequently, by harnessing the natural mechanisms of growth factor secretion, vascularization, and cell proliferation of the organism, we can further optimize the biological performance of these in vitro constructs, ultimately achieving the reconstruction of functional organs.

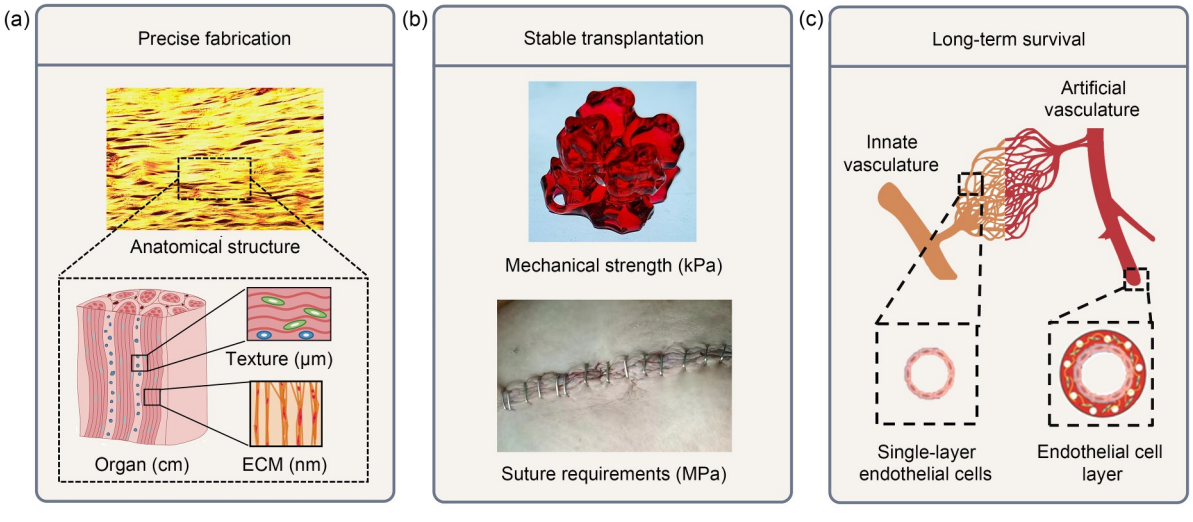

Fig. 3 Challenges of transplantable organs: (a) precise fabrication; (b) stable transplantation; (c) long-term survival. Part (b, upper) was reproduced from [42], Copyright 2023, with permission from Wiley

For example, the method of biomimetic trachea construction [27] reported by Yong He et al. first constructs a composite structure of cartilage and connective tissue rings in vitro, and then promotes vascularization through ectopic implantation in vivo, ultimately affording successful trachea transplantation. This strategy provides a novel paradigm for the fabrication of transplantable organs. By embracing the self-organizing capabilities of living organisms, we can circumvent the limitations of the current bioprinting technologies and achieve more robust and functional bioprinted tissues/organs. This approach holds immense promise for advancing tissue engineering and regenerative medicine, thus paving the way for the development of effective therapies for a wide range of tissue and organ damage.

3.2.2 Stable transplantation

During transplantation, fixation is crucial for ensuring the normal function of the implant, which renders suturing a necessary step of the process. However, this poses a challenge for soft tissue reconstruction. In 3D bioprinting (especially in cell-laden bioprinting), to ensure cell viability, Young's modulus of bioinks is typically on the order of kPa, whereas effective and stable surgical sutures typically require Young's modulus on the order of MPa [40]. Therefore, ensuring the effective suturing of soft tissues and guaranteeing their transplantation stability remain a significant challenge. One feasible solution is the employment of composite biomaterials to achieve a balance between overall toughness and local softness. For instance, by utilizing extrusion or photo printing, soft bioinks initially form a biomimetic structure. Subsequently, a polycaprolactone (PCL) fiber scaffold crafted via near-field direct writing is embedded. The fibers offer surgical suturing support, while the bioinks create a microenvironment that is conducive to cell growth [24]. Their synergy facilitates the attainment of the objectives mentioned above (Fig. 3b).

3.2.3 Long-term survival

Neuralization and vascularization are crucial for the long-term survival and functionalization of 3D-printed artificial tissues [41]. A macro-/microscale multilevel vascular network system can deliver adequate nutrients and oxygen to all areas of the entire tissue/organ, providing the essential material basis for cell growth and metabolism. Therefore, the construction of a multilevel vascular system is key to the fabrication of large-volume artificial tissues and even whole organs. Simultaneously, a multilevel artificial vasculature offers the possibility of direct connection to the host vasculature upon transplantation. This timely vascular integration can prevent cell apoptosis within the tissue and further promote cell and tissue development, thus ensuring the long-term survival of the transplanted tissue/organ (Fig. 3c). On the other hand, neuralization regulates and controls the functional activities of various systems by integrating the engineered tissue with the native tissue to form a cohesive unit. Concurrently, neuromodulatory mechanisms optimize the regenerative microenvironment, thus playing an indispensable role in the promotion of tissue regeneration. Neurovascularization is a fundamental physiological requirement for tissues and a critical factor in the enhancement of the overall performance and functional recovery of artificial tissues (Fig. 3c).

4 From scientific research to clinical application

4.1 Status

Innovation plays a pivotal role in scientific research, and researchers often showcase intricate designs. However, safety and effectiveness are the primary considerations in clinical applications. Clinical therapeutic products directly impact patient health and life safety; therefore, a stringent regulatory oversight of safety and efficacy is paramount. The 3D bioprinting technology can facilitate personalized customization to meet the unique needs of different patients. Despite extensive scientific research on the 3D bioprinting technology, few 3D-bioprinted products have been successfully applied in clinical practice. On the one hand, clinical translation research remains in its infancy; on the other hand, governmental departments need to establish a systematic and comprehensive regulatory and evaluation system.

For clinical therapeutic applications, 3D-printed products can be broadly categorized into two types: medical devices and pharmaceuticals. Medical devices refer to those used for the human body or its extracorporeal diagnosis, primarily achieving therapeutic purposes through physical means or auxiliary functions without relying on pharmacology, immunology, or metabolic effects. In turn, pharmaceutical products aim to regulate the physiological functions of the human body. Most of the 3D-printed products available currently are medical devices, and their clinical application requires a medical device registration certificate. If the printed product contains drugs (such as a drug-delivery system), it may be subject to regulation as a drug or a combination of drugs and devices, and a drug registration certificate is required. The process of research, development, and production of pharmaceutical products is relatively complex, with high demands on technology and equipment. In particular, when 3D-printed products involve biological agents (such as cells, antibodies, and vaccines), their management should be based on the specific properties (such as biological activity and immunogenicity) of the biological agents, which may entail a more complex and stringent clinical trial process.

In China, the materials that are currently approved for medical 3D printing are primarily limited to inorganic and nondegradable materials, such as titanium alloys and tantalum powders. These materials are highly inert and interact minimally with the body, thus facilitating a relatively straightforward regulatory approval process. However, the integration of these materials with tissues primarily relies on tissue growth into their rough surfaces, forming a mechanical interlock that is not robust and can easily trigger adverse reactions, such as inflammation and allergies. Consequently, the future trend will lean toward exploring and developing degradable materials for tissue regeneration. However, the clinical application of degradable materials is not straightforward. Although researchers hope for relaxed regulatory policies to accelerate the research progress, from a regulatory perspective, it is essential to comprehensively assess the degradation process, metabolites, and interactions with host tissues of these artificial implants in the body to ensure the safety of their behavior throughout the entire lifecycle. Therefore, degradable, absorbable, and cell-laden 3D-printed products largely remain in the research stage. The incorporation of biological components into a product necessitates in-depth technical considerations regarding both the manufacturing and regulatory aspects, which poses significant challenges. Therefore, a multi-stage, incremental development strategy may be more practical and feasible for the translation from research to clinical applications in this context. For example, in the production of 3D-printed medical devices, materials that have been widely applied clinically or have undergone simple modifications can be preferentially selected. However, in the long term, degradable materials, drug-laden materials, and biological-agent-laden materials for medical 3D printing will be key areas of future research.

4.2 Challenges

During the implementation of 3D-printed medical device products, "risk" and "quality" are the two core concerns. Based on these two issues, two major quality control focuses have been developed, i.e., "full-process quality control" and "full-lifecycle risk management" [43], which have highlighted the urgent need for standardization in the field of 3D printing. From the early design stage to the manufacturing stage, each link requires strict control to form a comprehensive product quality-control system (Fig. 4).

4.2.1 Raw material qualification

To meet the biocompatibility requirements of the 3D printing technology, degradable biomaterial inks are often chemically modified from proteins, saccharides, and lipids in natural biological tissues. Such animal-derived materials require strict traceability to their source to ensure that the entire supply chain meets strict quality system standards. Furthermore, 3D printing often recycles materials for re-use, which may lead to changes in performance or potential contamination risks, thus requiring special attention.

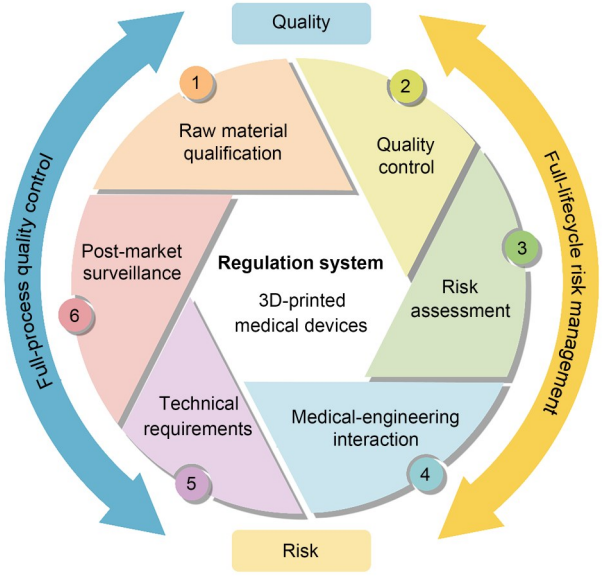

Fig. 4 Full-process quality control and full-lifecycle risk management in the supervision of 3D-printed medical devices

4.2.2 Quality control

Because of the significant differences between 3D printing and the traditional casting and cutting processes, the former may face additional risks and challenges in terms of manufacturing control, performance, biocompatibility, and sterilization. These new challenges require a comprehensive consideration of more factors during the processing to ensure stable product quality.

4.2.3 Risk assessment

The potential interactions of 3D-printed medical devices with the human body and their impact on human health are important aspects of their risk assessment. For example, implants, as medical devices that directly contact the human body, require a strict evaluation and control of their residues or leachates. Quality and safety risk management should be a comprehensive and systematic process that must carefully consider every factor that may affect human health.

4.2.4 Medical–engineering interaction

As medical–engineering interaction products, the research, development, and application of 3D-printed medical devices involve two main entities: engineering technicians and clinical doctors. To ensure product quality and safety, both parties

must have a deep understanding of, and strictly follow the quality-control process.

4.2.5 Technical requirements

Technical requirements are an integral part of product design by specifying the technical performance and quality standards of the product. Given the diversity of the 3D printing technologies and the complexity of the material system, it is particularly important to scientifically, comprehensively, and effectively formulate technical requirements and corresponding testing methods. However, currently, gaps remain in the technical requirements in the field of medical 3D printing in China, which requires the investment of additional resources toward in-depth research and exploration.

4.2.6 Post-market surveillance

Obtaining regulatory approval and market placement does not represent the end of the regulation of 3D-printed medical devices; on the contrary, the clinical applications of the devices after their launch are the true test of their effectiveness. If adverse events occur and the implants need to be removed, well-established removal procedures and post-removal product testing and analysis techniques should be established to identify the causes of product failure. Moreover, ensuring that 3D-printed medical devices have unique identification numbers and archiving production, sales, and subsequent handling records are crucial for achieving traceability from raw materials to the final sales link.

The management of medical devices is a complex engineering system that involves the participation of multiple parties, such as the government, manufacturers, suppliers, and research institutions. The emerging field of 3D-printed medical devices inevitably encompasses details that are difficult to fully cover, even with the support of laws and regulations. Therefore, all parties need to strengthen cooperation and jointly promote the implementation of the full-lifecycle management of medical devices.

5 Advances in 3D bioprinting technologies in China

Chinese research teams have made remarkable progress in the field of 3D bioprinting technologies. In terms of printing materials, notable achievements include advancing the standardization of photocurable inks and developing degradable bone materials for 3D printing, thereby providing safer and more efficient material solutions for biomedical engineering.

Regarding the printing processes, research efforts have converged on two core technological pathways: light-based printing and extrusion-based printing. The light-based printing technology has achieved breakthroughs in high-precision and multimaterial bioprinting, opening new avenues for the precise construction of complex biological structures. In turn, the extrusion-based printing technology has made significant progress in the optimization of printing windows and the enabling of high-cell-density printing, thus further enhancing the biological functionality of bioprinting. It should be noted that 3D bioprinting is not limited to these two technological pathways. Other printing technologies, such as powder bed technologies (e.g., selective laser melting (SLM) and selective laser sintering (SLS)), can also print biomaterials. However, they are commonly used in ceramic and metal printing, with limited application in biodegradable materials and bioinks for tissue repair. Therefore, this study focuses on two main technological pathways: light-based and extrusion-based bioprinting.

In the context of the exploration of printing methods, a series of innovative technologies, such as volumetric printing, micro-nano printing, embedded printing, gradient printing, piezoelectric material printing, and space printing, have been deeply investigated. These technologies not only expand the application boundaries of 3D bioprinting, but also offer additional possibilities for future biomedical research and clinical applications. Moreover, efforts are being directed toward the development of other biomimetic organ-on-a-chip and organoid technologies, aiming to accelerate disease modeling, drug screening, and regenerative medicine research through highly realistic physiological environment simulations (Fig. 5).

5.1 Printing materials

5.1.1 Standardization of photocurable bioinks

Because of the high biocompatibility, tunable physicochemical properties, and excellent printability of the photocurable bio-hydrogels, bioinks have gradually transitioned from ionic crosslinking to photocrosslinking. GelMA exemplifies the second generation of photocurable bioinks and has become the cornerstone consumable material for 3D bioprinting. However, the lack of standardization for this material can easily lead to contradictory results, as the properties and performance of GelMA vary under different synthesis conditions. To address this challenge, the group of Yong He has established a unified framework to understand and enhance GelMA applications [28]. First, those researchers initially defined the basic concept of hydrogels: the density of the molecular network (DMN). Second, the degrees of substitution and solid content ratio were identified as the key measurable parameters for determining the DMN. Subsequently, they elucidated the mechanisms and relationships between the DMN and hydrogel performance in diverse applications, including porosity, viscosity, formability, mechanical strength, swelling, biodegradation, and cytocompatibility.

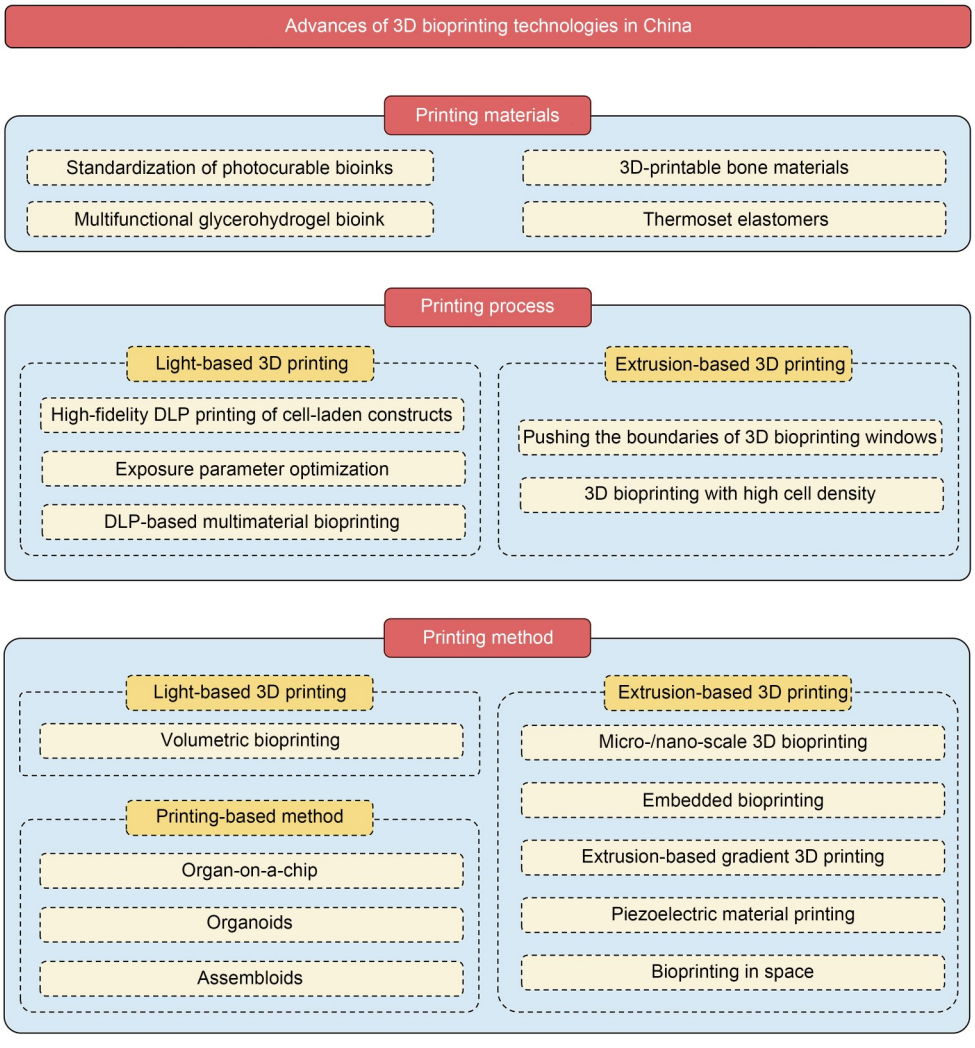

Fig. 5 Advances in 3D bioprinting technologies in China

This knowledge empowers researchers to bypass the need for cumbersome and repetitive pre-experiments, facilitates seamless result exchange between groups that adhere to the same standard, and unlocks the full potential of GelMA hydrogels (Fig. 6a). Based on this foundation, that group demonstrated the precise tailoring of the mechanical properties of the printed constructs by manipulating the hydrogel concentration, degree of substitution, and photocrosslinking time [33] (Fig. 6b). This enables the biomimetic fabrication of soft tissues with a spectrum of mechanical strengths [44], from the liver (6–8 kPa) to the skin (0.3–0.4 MPa). Furthermore, a profound understanding and quantification of the photocrosslinking process in bioinks are indispensable for achieving standardization and scalability in bioprinting. Therefore, the team of Yong He established the formation theory of photocurable hydrogels [32, 45]. They discovered that not all double bonds consumed during crosslinking contribute equally to polymerization, which then elicits the concept of effective double-bond conversion (EDBC) (Fig. 6c). Deriving from EDBC, they defined several critical formation indices. Moreover, by leveraging the principles of bioink photocrosslinking, they proposed a novel strategy for projection-based 3D printing (PBP), leading to significant enhancements in printing quality and efficiency. In conclusion, this work bridges the knowledge gap in the hydrogel formation theory, thereby paving the way for the accurate quantification of the formation process.

5.1.2 3D-printable bone materials (provided by the Xin Zhao group)

In the field of bone tissue engineering, various materials have been examined for their 3D printing potential. Traditional materials such as polycaprolactone (PCL), poly(lactic acid) (PLA), and poly(lactic-co-glycolic acid) (PLGA) are commonly used for bone repair [46]. However, to render these materials printable, the involvement of organic solvents or heating processes is required, which compromises their

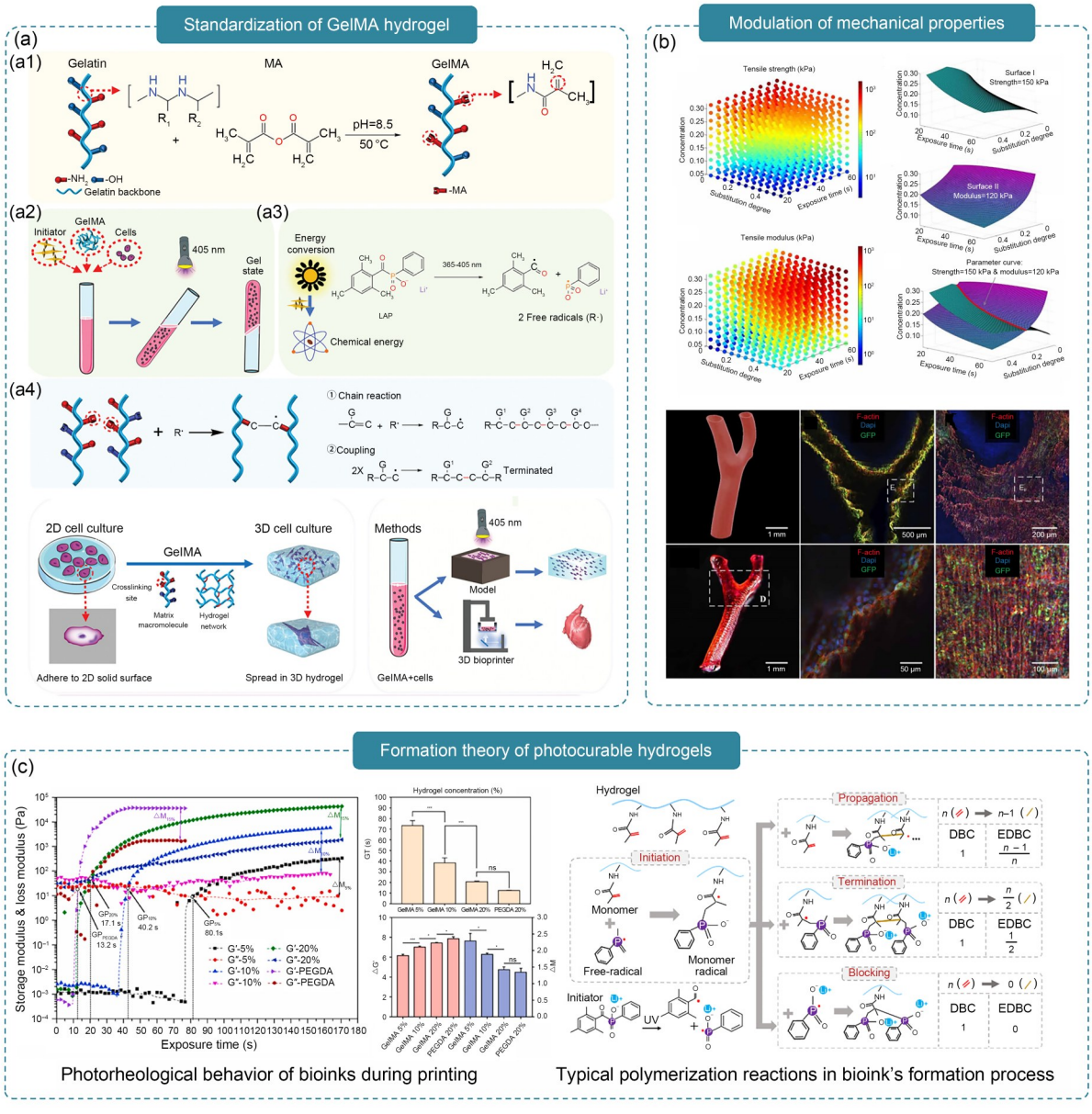

Fig. 6 Standardization of photocurable bioinks: (a) synthesis, photocrosslinking, 3D printing, and cell culture of gelatin methacryloyl (GelMA); (b) precise modulation of the mechanical strength of the bioinks to mimic various tissues; (c) photorheological properties of the bioinks under light irradiation and characteristics of the three typical reactions that occur during polymerization. Part (a) was reproduced from [28], Copyright 2023, with permission from Wiley. Part (b) was reproduced from [33], Copyright 2021, with permission from IOP Publishing. Part (c, first panel) was adapted from [32], Copyright 2021, with permission from the authors, licensed under CC BY 4.0. Part (c, second panel) was reproduced from [42], Copyright 2023, with permission from Wiley

ability to encapsulate bioactive molecules. Calcium-phosphate-based materials, such as hydroxyapatite, are bioactive and chemically similar to bone minerals but are generally brittle and unsuitable for load-bearing applications because of their mechanical limitations [47]. After 3D printing and sintering, these materials can form various topological structures and scaffolds [48]. However, they exhibit a poor drug-loading capacity and the sintering process is complex and time-consuming. In addition, these scaffolds face challenges such as inhomogeneous filler distribution and nozzle clogging during 3D printing. To address these challenges, the Xin Zhao group developed a novel photopolymerizable material, i.e., poly(lactide-co-propylene glycol-co-lactide) dimethacrylate (P_mL_nDMA), which enhances printability and injectability through the use of propylene glycol, increases biodegradability via the use of lactide, and incorporates methacrylate to enable photocrosslinking [49–51]. Furthermore, the Xin Zhao group enhanced this material by developing a biomimetic photopolymerizable nanocomposite (BPN) (Fig. 7a) that integrates functionalized nano-hydroxyapatite to further

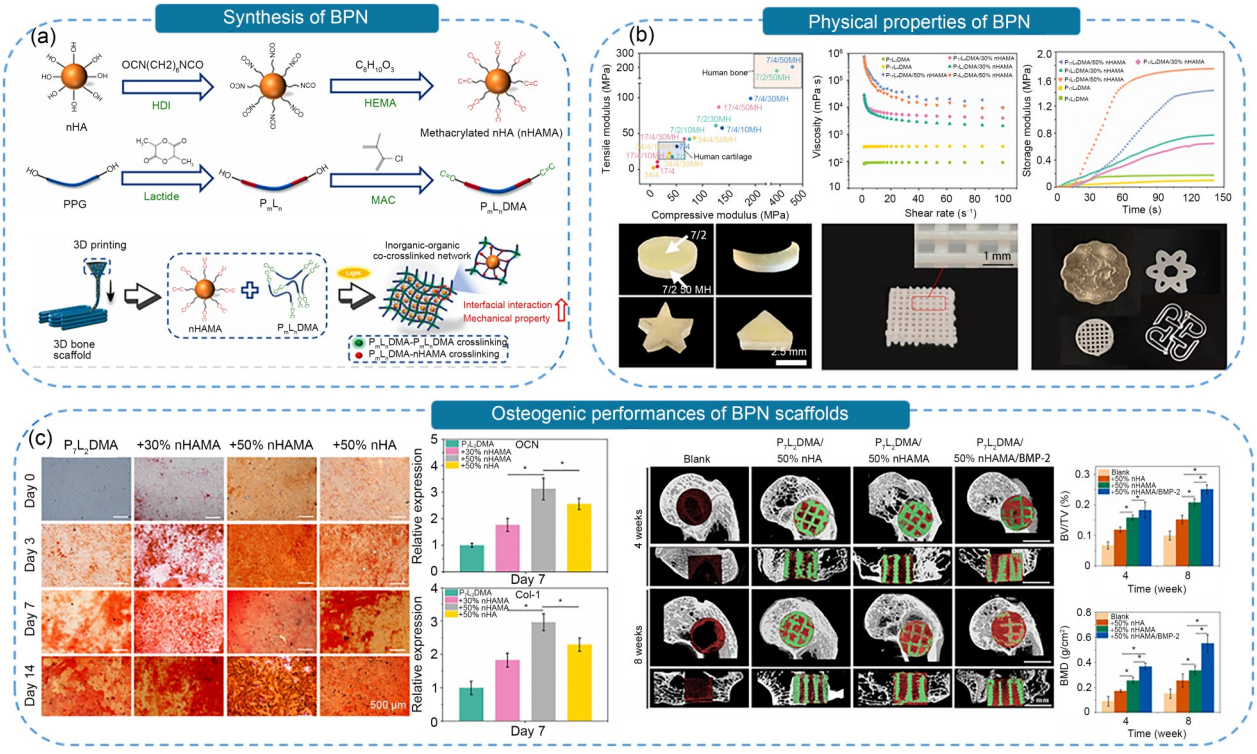

Fig. 7 Three-dimensionally printable bone materials—P_mL_nDMA-based biomimetic photopolymerizable nanocomposite (BPN) scaffolds: (a) synthesis and application of P_mL_nDMA and methacrylated hydroxyapatite nanoparticles (nHA) in the construction of 3D-printed BPN scaffolds; (b) tunable physical properties of BPN, including mechanical properties, rheology, and printability; (c) in vitro (left) and in vivo (right) osteogenic performances of BPN scaffolds. Part (a), Part (b, second and third panels), and Part (c) were reproduced from [49], Copyright 2020, with permission from Elsevier. Part (b, first panel) was adapted from [52], Copyright 2023, with permission from Wiley

enhance the mechanical properties. The tunable mechanical properties of BPN (from 40 to 400 MPa) can be adjusted to meet the requirements of various tissue types, ranging from hard bone to softer cartilage [52] (Fig. 7b). The excellent rheological properties of P_mL_nDMA render it compatible with advanced fabrication techniques, such as 3D printing, thus allowing the creation of complex scaffold structures that promote effective tissue regeneration. Reportedly, this affords complete crosslinking within 140 s with minimal heat, thus facilitating the sustained release of therapeutic molecules [53]. This material supports mechanical stability and stimulates osteogenesis through the controlled release of bioactive molecules, thereby significantly augmenting bone healing and tissue regeneration. Furthermore, in the rabbit femoral defect model, BPN scaffolds that incorporated bone morphogenic protein-2 (BMP-2) exhibited a 1.6-fold increase in bone mineral density compared with the unmodified BPN scaffolds and a 3.6-fold increase compared with the blank control group [49] (Fig. 7c).

5.1.3 Multifunctional glycerohydrogel bioink (provided by the Huixia Xuan group)

Hydrogels are currently the most commonly used bioinks because of their biomimetic ECM properties. Previous studies employing hydrogel bioinks have mainly focused on their cytocompatibility and cell survival after the 3D bioprinting of tissues [54, 55]. However, the free water in hydrogel bioinks forms fatal ice crystals at low temperatures, which poses a challenge to the cryopreservation of the printed constructs. In addition, free water will evaporate and provide a living environment for bacteria, which limits the application of the hydrogel bioink. The group of Xuan at Donghua University demonstrated that the incorporation of glycerol into a hydrogel may address the aforementioned limitations of hydrogels [56–58]. Inspired by these results, they introduced glycerol to regulate the state of water by forming extensive hydrogen bonds between glycerol and water to transform free water into bound water and create a multifunctional binary gelatin glycerohydrogel bioink (Fig. 8) [59]. Compared with the existing hydrogel bioinks, the glycerohydrogel bioink displays a series of favorable properties, including bacteriostatic characteristics, excellent shape maintenance, and an intrinsic ability of direct cryopreservation at 80 °C, which are highly desired but difficult to achieve in existing bioinks. This study establishes a new paradigm of bioinks and is expected to facilitate the practical utilization of 3D bioprinting in diverse fields, such as regenerative medicine and in vitro disease modeling.

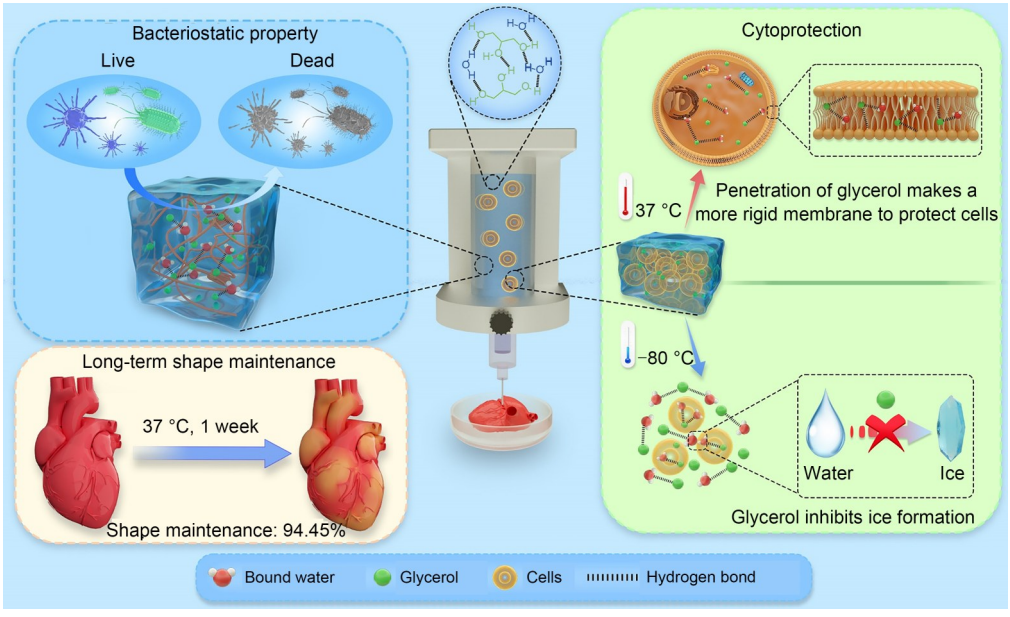

Fig. 8 Design of a multifunctional glycerohydrogel bioink. Reproduced from [59], Copyright 2023, with permission from Elsevier

5.1.4 Thermoset elastomers (provided by the Huixia Xuan group)

Thermoset elastomers can resemble the mechanical properties of the ECM and soft tissues and are compliant with the dynamic mechanical environment of the body; thus, they are very useful for many biomedical applications [60–62]. However, the permanent chemical crosslinked networks of thermoset elastomers are typically insoluble and infusible, which greatly restricts their processing and design freedom. Time-consuming crosslinking reactions, such as esterification, render it difficult to match the demand for fast curing of the prepolymer in processing. Thus, the 3D printing of thermoset elastomers remains a significant challenge. You and coworkers proposed an innovative approach to addressing this problem. They designed composite inks containing prepolymer and carrier materials, serving as binder and aggregate, respectively, to ensure efficient 3D printing and structural integrity during subsequent curing, even in harsh conditions [63] (Fig. 9a). After curing, the carrier materials can be either removed to provide porous 3D constructs or retained as functional fillers. Those authors demonstrated that this is a general strategy to 3D print various thermosets directly, as exemplified by crosslinked polyester, polyurethane, and epoxy resin. Taking a representative biomedical elastomer poly(glycerol sebacate) (PGS) as an example, they used biosafe sodium chloride particles as sacrificial carrier materials to efficiently 3D print tunable and well-organized hierarchical porous architectures [64–68]. They demonstrated the power of the 3D-printed PGS constructs as tissue-engineered scaffolds, myocardial patches, and soft robots [63, 69, 70]. Moreover, conductive substances, such as carbon nanotubes, were incorporated into the composite ink to 3D print for the first time integrated triboelectric nanogenerators (TENGs) without additional assembling steps [71]. The 3D-printed TENGs efficiently converted mechanical energy into electrical energy through triboelectrification and electrostatic induction. Recently, a new concept of triboelectric scaffolds and nonadjacent wireless self-powered electrotherapy was proposed using 3D-printed TENGs to efficiently promote the regeneration of cartilage, skin, and muscle tissues [72, 73]. Similarly, magnetic particles were integrated to develop a magnetic epicardial patch for rapid vascular reconstruction and drug delivery [74] (Figs. 9c–9e). Based on their previously developed 3D-printing strategies, the You group further developed four-axis printing [75] (Figs. 9b and 9f). Traditionally, the collecting plate is replaced with a continuously rotating axis to fabricate a hollow tubular scaffold for tracheal cartilage regeneration and external stents on vein graft [76]. This approach has also been adopted by Wu and coworkers to fabricate a 3D porous vascular graft for the efficient regeneration of small-caliber arteries, which is promising for clinical translation [77]. In conclusion, these works bridge the long-standing challenges of the processing of thermoset elastomers with personalized 3D printing, thus paving a new avenue for the application of thermoset elastomers.

5.2 Printing process

5.2.1 High-fidelity digital light processing (DLP) printing of cell-laden constructs (provided by the Xiaoxiao Han group)

Complex tissues require engineered constructs with multiscale features to mimic their microenvironment and support

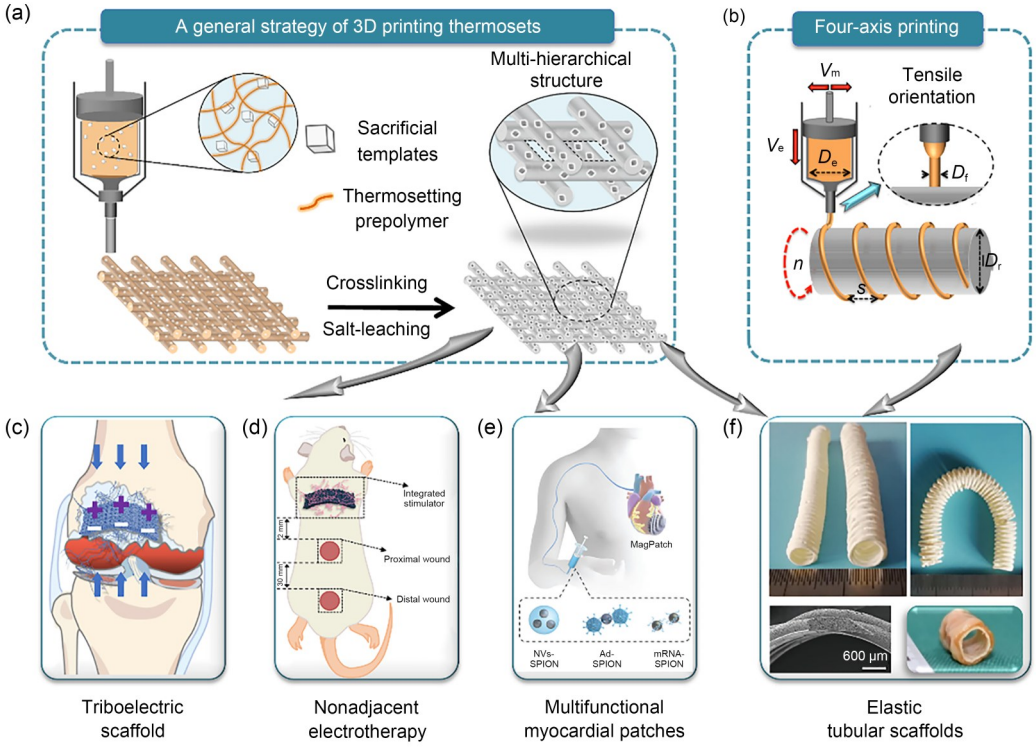

Fig. 9 Three-dimensional printing of thermoset elastomers and their biomedical applications: (a) schematic diagram of 3D printing thermosets; (b) illustration of four-axis printing; thermoset elastomers prepared by 3D printing and four-axis printing as a triboelectric scaffold (c), nonadjacent electrotherapy (d), multifunctional myocardial patches (e), and tubular scaffolds for tissue regeneration (f). Part (a) was reproduced from [63], Copyright 2019, with permission from the Royal Society of Chemistry. Part (b) and Part (f) were reproduced from [75], Copyright 2019, with permission from Science China Press and Springer-Verlag GmbH Germany, part of Springer Nature. Part (c) was adapted from [72], Copyright 2024, with permission from Wiley. Part (d) was reproduced from [73], Copyright 2023, with permission from the American Chemical Society. Part (e) was reproduced from [74], Copyright 2023, with permission from the authors, licensed under CC BY

cell function. This includes interconnected channels for nutrient exchange and specific geometries for cell guidance. The optimization of these features is crucial for tissue engineering. Traditional trial-and-error methods are inefficient; thus, computer modeling is used to predict cell behavior and optimize the design parameters for engineered tissues. Therefore, a theoretical framework describing the degradation process of biocompatible polymers was established by Han and her coworkers and applied to guide the design of implantable devices, such as bone screws and heart stents [78–81]. To promote mechanical stimulation for cell differentiation and tissue formation, the Han group optimized the mechanical and permeability properties of a three-periodic minimal surface (TPMS) structure via finite element modeling [82]. The human adipose stem cell-laden hydrogel was then infused into the optimized TPMS structure to form a scaffold, which exhibited an elastic modulus that was comparable to that of human breast tissue (0.20–0.83 MPa). To further expand the modeling capability to optimize cell-laden constructs, they established a mechanistically realistic modeling framework that is capable of capturing the phenomena observed during the cultivation process [83]. The model accounted for the coupled physical–biological process (the fluid dynamics when nutrient medium passed through the construct, oxygen transport process, oxygen consumption by cells, and cell growth kinetics) and parameters including material, geometry, and cells. The model's accuracy was verified by comparing the simulated results with those of the cell-proliferation experiments, and it was substantially applied to optimize the diameter of the microchannels and their spatial distribution within the scaffold, thereby providing a valuable tool for guiding the design of scaffolds and engineered tissues (Fig. 10a).

From a manufacturing perspective, light-based 3D printing (such as DLP, two-photon polymerization, and volumetric printing) is gaining popularity in tissue engineering because of its high resolution and flexibility. However, the cells in the bioink cause nonuniformities and light scattering, thus deviating light to nontarget areas. This leads to excessive solidification, which reduces the printing resolution and limits the fabrication of complex cell-laden constructs. To address this challenge, the Han group proposed an innovative photoinhibition approach that effectively suppresses the inherent light-scattering effect of light-based 3D printing platforms via simultaneous photoabsorption and free-radical reaction [84]. Based on this mechanism, a new photoinhibition additive (curcumin-Na (Cur-Na)) was synthesized. Cur-Na confines

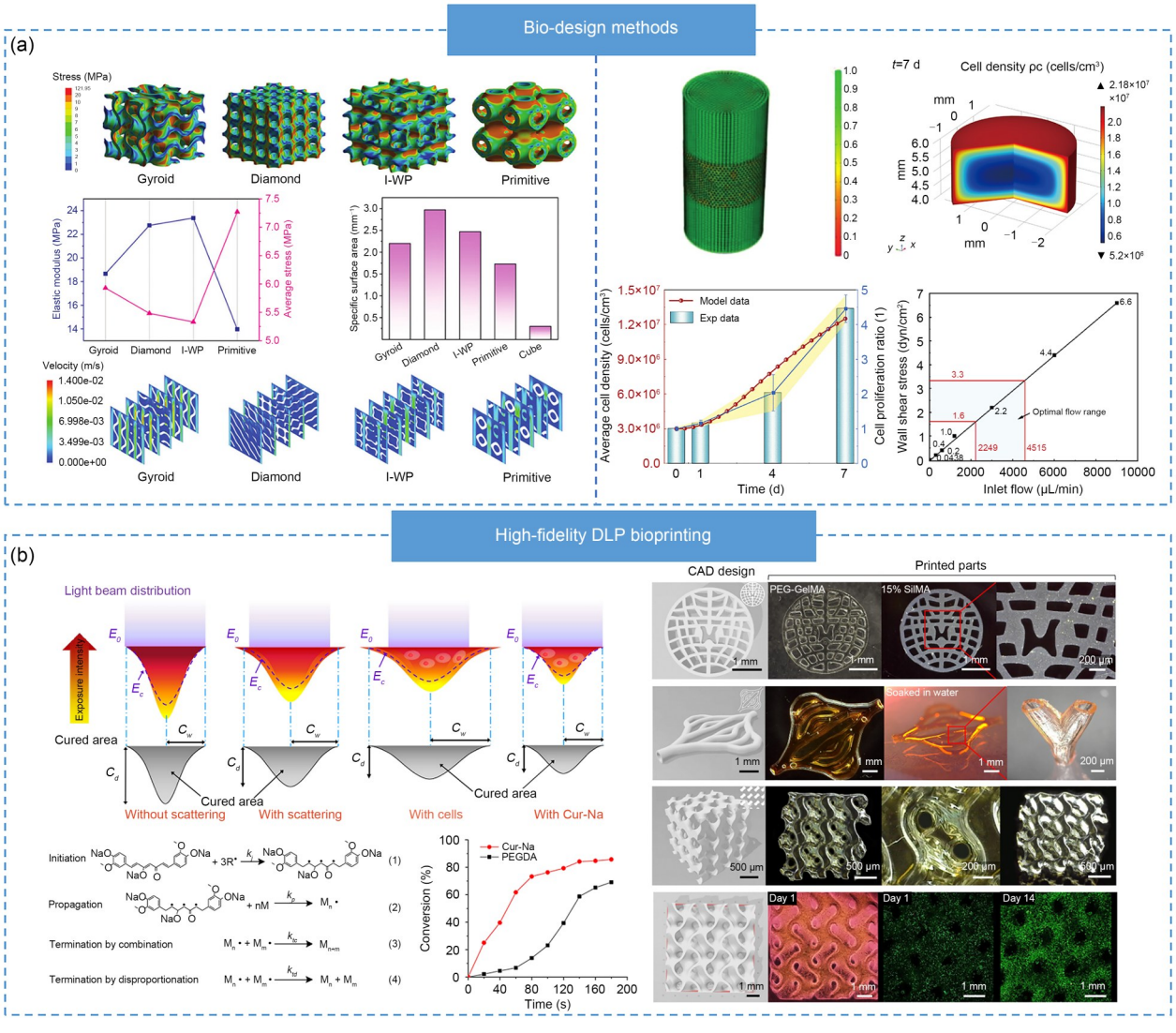

Fig. 10 Optimal design and high-fidelity 3D printing of cell-laden constructs. (a) Optimization of the mechanical and permeability properties of a three-periodic minimal surface structure utilizing finite element modeling to match the elastic modulus to that of human breast tissue (0.20–0.83 MPa) (left); modeling of cell growth behaviors in a cell-laden construct (right). (b) Mechanism used for mitigating the light scattering effect (left); 3D complex constructs and functional cellularized gyroid scaffolds (HepG2) fabricated with high fidelity using the new photoinhibition additive (right). Part (a, left) was reproduced from [82], Copyright 2023, with permission from the authors, licensed under CC BY 4.0. Part (a, right) was adapted from [83], Copyright 2024, with permission from the authors, licensed under CC BY 4.0. Part (b) was adapted from [85], Copyright 2023, with permission from the authors, licensed under CC BY 4.0

the vertical light penetration depth by physically absorbing excessive light, thus promoting vertical resolution. In turn, the reactive functional groups of Cur-Na (three C=C double bonds of alkene) rapidly consumed free radicals in the scattered region via a chain-growth chemical reaction, thereby preventing unwanted solidification and improving the horizontal resolution. Using this approach, the authors demonstrated that the printing resolution was enhanced to approximately 1.2–2.1 pixels depending on swelling degree, and that the geometric error was lowered to less than 5%. This photoinhibition strategy significantly advances the printability of light-based 3D bioprinting systems, enabling the successful fabrication of various 3D complex constructs and functional cellularized (e.g., HepG2) gyroid scaffolds, thereby opening numerous new applications for tissue engineering (Fig. 10b).

5.2.2 Exposure parameter optimization (provided by the Jun Yin group)

As a 3D-printing technology with high precision and efficiency, the DLP technology requires the fine-tuning and optimization of various critical parameters before printing, which is a complicated process. The Jacob working curve is conventionally applied to demonstrate the relationship between the light energy absorbed and the cured thickness of the photocurable bioink under light exposure [86], in which these

technical details need to be acquired through extensive experiments. This is a time-consuming process that is wasteful of materials. To simplify and improve the process of obtaining DLP parameters, an analytical model was established to describe the relationship between the ultra-violet (UV) light exposure time and the cured layer thickness. In this model, the Jacob working curve can be demonstrated as being solely dependent on three constant properties of the photocurable bioink, i.e., solid absorbance, liquid absorbance, and gelation time, which then contribute to the prediction of the printing parameters under any printing requirements of this type of bioink. Overall, the model lays the foundation for determining appropriate DLP parameters and affords high-precision DLP printing (Fig. 11a).

Having established a systematic theory for determining parameters in DLP printing, conventional DLP printing still has flaws in fidelity, such as staircase effects and an over-curing state, caused by repeated positioning and excess exposure. Based on the curing condition controlling theory, a continuous pre-curing DLP approach has been further achieved [87], which introduces the concept of pre-curing into the slice thickness and light exposure time. The printing process is divided into two sub-processes: pre-curing and further curing. In the pre-curing step, the excess exposure on the bottom layer can pre-cure the bioink of the next layer and maintain it at a pre-gelled state. In the subsequent further curing step, the pre-cured layer can be fully cured in a very short time by the light energy that was absorbed beforehand. By theoretically determining the relationship between the photocured layer thickness and the exposure time in continuous DLP printing, the printing time is reduced to 5.6% of the conventional printing time. By utilizing excess light exposure in pre-curing and replacing the repeating positioning with a continuous lift, the printing fidelity is improved (Fig. 11b).

5.2.3 DLP-based multimaterial bioprinting (provided by the Yang Wu group)

DLP technology works based on the layer-by-layer UV light curing of photocurable bioinks under the deflection and refraction of a digital micromirror device. Compared with droplet-based and extrusion-based bioprinting, the DLP-based technology holds significant potential because of its high printing precision, absence of shear forces, and rapid printing rate [88]. DLP-based multimaterial bioprinting has been proposed for the construction of tissues and organs with structural and functional heterogeneity. Multimaterial bioprinting devices must address issues such as material switching and the cleaning of residual materials. Popular material switching methods include liquid vat switching, fluid microcavity, liquid deposition, and multiwavelength photopolymerization [88]. As a pioneer work in this field, Ma et al. created an in vitro liver model using sequential material switching, which was in the shape of microscale hexagons [89] (Fig. 12a). In turn, Wang et al. developed a DLP system that integrated a microchannel to create a helical flow for the ink mixture at the inlet of the fluidic chip [90]. By fine-tuning the flow of different inks in the microchannel, the ink composition at the outlet of the fluidic chip could be precisely controlled, thus realizing multimaterial printing with a continuous or discrete cell-density gradient. The group of Yang Wu built a DLP-based multimaterial bioprinter based

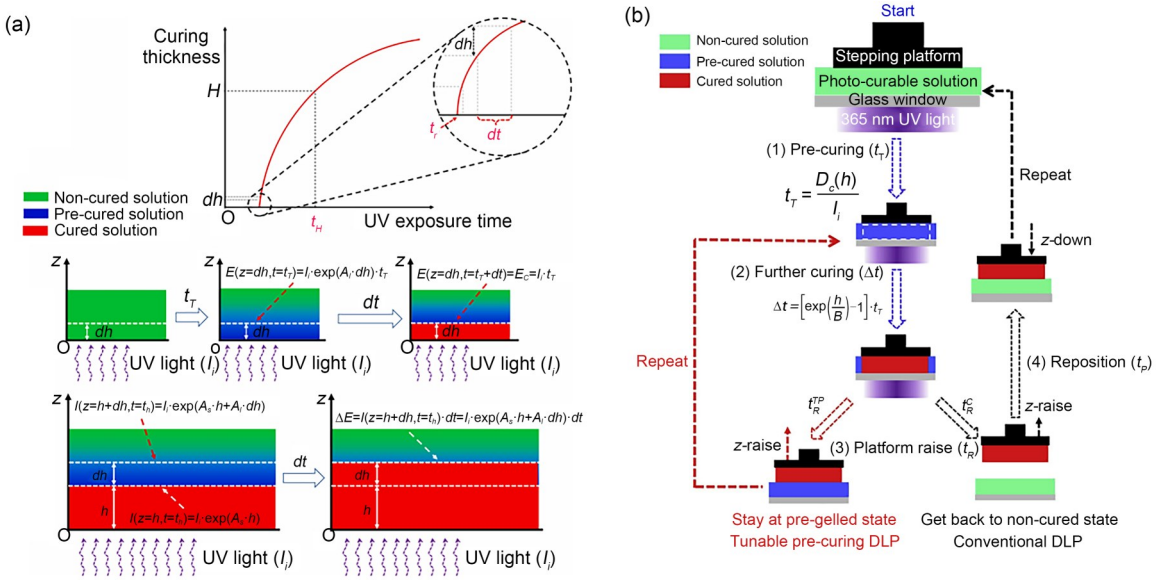

Fig. 11 Exposure parameter optimization of digital light processing (DLP): (a) Jacobs working curve; (b) pre-curing DLP printing. Part (a) was reproduced from [86], Copyright 2020, with permission from Elsevier. Part (b) was reproduced from [87], Copyright 2019, with permission from Elsevier

on the liquid vat switching mechanism, which included a bottom-up cleaning nozzle with a drying fan and enabled the printing of complex structures with multiple popular biomaterials (e.g., lattice structures with different colors and pyramid-containing polyethylene glycol diacrylate (PEGDA) and GelMA) [91]. A tracheal construct with a heterogeneous organization was also successfully bioprinted, which imitated the anatomy of the natural gas pipe and supported the viability of the embedded mesenchymal stem cells (MSCs). Recently, Yang et al. incorporated DLP-based multimaterial bioprinting with PEGDA-acrylamide (AAm) bioinks to develop cell-laden hydrogel constructs with multiple components and moduli, which exhibited not only heterogeneous mechanical properties, but also complex architectures and surface microstructures [92] (Fig. 12b). The mechanical moduli of different biological tissues (e.g., liver lobules, bone

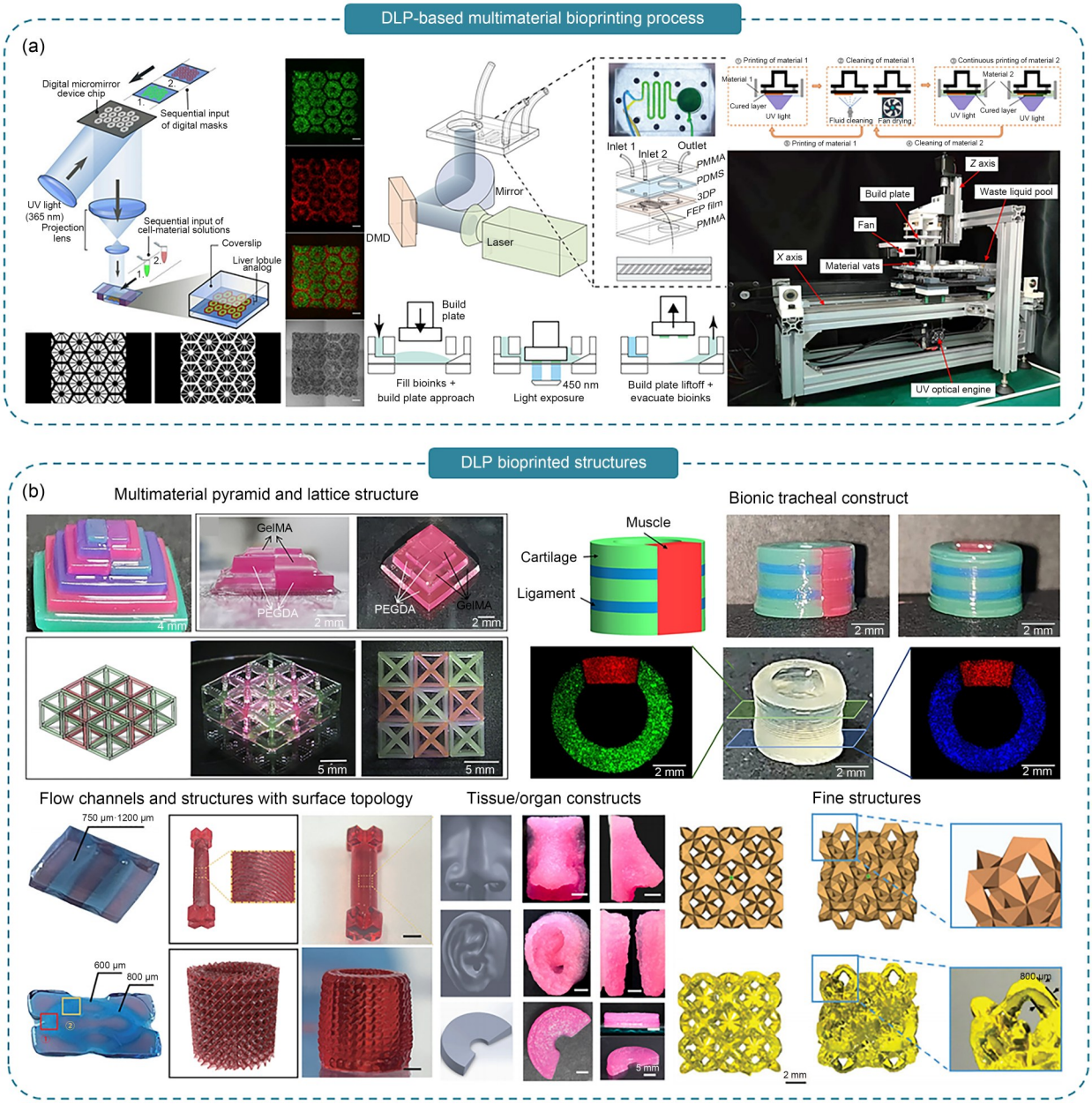

Fig. 12 Digital light processing (DLP)-based multimaterial bioprinting processes and structures: (a) schematics of DLP-based multimaterial bioprinting processes; (b) different structures created by DLP bioprinting. Part (a, left) was reproduced from [89], Copyright 2016, with permission from the National Academy of Sciences. Part (a, middle) was reproduced from [90], Copyright 2021, with permission from Wiley. Part (a, right) and Part (b, upper) were adapted from [91], Copyright 2023, with permission from the Royal Society of Chemistry. Part (b, lower left) was adapted from [92], Copyright 2024, with permission from Wiley. Part (b, lower middle) was adapted from [93], Copyright 2023, with permission from the authors, licensed under CC BY-NC-ND 4.0. Part (b, lower right) was adapted from [94], Copyright 2024, with permission from the authors, licensed under CC BY

tissue, and vascular networks) were replicated. In addition, DLP-based multimaterial bioprinters have been commercialized by companies in China, such as EFL-BP8601 Mix from Yongqinquan Intelligent Equipment Co., Ltd. and Bioarchitecht Parrot from Regenovo Biotechnology Co., Ltd.

5.2.4 Pushing the boundaries of 3D bioprinting windows (provided by the Liliang Ouyang group)

3D bioprinting is very often restricted by the narrow biofabrication windows caused by the complex rheological properties of the ink materials [95]. Recently, researchers have made many efforts to push the boundaries of 3D bioprinting windows to enhance biofabrication capabilities (Fig. 13a). For example, it is usually challenging to print liquid-like ink formulations and supersoft structures using extrusion-based 3D bioprinting, and nonstandard process optimization for individual inks further compromises the reproducibility of the process. To this end, Ouyang et al. proposed a generalizable approach termed the complementary network bioink (CNB) strategy (Fig. 13b), in which a miscible and sacrificial component is incorporated into the crosslinkable matrix component [96]. The sacrificial component, such as biocompatible and thermo-sensitive gelatin, affords the CNB a consistent rheological outcome, which is suitable for extrusion-based 3D bioprinting regardless of the type and concentration of the matrix components. The authors demonstrated the successful generalization of this approach to a library of photocrosslinkable bioinks (i.e., 12 different formulations covering natural or synthetic representatives), thus achieving the standard bioprinting of reproducible 3D structures throughout the library. The great expansion of the matrix concentration and easy removal of the gelatin (i.e., incubation at 37 °C

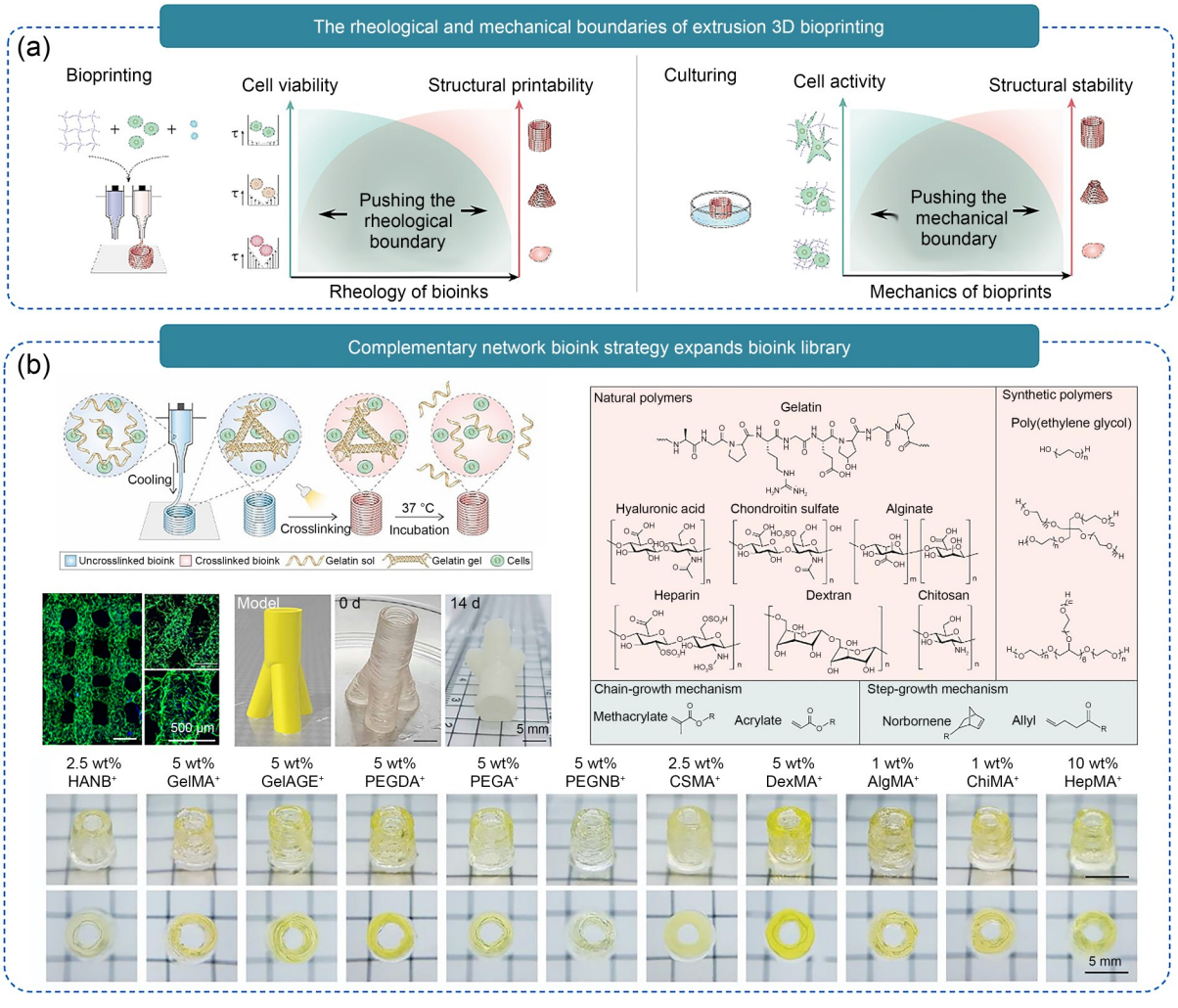

Fig. 13 Pushing the boundaries of 3D bioprinting windows: (a) schematic representation of two typical bioprinting windows regarding the rheology of bioinks and mechanics of imprints during the bioprinting and culturing processes, respectively; (b) the complementary network bioink strategy is generalizable to a library of bioinks with standard printability, thus benefiting the engineering of soft tissues. Part (a) was adapted from [95], Copyright 2022, with permission from Elsevier. Part (b) was adapted from [96], Copyright 2020, with permission from the authors and exclusive licensee American Association for the Advancement of Science

free of intentional washing steps) allow the bioprinting of a supersoft structure (e.g., 2.5% GelMA with Young's modulus of about 1 kPa) that benefits the 3D culture of native cells of soft origin (e.g., brain-derived cells). Similarly, Zhang et al. used hyaluronic acid methacrylate (HAMA) as the complementary sacrificial component in bioinks to expand the biofabrication window of DLP-based bioprinting [97]. The inclusion of well-printed HAMA in the bio-resin allows the high-fidelity printing of various photocrosslinkable hydrogels. The soft-tissue-matching mechanical properties of the bioprinted constructs can be achieved via the selective enzymatic digestion of HAMA.

In addition to pushing the mechanical boundaries toward the unusual softness of bioprinted structures, researchers have renewed the boundaries of other aspects using different approaches. For example, in situ crosslinking on the nozzle site [98] and suspended bioprinting strategies [99] allow the use of low-viscosity bioinks in extrusion-based bioprinting. By thinking outside the box, the granular bioink strategy has been proposed and recently drawn much attention because of its wide applicability to numerous hydrogels [100]. Additional discussion of the expansion of bioprinting windows can be found in a relevant review article [95]. We can envision continuous progress in pushing such boundaries and other methods, such as single-cell resolution bioprinting [101] and high-cell-density bioprinting [102].

5.2.5 3D bioprinting with high cell density (provided by the Yang Wu group)

Natural human tissues possess a high cell density, generally ranging from 1×10^9 to 3×10^9 cells/mL. However, the typical cell density reported in studies of conventional scaffold-based bioprinting is 2 to 3 orders of magnitude lower than that of natural tissues, which limits the maturation of bioprinted tissues because of insufficient chemical and physical communication between cells [103]. To address this limitation, scaffold-free bioprinting has attracted widespread attention in recent years, and several innovative works have been published worldwide [104–108]. Cell aggregates were generated in the form of spheroids, honeycombs, and strands, serving as the building blocks for bioprinting, to construct biomimetic tissues with a high cell density. For example, Zhang et al. reported the mass production of adipose-derived stem cell (ADSC) spheroids using a composite granular hydrogel, which were then used in bioprinting [109]. While ensuring a high cell density, regional cellular heterogeneity, which relies on the precise positioning of cell aggregates, is also important to closely recapitulate the native tissues.

In this regard, the group of Yang Wu has made several innovative contributions to expanding strategies for the scaffold-free biofabrication of cartilage and tendons. Those authors developed a hybrid approach that integrates the extrusion-based and aspiration-assisted bioprinting (AAB) techniques to generate zonally stratified cartilage, thus achieving the construction of a bioprinted cartilage that harmonizes an anatomical similarity with biological functions [110] (Fig. 14a). Furthermore, the AAB technology was used for the positioning of chondrogenic and osteogenic spheroids to build the osteochondral interface (Fig. 14b), at which the two types of spheroids were tightly fused while their respective morphologies were maintained [111]. In addition, a composite tendon construct was developed by integrating the electrohydrodynamic jet 3D printing technique and the fabrication of tissue strands, which exhibited a fibrous arrangement, a high cell density, and an enhanced cell alignment [112] (Fig. 14c). In the presence of cyclic stretching, the expression of tendon-specific proteins and cellular orientation in the tissue strands exhibited significant enhancement. Moreover, to improve the cell viability of scaled-up cell aggregates with diameters over 500 μm, sodium alginate porogens were blended with human ADSCs to generate tissue building blocks with micropores, which were termed porous tissue strands (pTSs) [113]. Compared with their solid counterparts, pTSs enabled the perfusion of oxygen and nutrients to the deeper region, enhanced cellular viability, and promoted tissue maturation for the long term, which represented an alternative solution for vascularization (Fig. 14d).

5.3 Printing method

5.3.1 Volumetric bioprinting (VBP) (provided by the Maobin Xie group)

Layer-by-layer printing (such as extrusion-based printing or DLP printing) techniques show limitations such as a low printing speed and high-concentration bioink, resulting in reduced cell activity. Therefore, the improvement of the printing speed and cytocompatibility represents a challenge. VBP facilitates the rapid photopolymerization of 3D objects at the centimeter scale within tens of seconds by projecting dynamic light patterns throughout the build volume [114]. The current VBP relies on high-energy UV light as the projecting light and high-concentration or high-viscosity bioinks, which may reduce the bioactivity of the embedded cells. To overcome these limitations, the Maobin Xie group developed a green-light-based VBP strategy and system (Fig. 15a) and provided a series of tyrosine-containing protein-based low-concentration bioinks [115, 116] (Fig. 15b). These tyrosine-containing protein-based bioinks are crosslinked by oxidizing tyrosine groups in the presence of a photoinitiator system (i.e., ruthenium/sodium persulfate (Ru/SPS)). In detail, Ru/SPS is activated by irradiation with a green light at a wavelength of 525 nm, whereby the tyrosine moiety is oxidized into tyrosine radicals; subsequently, these radicals form

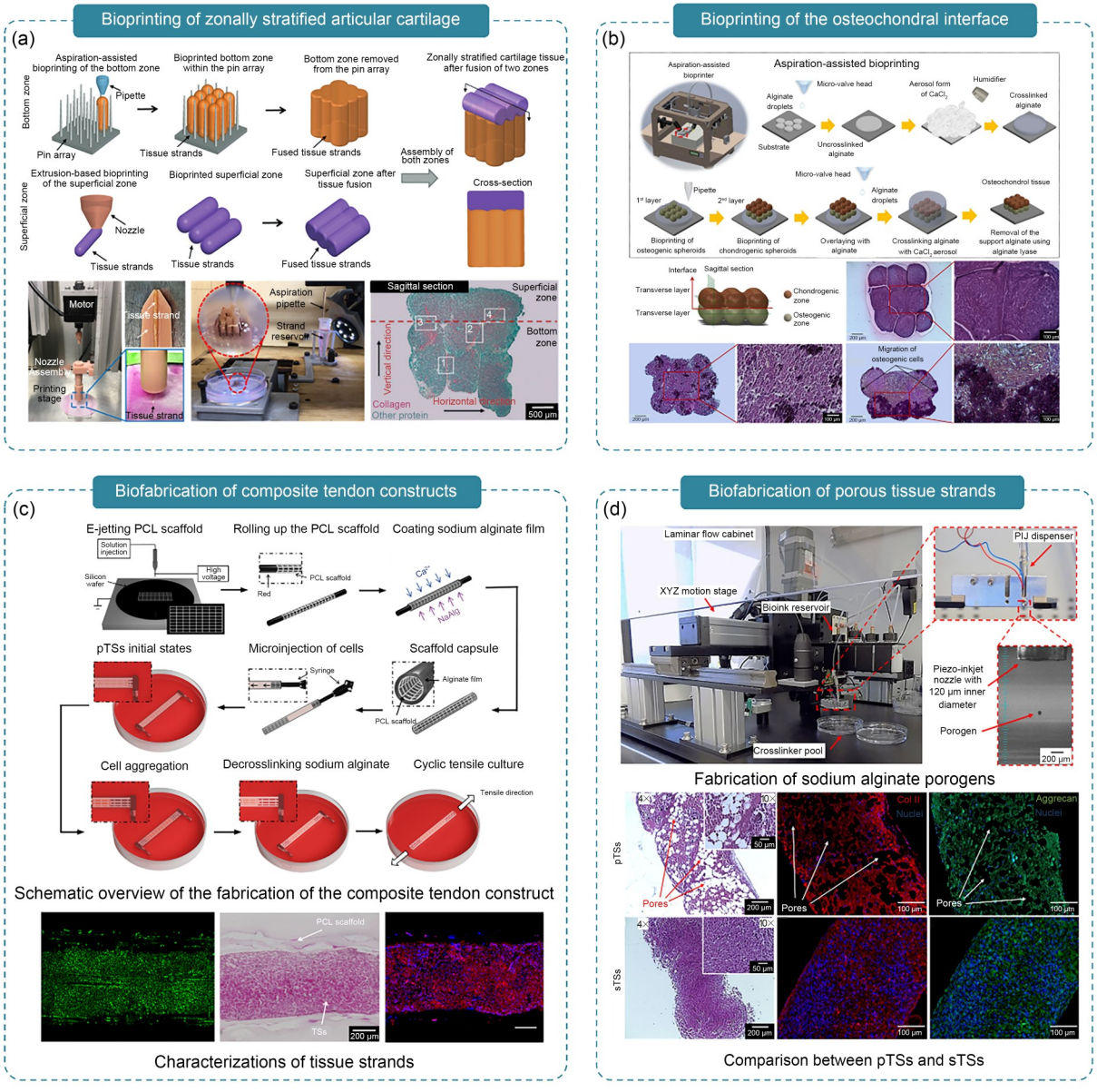

Fig. 14 Bioprinting based on cell aggregates: (a) bioprinting of zonally stratified articular cartilage; (b) bioprinting of the osteochondral interface; (c) biofabrication of composite tendon constructs; (d) biofabrication of porous tissue strands. Part (a) was adapted from [110], Copyright 2020, with permission from Wiley. Part (b) was adapted from [111], Copyright 2020, with permission from the authors, licensed under CC BY 4.0. Part (c) was adapted from [112], Copyright 2023, with permission from the American Chemical Society. Part (d) was adapted from [113], Copyright 2018, with permission from IOP Publishing

covalent di-tyrosine bonds with nearby tyrosine portions (Fig. 15c).

The reconstruction of artificial organs is of paramount importance for human health. However, the rapid construction of artificial organs with physiological dimensions and heterogeneous microenvironments remains a significant challenge. Based on the advantages of non-contact, ultra-fast, and low-concentration printing, the VBP methods have shown significant advantages for the rapid construction of complex bioconstructs. Despite these advantages, VBP currently relies primarily on photopolymerization, which is limited by the penetration depth of the projected light, which is typically less than 3 cm. To fabricate large-scale constructs, there is a need to optimize the bioink compositions and projection algorithms to enhance light penetration. Moreover, exploring alternative energy sources, such as ultrasound, which can penetrate up to 100 times deeper than light, could be a promising approach [117]. Simulating the microenvironment based on the physiological dimensions and structure is also crucial. Human tissues and organs are composed of a complex microenvironment involving multiple cell types and extracellular matrices. The current VBP techniques using

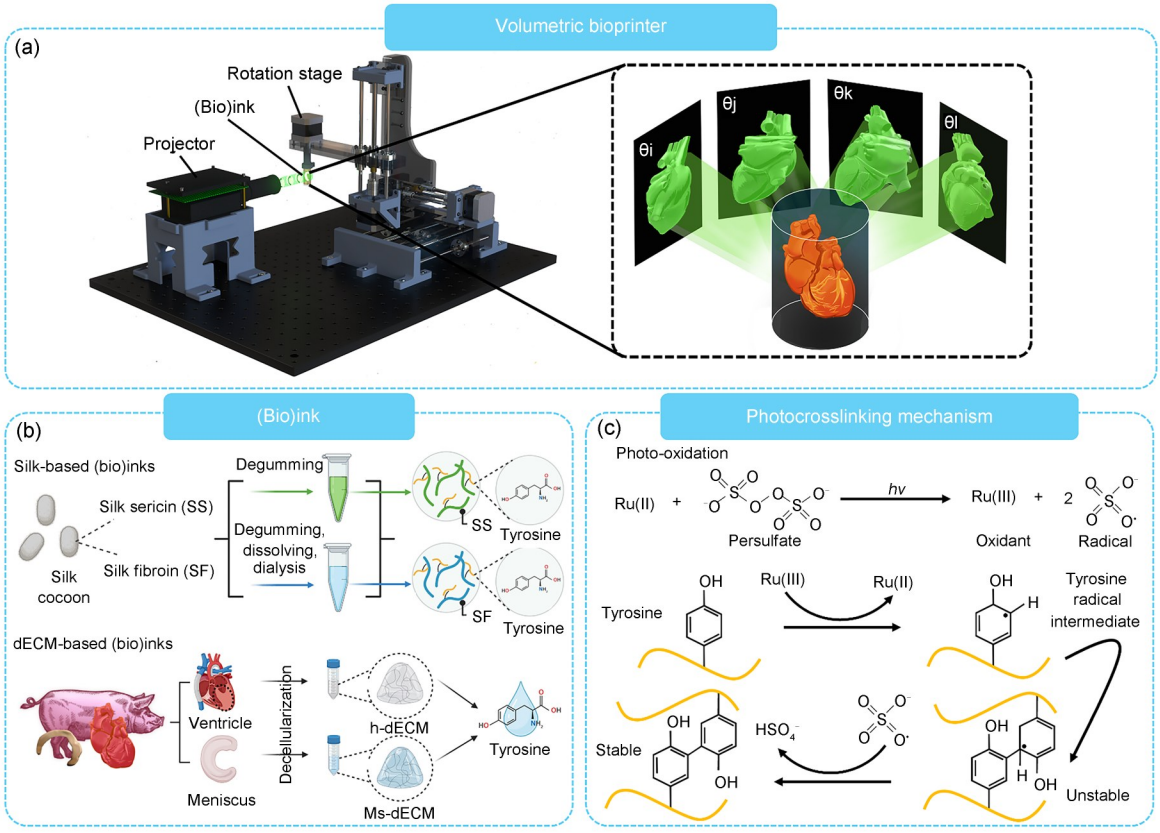

Fig. 15 Volumetric bioprinting (VBP) using silk-based and decellularized extracellular matrix (dECM)-based bioinks: (a) schematic representation showing the VBP setup and printing principle; (b) preparation of silk-based and dECM-based bioinks; (c) photocrosslinking mechanism of tyrosine-containing protein-based bioinks. Part (a) was adapted from [118], Copyright 2024, with permission from Wiley. Part (b, upper) was adapted from [115], Copyright 2023, with permission from the authors, licensed under CC BY 4.0. Part (b, lower) was adapted from [118], Copyright 2024, with permission from Wiley

single-material or single-cell bioinks are not well suited to the replication of these intricate microenvironments. Therefore, the development of multimaterial and multicellular VBP is essential for accurately simulating the complex microenvironment of artificial organs. It is anticipated that VBP will become a key technology in the future for the fast fabrication of tissue structures with physiological anatomical features and specific functions, which renders it a hot topic in the field of tissue engineering and regenerative medicine.

5.3.2 Micro-/nano-scale 3D bioprinting (provided by the Jiankang He group)

Micro-/nano-scale 3D bioprinting can precisely control the spatial arrangement of biomaterials and cells at the micronanometer scale, thus showing great potential for the regulation of cell behavior and tissue regeneration. Electrohydrodynamic (EHD) bioprinting has gradually developed into a promising micro-/nano-scale 3D bioprinting technology. However, EHD bioprinting faces challenges regarding the fabrication of tiny architectures, large-height structures, high-fiber-density architectures, and cell–hydrogel composite constructs. To address these challenges, the group of Jiankang He at Xi'an Jiaotong University developed an EHD bioprinting strategy (Fig. 16a) using a biopolymer solution to fabricate submicroscale ((193±51) nm) biopolymer fibers that mimic the tiny architectures of the native ECM, thus enhancing cell adhesion, proliferation, and orientation [119]. Furthermore, by maintaining a constant electric field strength and in situ charge neutralization during EHD bioprinting, they successfully achieved, for the first time, the EHD bioprinting of microfibrous structures with centimeter-scale heights ((10.01± 0.18) mm), thereby providing topographical contact cues for 3D large-area cellular arrangements [120] (Fig. 16b). The embedding of the cell–hydrogel mixture into EHD-bioprinted 3D microlattices can guide various tissues, such as cardiac and skeletal muscles, to form 3D densely populated and highly aligned cell bands with layer-specific orientations [121, 122]. To address the challenge of manufacturing high-fiber-density architectures using EHD printing, the authors studied the effects of fiber diameter and spacing. They found that a uniform fiber arrangement can be achieved when the fiber spacing is five times the fiber diameter [123] (Fig. 16c).

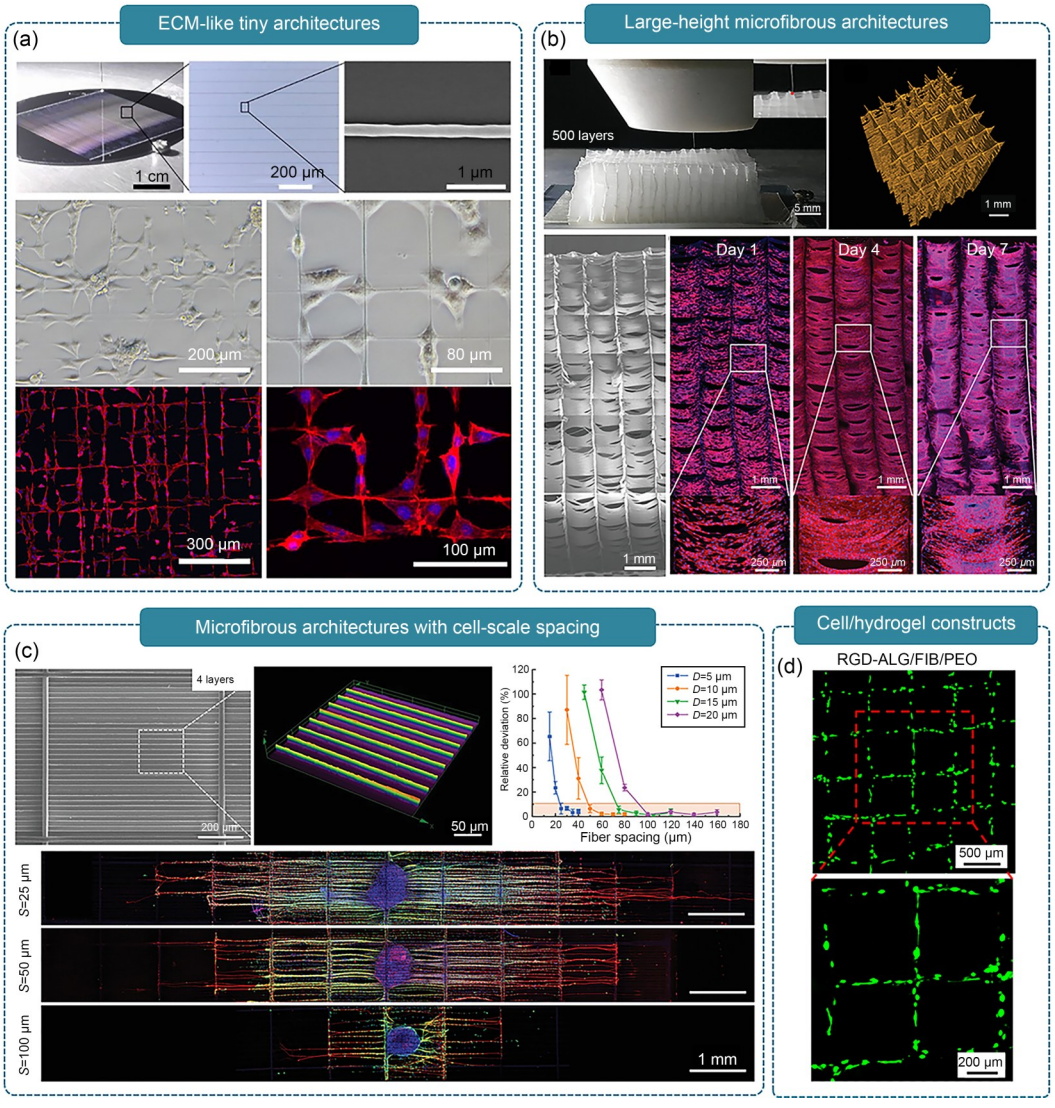

Fig. 16 Micro-/nano-scale 3D bioprinting technology: (a) electrohydrodynamic (EHD)-bioprinted extracellular matrix (ECM)-like tiny architectures; (b) EHD-bioprinted microfibrous architectures with a centimeter-scale height; (c) EHD-bioprinted microfibrous architectures with cell-scale spacing; (d) EHD-bioprinted cell/hydrogel constructs. Part (a) was reproduced from [119], Copyright 2019, with permission from Taylor & Francis. Part (b) was reproduced from [120], Copyright 2021, with permission from Wiley. Part (c) was reproduced from [123], Copyright 2023, with permission from Wiley. Part (d) was reproduced from [124], Copyright 2022, with permission from Zhejiang University Press

Based on this finding, they controllably fabricated microfibrous architectures with a fiber diameter of about 5 μm and a fiber spacing of about 25 μm. Furthermore, they discovered that the reduction of the fiber spacing from 100 to 25 μm allowed the formation of microfibrous architectures with cell-scale spacing to promote the directional growth of neurites and increase the migration speed and density of Schwann cells, thus providing a new method for repairing peripheral nerve injuries. Moreover, they established an electrostatic field force-driven cell-printing strategy to achieve the high-precision EHD bioprinting of 3D cell/hydrogel constructs with a minimum printed fiber size of (25.6±2.5) μm and cell viability of over 90% [124]. The addition of conductive polymer materials to the cell/hydrogel mixtures enabled the formation of EHD-bioprinted constructs with a minimum feature size of (48.91±3.44) μm, thereby offering a promising approach for creating electro-conductive and cell-laden constructs for electroactive tissue engineering (Fig. 16d).

5.3.3 Embedded bioprinting (provided by the Hongzhao Zhou group)

Embedded bioprinting is a technique that utilizes a yield-stress fluid supporting matrix to stabilize structures during the printing process, thus enabling the creation of intricate and multilayered tissues that closely resemble the complex architecture found in natural tissues and organs. This technique addresses a key issue in conventional extrusion-based

bioprinting, i.e., the maintenance of a balance between the printability of materials and their compatibility with biological systems. Nevertheless, embedded bioprinting has its challenges, including a limited printing window, compatibility concerns between support mediums, bioinks, and crosslinkers, and difficulties in the removal of the support matrix after printing. Furthermore, the inherent inertia of the support matrix often necessitates a compromise between the structural integrity and the precision of the printed tissues, particularly when employing multiple nozzles for varied structures.

The group of Dr. Hongzhao Zhou has improved embedded bioprinting by creating an adaptable embedding medium that accommodates various bioinks and crosslinking techniques (Fig. 17a). Their composite gel, which is composed of hydrophobically modified hydroxypropylmethyl cellulose and Pluronic F-127, permits the simultaneous patterning of multiple bioinks with distinct crosslinkers [125, 126]. This flexibility is key for constructing diverse tissues, which is essential for tissue regeneration. By tailoring the rheological properties of the matrix, Dr. Zhou's team provided a systematic approach to aligning the bioinks with the support bath, thus enabling the printing of low-viscosity bioinks into fine 3D structures. They have also introduced an innovative multimaterial printing method that allows the high-fidelity creation of layered structures with strong interlayer connections by utilizing multiple independently controlled nozzles to deposit different biomaterials into the same area, which minimizes the unwanted spreading and contamination of the embedding medium within the printed structure [127]. Through the quantitative analysis of the behavior of the bioink and the effects of the printing parameters on the 3D filament shapes, this multimaterial approach promises advancements in personalized medicine.

Dr. Yang Wu and his team have also made significant strides toward optimizing embedded bioprinting for complex tissue assembly (Fig. 17b). They have introduced a novel support bath that can be crosslinked with a bioink via the Schiff base reaction, which is known for its precise and efficient bonding [110, 128, 129]. They further developed a numerical model to evaluate the extrusion process and support bath dynamics, thus establishing essential parameters for consistent fiber formation and structural integrity. This led to the creation of a zonally stratified artificial cartilage with a complex three-layer structure that promoted cellular integration, proliferation, and characteristic protein presence. The work of Dr. Wu's team represents progress in embedded bioprinting by providing a detailed operational framework and achieving a biologically relevant articular cartilage construct, thereby marking an important step toward the generation of clinically applicable bioprinted tissues.

Prof. Zhuo Xiong's team has expanded the horizons of 3D bioprinting to produce complex tissues that replicate the structure and function of natural tissues (Fig. 17c). They introduced a granular aggregate-prevascularized bioink for engineering vascularized bone tissue, which capitalizes on the self-organizing nature of mesenchymal spheroids [130]. This bioink enables the printing of highly viable structures with dense cell populations, leading to the postprinting formation of an interconnected vascular network. Its potential for creating patient-specific vascularized tissues is further enhanced by its osteogenic and angiogenic properties. Moreover, the team of Prof. Xiong developed a sequential printing in a reversible ink template (SPIRIT) strategy using a microgel-based biphasic bioink that was conducive to cell encapsulation and embedded printing [131]. This method has been successfully applied to the bioprinting of cardiac tissues with significant cellular proliferation and differentiation, including a model ventricle with a perfusable vascular network, thus demonstrating the potential to produce complex organ geometries for therapeutic use. Prof. Xiong's work underscores the synergy between innovative bioinks and strategic printing methods for creating vascularized, functional tissues.

5.3.4 Extrusion-based gradient 3D printing (provided by the Changshun Ruan group)

Extrusion 3D printing is one of the most widely used additive manufacturing technologies, and it has been employed in a variety of industries, including tissue engineering [132], flexible electronics [133], robotics [134], time-driven devices [135], etc. [136, 137]. The layer-by-layer stacking of filaments along the longitudinal direction affords extrusion 3D printing the advantages of simplicity, efficiency, and low cost. However, the conventional filament crossing angles (e.g., 0°/90°) and constant filament diameters limit the ability of extrusion 3D printing to produce samples with internal complex gradient porous structures. To address this challenge, the group of Changshun Ruan has established new strategies for fractal-design-based filament-filled patterning [138] and filament-diameter-adjustable 3D printing (FDA 3D printing, FDA-3D printing, or FDA-3DP) [139]. Specifically, as demonstrated in Figs. 18a–18h (Strategy 1), inspired by the Koch snowflake fractal iteration, they designed a new filament-filled patterning (print trajectories) that can be used for the extrusion 3D printing of radial-gradient porous scaffolds [138]. To promote the printability and stability of the designed model, the authors developed a new format of fractal and circular layer-by-layer stacking, with the results showing that the fractal design strategy accomplished the construction of radial-gradient porous samples; this design is expected to be applied to bone tissue engineering in the future. Conversely, as shown in Figs. 18i–18o (Strategy 2), based on the volume conservation law and the working principle of conventional extrusion 3D printing, they developed a new strategy, i.e., the FDA 3D printing,

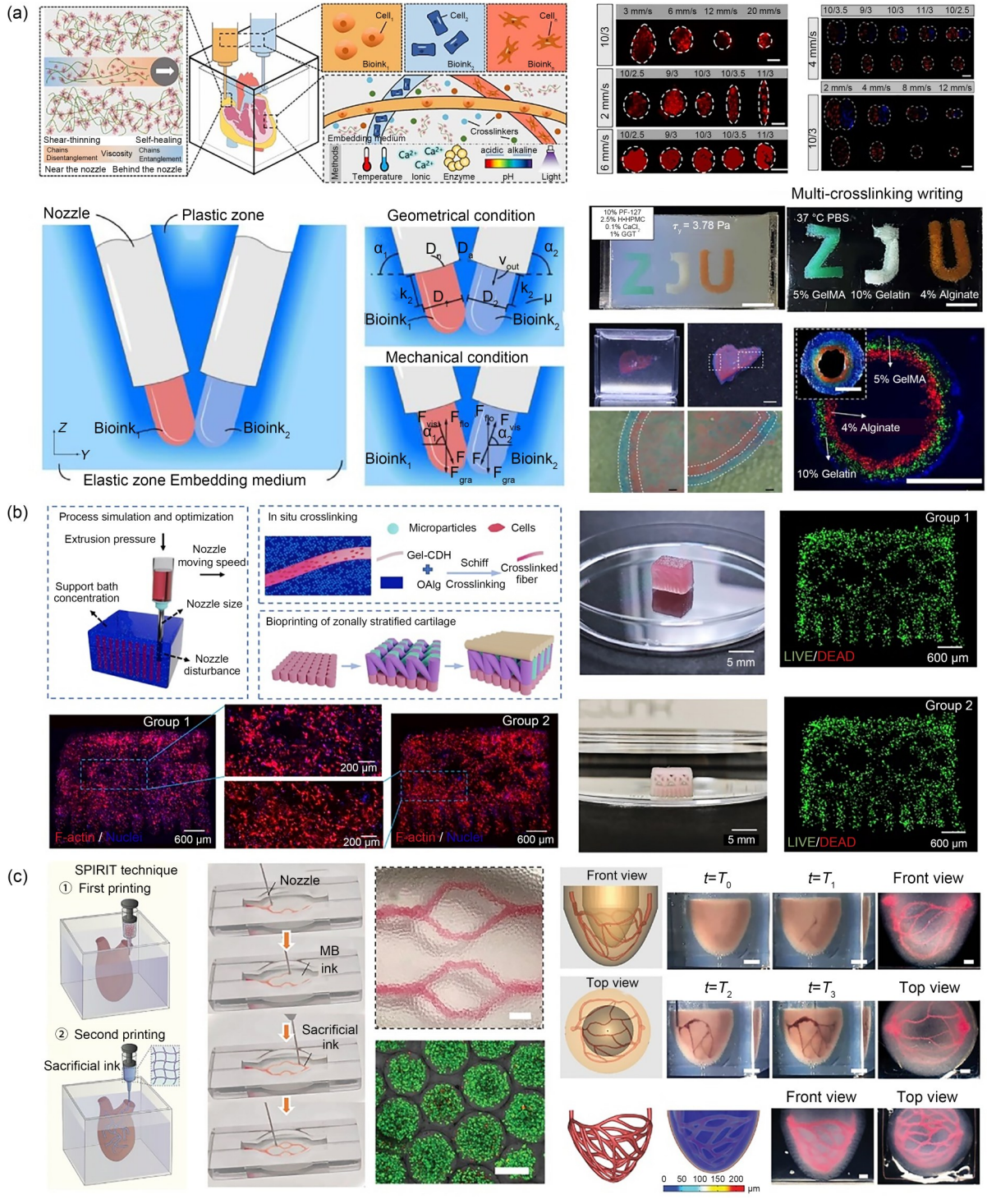

Fig. 17 Embedded bioprinting in the yield-stress fluid supporting matrix. (a) Embedded medium designed for a variety of bioinks with different crosslinking methods. Using this embedded medium, a simultaneous printing method was developed for multimaterial printing. (b) Schematic diagram of the embedded bioprinting method for complex tissue assembly. Using this method, a zonally stratified artificial cartilage was manufactured that promoted cellular integration, proliferation, and characteristic protein presence. (c) The sequential printing in a reversible ink template (SPIRIT) strategy enables the fabrication of tissue and organ constructs via the sequential printing of a microgel-based biphasic (MB) bioink and a sacrificial bioink. A perfusable sacrificial channel and ventricular constructs were fabricated using this technique. Part (a, upper left) and Part (a, lower right) were adapted from [126], Copyright 2022, with permission from IOP Publishing. Part (a, upper right) was adapted from [125], Copyright 2022, with permission from the American Chemical Society. Part (a, lower left) was adapted from [127], Copyright 2023, with permission from the authors, licensed under CC BY 4.0. Part (b) was adapted from [129], Copyright 2024, with permission from the authors, licensed under CC BY 4.0. Part (c) was adapted from [131], Copyright 2023, with permission from Wiley

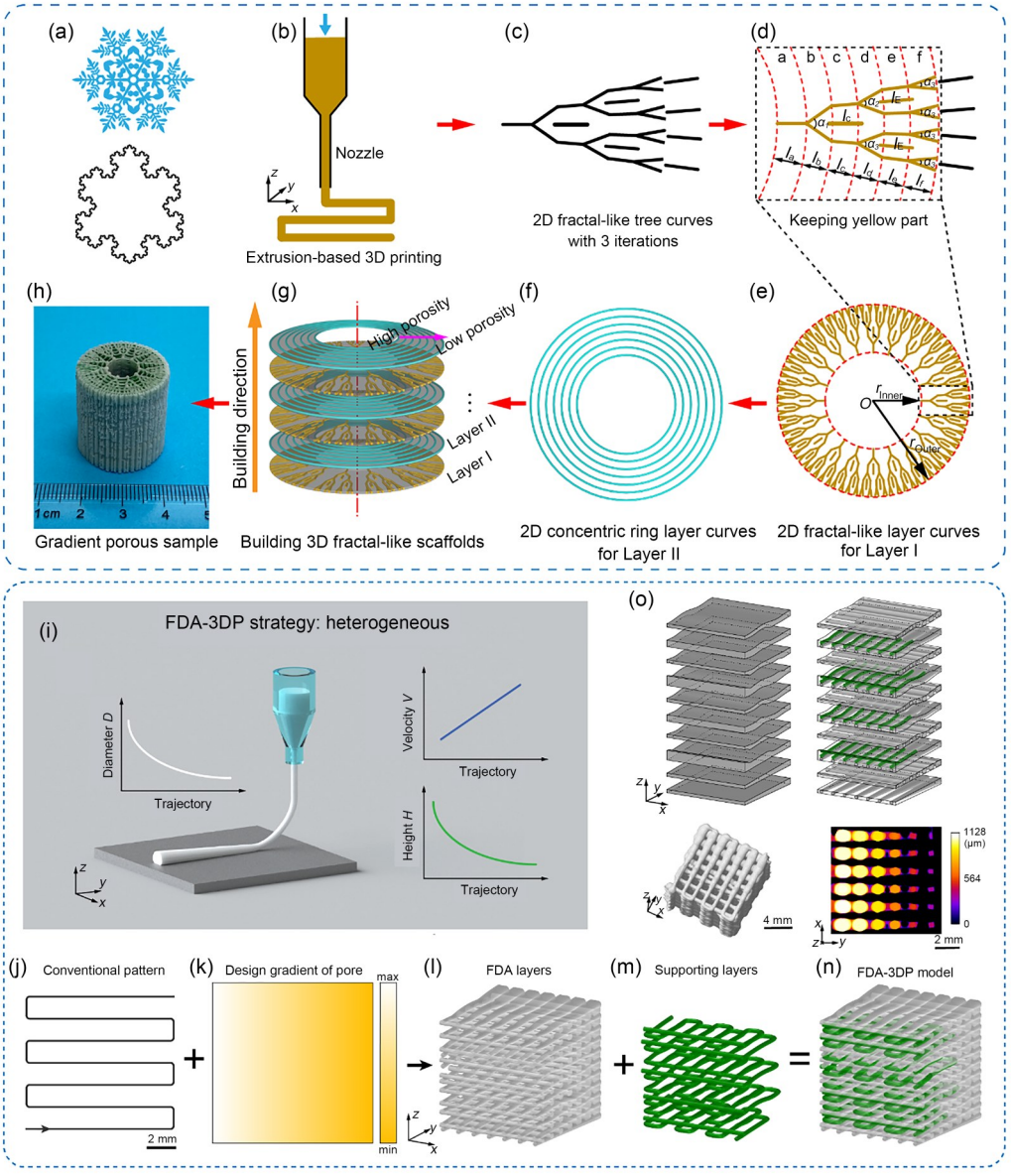

Fig. 18 Extrusion 3D printing of gradient porous structures via fractal-design-based filament-filled patterning: (a) snowflake digital modeling and fractal-based Koch snowflakes; (b) extrusion 3D printing; (c) fractal-like print trajectories inspired by Koch snowflakes; (d) a fractal-like cell on a circular array; (e) fractal layer; (f) circular layers; (g) schematic diagram of the layer-by-layer stacking of fractal and circular layers; (h) radial-gradient porous sample with fractal and circular layers fabricated by extrusion 3D printing; (i) schematic representation of filament-diameter-adjustable (FDA) 3D printing with variable filament diameters by tailoring the print velocity and print height; (j–n) parametric design for the FDA 3D printing of horizontal gradient porous samples; (o) unconventional slices for FDA 3D printing and the horizontal gradient pore size distribution of the fabricated sample. Parts (a–h) were adapted from [138], Copyright 2021, with permission from the authors and exclusive licensee Science and Technology Review Publishing House. Parts (i–o) were adapted from [139], Copyright 2024, with permission from the authors, licensed under CC BY 4.0

which can accomplish the extrusion 3D printing of complex gradient porous structures in response to the desired pore size. The FDA 3D printing strategy controls the diameter (i.e., ink volume) and state (to avoid line discontinuities and rope-winding effects) of the deposited filaments by customizing the print velocity and print height, respectively. Excitingly, the FDA 3D printing results illustrate its promise for applications in fields such as embedded alphabet structures, mechanical meta-structures, tissue engineering (bone, meniscus, and blood vessels), flexible electronics, and four-dimensional (4D) printing. In summary, Huawei Qu et al. revolutionized the filament-filling mode in extrusion 3D printing via fractal design [138] and FDA 3D printing [139] strategies. This breaks through the dilemma that extrusion printing is usually considered to be able to process homogeneous porous structures exclusively.

5.3.5 Piezoelectric material printing (provided by the Cijun Shuai group)

The electrical microenvironment is an important composition in human tissues that plays an important role in promoting cell growth and tissue function reconstruction. Piezoelectric materials can generate electrical signals in response to a microdeformation of the body without the use of an external power supply and wires, and directly build a bionic electrical microenvironment to induce cell growth. In recent years, the introduction of piezoelectric ceramic nanoparticles into piezoelectric polymer implants to reconstruct the electrical microenvironment has attracted great attention [140, 141]; however, the great difference in the dielectric constant between ceramics and polymers hampers polarization. To this end, the team of Cijun Shuai used ion chelation and an in situ growth technology to grow nano-silver on barium titanate piezoelectric nanoparticles, and synthesized a silver–barium titanate nanosystem with a strawberry-like structure to enhance the piezoelectric activity of the implants [142]. In vitro cell culture confirmed that the enhanced piezoelectric activity promoted cell proliferation and differentiation. In addition to bioelectric effects, human tissues are affected by biomagnetic effects. Based on this observation, the team introduced magnetic nanoparticles into implants, with the aim of building biomimetic magnetic microenvironments that speed up tissue regeneration via the magnetic stimulation effect [143]. However, the random arrangement of the nanoparticles easily leads to the mutual consumption of magnetic poles between the different particles, thereby weakening the therapeutic effect of the implant.

To address this challenge, the authors constructed magnetic nanochains via the magnetic-field-guided interface coassembly of nanoparticles (Fig. 19a), and then introduced them into the implant [144]. The magnetic energy coupling between the nanoparticles in the nanochains significantly enhanced the magnetic stimulation effect of the implant on the surrounding cells and tissues, thereby improving cell activity and promoting cell proliferation and mineralization. Considering that human tissues are affected by both the bioelectrical and magnetic microenvironments, this team further constructed a biomimetic microenvironment with dual electrical and magnetic stimulation in the implant based on the electromagnetic induction effect [145, 146]. Specifically, nano-conductive materials (MXene) were used to coat the polymer particle surface via an ultrasonic-assisted solution mixing process (Fig. 19b). Under the near-zero shear action of laser 3D printing, the MXene was driven by the surface tension of the molten polymer and distributed in the interfacial regions among adjacent polymer particles, finally forming an interconnected conductive network in the implant. In this case, the implant was used as a coil to cut the magnetic induction line and generate a spontaneous current under an alternating magnetic field, thus forming an electric and magnetic dual-stimulation microenvironment. The results of this approach showed that the dual stimulation was superior to the single electrical or magnetic stimulation for enhancing cell proliferation and differentiation. Mechanically, the continuous electrical and/or magnetic signals acting on cells are transformed into internal biochemical signals via the mechanical transduction effect, which activates cell membrane surface receptors, regulates calcium ion channels and signaling

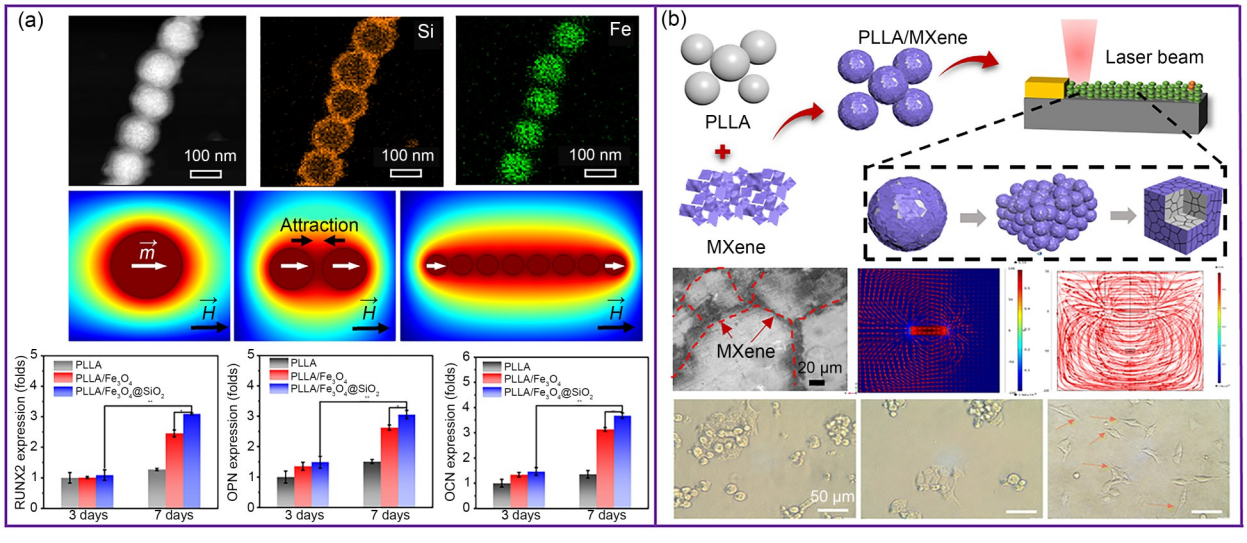

Fig. 19 Construction of a biomimetic electromagnetic microenvironment: (a) structure of the magnetic nanochains and their effects on cell activity and differentiation in the implants; (b) synthesis, 3D printing, conductive network, and electromagnetic effects on nerve cells. Part (a) was adapted from [144], Copyright 2022, with permission from the authors, licensed under CC BY 4.0. Part (b, upper) was reproduced from [145], Copyright 2022, with permission from Elsevier. Part (b, lower) was adapted from [146], Copyright 2023, with permission from the Royal Society of Chemistry and the Chinese Chemical Society

pathways, and upregulates the expression of related genes, thereby enhancing cell activity and promoting cell growth and proliferation.

5.3.6 Bioprinting in space (provided by the Zhuo Xiong group)

With the rapid advancements in manned spaceflight, humanity is witnessing a renaissance of space exploration. Compared with the use of microgravity-simulation equipment, such as the random positioning machine and rotating wall vessel used for research [147], or the two-dimensional (2D) cell culture performed at space stations [148], bioprinting in space presents a revolutionary improvement. It offers a more accurate reflection of the impact of complex spatial environments on organisms and enables the construction of 3D heterogeneous structures with enhanced biomimicry [149]. In recent years, the International Space Station has become a pivotal platform for groundbreaking studies of 3D bioprinting. In 2020, the group of Vladislav A. Parfenov from Russia developed a magnetic levitation assembly technology to construct 3D cartilage spheroids (Fig. 20a), demonstrating the potential of 3D bioprinting in space, despite the challenges in the fabrication of complex structures [150]. Moreover, the 3D biofabrication facility (BFF) developed by Techshot from the US created complex heart structures that incorporated multiple cell types using a multinozzle bioprinter [5]. In 2024, the group of Nathanael Warth from Germany developed a compact in situ bioprinter that was capable of printing biological patches directly onto the skin for tissue repair, demonstrating good cell proliferation, albeit with limited cell spreading; this indicated the potential for on-orbit medical treatments [151]. In 2023, the Zhuo Xiong group developed a satellite-based 3D bioprinting device and embedded the bioprinting technology to construct 3D tumor models in space and conduct drug-sensitivity tests. Their research showed that microgravity enhanced the structural fidelity of the models and increased the drug sensitivity of the tumor cells, thus offering new avenues for cancer treatment [152] (Fig. 20b).

Space bioprinting technology holds immense potential for advancing space physiology and biomedical research, as well as providing crucial and timely support to on-orbit personnel. However, research in the field of space bioprinting remains in its nascent stages, with the following significant challenges.

5.3.6.1 Exploring space bioprinting technologies

The unique microgravity conditions of space significantly alter the behavior of bioinks compared with conventional environments [153]. In this regard, comprehensive studies using numerical simulations and microgravity-simulation equipment are essential [154]. These studies aim to build theoretical models for space bioprinting, develop suitable bioprinting techniques, and optimize bioink properties (such as rheological behavior and gelation) [155], thus enhancing the quality and reliability of bioprinting in space.

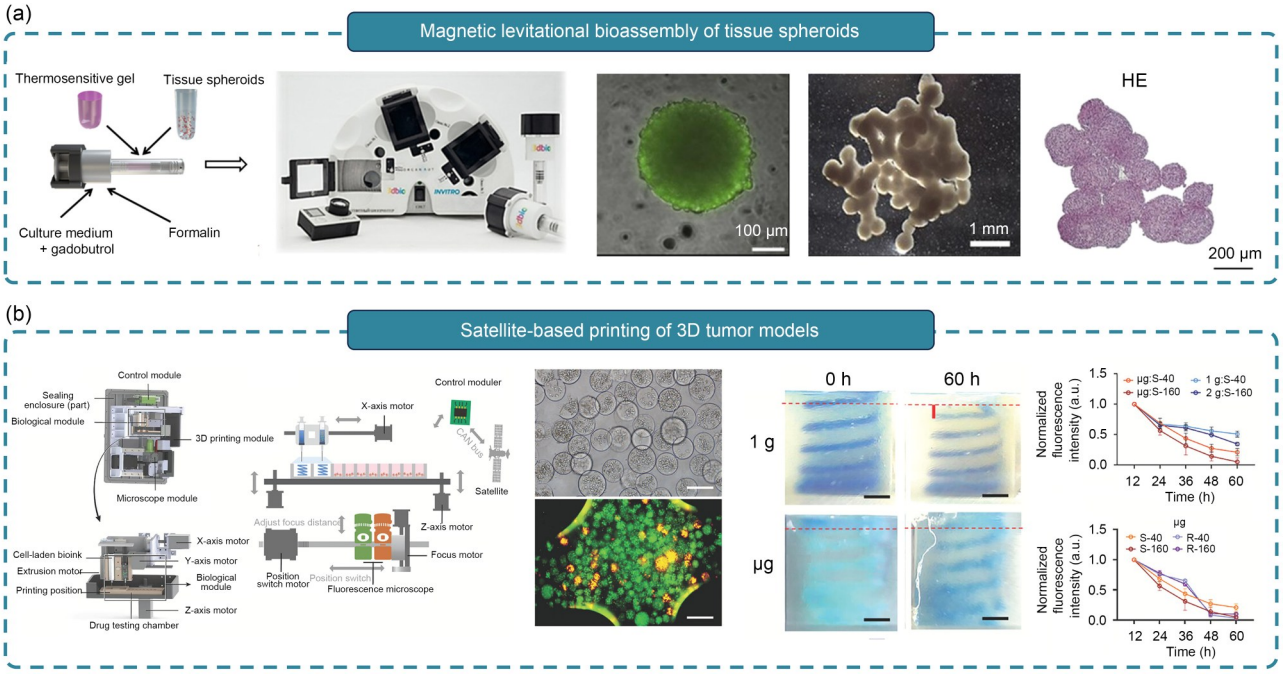

Fig. 20 Bioprinting in space: (a) magnetic levitational disassembly of tissue spheroids consisting of human chondrocytes; (b) manufacturing of 3D tumor models for drug-sensitivity research. Part (a) was adapted from [150], Copyright 2020, with permission from the authors and exclusive licensee American Association for the Advancement of Science. Part (b) was adapted from [152], Copyright 2023, with permission from Wiley

5.3.6.2 Development of 3D bioprinting devices

The constraints of space environments, such as those found aboard space stations or satellites, impose strict requirements on the size, weight, and energy consumption of bioprinting devices. The limited possibility for manual intervention in space also necessitates a higher degree of automation and intelligence of these devices. Moreover, integrating functionalities such as cultivation, observation, and analysis into the bioprinting devices is critical for the long-term cultivation, tissue functionalization, and real-time characterization of bioprinted structures [156]. Thus, the development of automated, compact, and intelligent bioprinting devices is crucial for advancing research on bioprinting in space. Overcoming these challenges will facilitate the establishment of 3D bioprinting as a crucial tool for space science research, thereby significantly enhancing the capabilities in space biopathology, drug development, and on-orbit tissue regeneration and repair.

5.3.7 Organ-on-a-chip (provided by the Liang Ma and Jing Nie groups)

By integrating basic living units, such as cells/organoids, and their corresponding controllable microenvironment onto microfluidic chips, the organ-on-a-chip (OOC) technique can reproduce the specific structure and function of human tissues/organs on physically microscale chips, which can be applied to the in vitro research of physiology/pathology/pharmacology/cancer, drug development, regenerative medicine, etc., thereby providing a basic tool and platform for biomedical-related research by reducing the number of animal experiments, potentially being a "sharp knife technology" that subverts the process of precision medicine [157]. However, OOC encounters three significant limitations that are inherent to traditional processes. First, the limited material options impede the formation of biomimetic geometries and the growth of internal cells/organoids. Second, the restricted processing precision and complexity of low-strength bio-hydrogels, which are characterized by their softness and brittleness, lead to poor mechanical properties, which can easily damage the hydrogel structure during demolding. In addition, their high water content and wet–soft interface hinder their compatibility with conventional microfluidic chip bonding processes, thus worsening the manufacturing difficulties. Third, the lack of effective cell-manipulation methods prevents the direct manipulation and directional deposition of cells within closed channels.

To address these challenges, the team of Jing Nie focused on the controllable manufacturing of OOC by specifically targeting the key scientific issues involved in this process (i.e., OOC substrate for simulating the ECM microenvironment, multiscale channel manufacturing process for biomimicking tubular organ structure, and cell manipulation and deposition method for the precise regulation of cell distribution). The authors proposed the concept of a hydrogel-based OOC that breaks through the bottleneck that the current OOC substrate cannot fully simulate the in vivo microenvironment required for cell growth, thus endowing OOC with a broader definition based on the aspects of form and function, while opening up a broader research direction for OOC [158]. They developed a new method for the fabrication of hydrogel chips based on the principle of twice crosslinking, which can realize the reliable encapsulation and high-fidelity structure of the hydrogel channels, thus solving the problem of incompatibility between the new material and the traditional process and laying the processing foundation for hydrogel-based OOC [159]. These researchers proposed a new idea of damage-free demolding based on a flexible wireframe template, which greatly decreases the demolding force by shifting from 2D surface-contacting to zero-dimensional point-contacting. Moreover, it overcomes the difficulty of manufacturing a complicated and fine-channel network on a kPa-level, low-strength bio-hydrogel. They developed a high-precision multiscale 3D printing process that is approved for the personalized manufacturing of flexible wireframe templates and the precise processing of corresponding micro-nano structures on a low-strength hydrogel, thereby laying the technical foundation for the creation of a biomimicking structure on a hydrogel-based OOC [160]. They proposed a cell-preloading seeding technique based on a sacrifice template, which is different from the traditional idea of injecting cells into a preformed channel, thereby avoiding difficult cell manipulations within a closed channel. This provides an effective solution for controllable cell deposition in OOC, solves the issue of directional cell manipulation during OOC manufacturing, and realizes biomimicking and precise cell distribution within a hydrogel channel [161]. The authors reported a multiscale vascular-on-a-chip that can simulate an artery–capillary–vein structure for the first time, and further realized the efficient modeling of vascular diseases, such as stenosis and atherosclerosis, as well as the tumor–vascular interaction, thereby paving the way for the study of the physiological/pathological process of vascularization and the mechanism of tumor angiogenesis. In conclusion, these works bridge the gap between the manufacturing and application of OOCs, improve the quality and performance of OOCs, and pave the way for the transformation from a microfluidic mechanical model into a living tubular system (Figs. 21a–21f).

The OOC technology is increasingly focused on creating 3D tissue structures, and bioprinting has proven to be a promising tool for this purpose [163, 164]. For instance, Liang Ma's team used a hyaluronic-acid-based cell-laden bioprinted scaffold to mimic the brain microenvironment, thus providing an accurate experimental model to explore the mechanisms

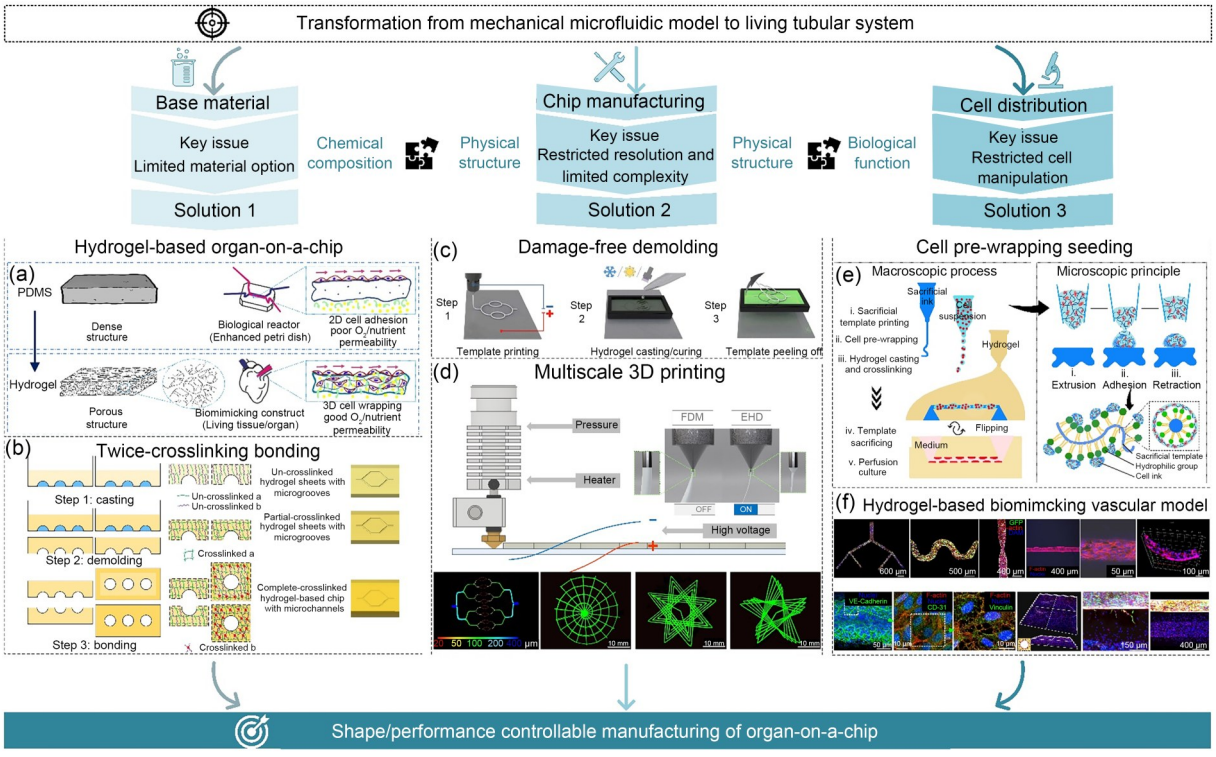

Fig. 21 Construction of a hydrogel-based organ-on-a-chip: (a) proposal of a hydrogel-based organ-on-a-chip concept; (b) schematic diagram of the fabrication process of the hydrogel-based chips based on the twice-crosslinking strategy; (c) micro/nanofabrication of brittle hydrogels based on damage-free demolding using a 3D-printed soft fiber template; (d) schematic diagram of multiscale 3D printing and display of channel patterns; (e) schematic diagram of the cell pre-wrapping seeding technique used for the hydrogel-based tubular organ-on-a-chip; (f) display of the hydrogel-based biomimicking vascular models. Part (b) was reproduced from [159], Copyright 2018, with permission from Wiley. Part (c) was reproduced from [162], Copyright 2020, with permission from IOP Publishing. Part (d, first, second, and third panels) and Part (f, first, third, and fourth panels) were reproduced from [160], Copyright 2020, with permission from the Royal Society of Chemistry. Part (e) and Part (f, second panel) were reproduced from [161], Copyright 2024, with permission from the authors, licensed under CC BY

of glioblastoma (Fig. 22a) [165, 166]. The successful integration of 3D tissues into OOC platforms reported by various research teams has yielded promising results. Bioprinting techniques offer a particularly powerful approach for constructing these structures. Sacrificial extrusion bioprinting, for example, allows researchers to create vascularized OOC models. The team of Liang Ma has extensively investigated the vascularization of OOCs using bioprinting and other biofabrication techniques, focusing mainly on the liver and brain tissues, which are among the most complex tissues in the human body (Fig. 22b) [167 – 169]. Beyond the vasculature, bioprinting can generate even more complex structures. Microfluidic-based gradient bioprinting, which was also studied by his team, holds immense potential for recreating the heterogeneous composition of real tissues. The team has developed a new micromixing technology that enables precise control over biomaterial gradients, thereby opening new avenues for creating gradient bioprinted tissues-on-a-chip (Fig. 22c) [170]. In addition to biofabrication methods, disassembly methods can be used to generate 3D heterogeneous tissue structures, such as spheroids or more complex organoid structures, within the OOC platform. The combination of organoid bioprinting and organ-on-a-chip technologies holds particular promise for creating tissues with complex vascularization and structures that mirror the intricate architecture of real organs. This synergy is a growing area of research.

One of the major current obstacles of the OOC technology is the lack of a functional vascular system. A biomimetic design and dynamic control are crucial for achieving this goal. The key challenges involve the construction of multiscale vascular networks within hydrogels and the regulation of their growth over time. Hydrogel biomaterials and 3D bioprinting offer promising solutions by enabling precise spatial control and dynamic microenvironment cues. Future OOC models will integrate engineered vascular networks with perfusable channels and spatiotemporal control of cellular behaviors to realize living, multiscale vascular systems.

The ideal OOC model necessitates precise control over the cells, matrices, and microenvironments. The traditional OOC construction often lacks cellular specificity resolution because of limitations in cell manipulation. Although 3D bioprinting provides a solution for precise cell deposition, it is hindered by the enclosed nature of conventional OOCs.

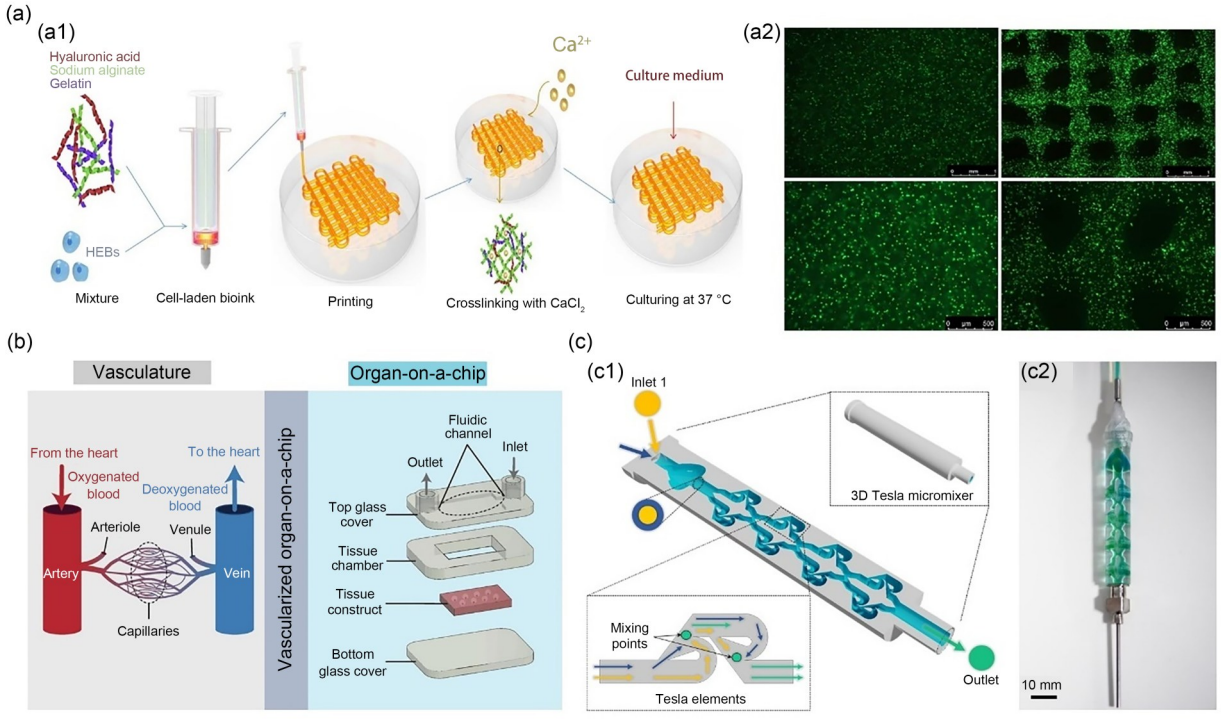

Fig. 22 Three-dimensional bioprinting of an organ-on-a-chip. (a1) Schematic diagram of the 3D cell-laden scaffold printing process; (a2) live/dead staining of HEBs at Day 1 after printing in a monolayered solid membrane and multilayered grid model (scale bar: 1 mm (upper) and 500 μm (lower)). (b) Main elements of the vasculature and the organ-on-a-chip, and their intersection on a vascularized organ-on-a-chip. (c1) Overview of the 3D Tesla micromixer design and operational flow dynamics [170]; (c2) real-world implementation of the micromixer with a nozzle. Part (a) was reproduced from [166], Copyright 2020, with permission from Zhejiang University Press. Part (b) was reproduced from [169], Copyright 2021, with permission from the authors, licensed under CC BY-NC-ND 4.0. Part (c) was reproduced from [170], Copyright 2023, with permission from Zhejiang University Press

This challenge can be addressed using sacrificial templates to guide cell printing and create lumens with the desired geometries. Further research is needed on the printability of cell inks, template–ink interface coupling, and template design optimization to improve the feasibility and controllability of this approach. This will enable a more flexible cell distribution and pave the way for the robust integration of cell printing with OOC fabrication.

5.3.8 Organoids (provided by the Shuo Bai group)

The precision deposition of cells and matrix materials in a predetermined manner afforded by 3D bioprinting holds immense potential for creating organoids that faithfully replicate the microstructure of native organs [171]. In the realm of engineered organoid construction, two primary strategies have emerged: scaffold-free and scaffold-based approaches. In the former, organoids form as cells that self-assemble via surface adhesion, albeit with a lack of the biomimetic complexity of the native structure and of a matrix microenvironment. In contrast, scaffold-based methods introduce materials that occupy space, thus requiring that the scaffold degradation rates align with the cell proliferation and ECM secretion rates during culture. To address this challenge, the team of Prof. Bai pioneered the development of short-peptide self-assembled hydrogels as bioink materials for the 3D bioprinting of organoid constructs, including cancer and liver organoids boasting biomimetic lobular structures. Short peptides facilitate the formation of a dynamic noncovalent gel network through electrostatic forces, the Hofmeister effect, and enzyme catalysis [172] (Fig. 23b). This dynamic hydrogel characteristic not only mitigates the shear-force-induced cell damage that occurs during printing, but also adapts to the stress caused by cell proliferation and tissue formation. In cancer organoid construction, hundreds of uniformly sized organoids with 3D multicellular spherical structures are produced in batches via postprinting culture, with nondestructive release being facilitated by the degradation of the short-peptide self-assembled hydrogel materials [173, 174] (Fig. 23a). Compared with 2D monolayer cultures, 3D lung cancer organoids exhibited heightened cellular activity and increased expression of pan cytokeratin (P-CK), antiprosurfactant protein C (ProSP-C), mucl protein 1 (MUC1), and Caveolin-1, together with enhanced resistance to anticancer drugs and lower half maximal inhibitory concentration (IC_{50}) values. Furthermore, liver organoids mimicking cellular heterogeneity, spatial structure, and ECM characteristics displayed elevated cell viability, albumin (ALB) secretion,

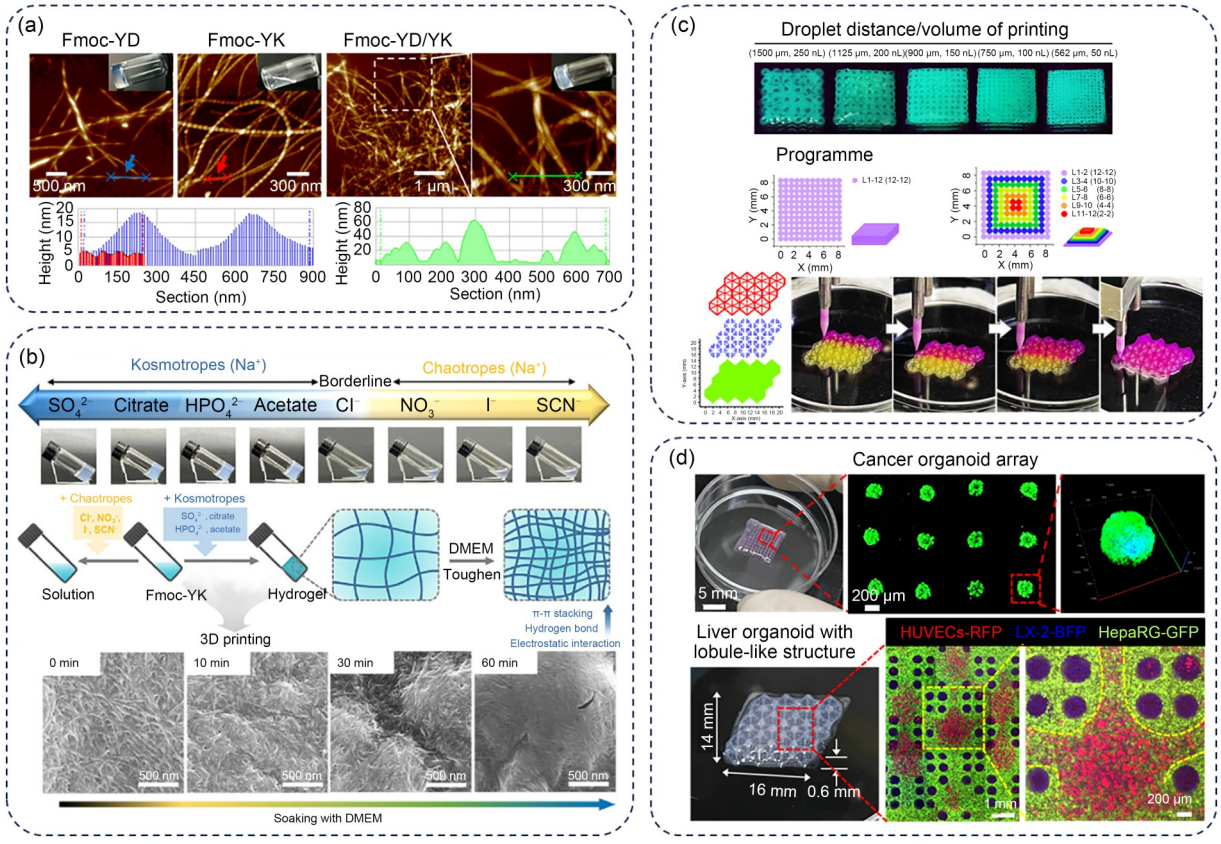

Fig. 23 Three-dimensional bioprinting-based in vitro construction of organoids: (a) atomic force microscope (AFM) images of the dipeptide self-assembled bioink system based on an electrostatic interaction; (b) cell culture medium-toughened dipeptide hydrogel scaffolds with the Hofmeister effect; (c) 3D bioprinting of short-peptide-based bioink materials to construct various hydrogel scaffolds; (d) in vitro construction of a cancer organoid and liver organoid with a lobule-like structure. Part (a) and Part (c, upper) were adapted from [173], Copyright 2019, with permission from the American Chemical Society. Part (b) was adapted from [172], Copyright 2023, with permission from Elsevier. Part (c, lower) and Part (d, lower) were adapted from [175], Copyright 2023, with permission from the authors, licensed under CC BY. Part (d, upper) was adapted from [174], Copyright 2023, with permission from Elsevier

and urea synthesis levels compared with 2D monolayer cultures [175] (Figs. 23c and 23d). In summary, Bai's research represents a significant advancement in tissue engineering that offers applications for high-throughput drug screening, disease modeling, and precision medicine.

5.3.9 Assembloids with a heterogeneous microenvironment (provided by the Yuan Pang group)

The growth, development, and health status of tissues and organs in the human body are affected by their interaction with the complex microenvironment. The microenvironment refers to the local environment surrounding tissues or organs, which is composed of the ECM, vascular system, immune cells, signaling molecules, and other supportive cells. These factors collectively maintain tissue structure and function and regulate cell behavior, and abnormal microenvironments may be associated with tissue and organ pathologies or lead to disease progression, including the development of drug resistance. To recreate these interactions between the microenvironment and organs in vitro, it is necessary to reconstruct tissue models with complex and heterogeneous microenvironments. Assembloids, which are an emerging technology for constructing in vitro tissue models, have cell densities similar to in vivo conditions and can reproduce important components of the microenvironment, such as vascular networks, thereby significantly enhancing tissue survival and development. Assembloids hold promise as a powerful tool for reconstructing heterogeneous microenvironment models in vitro. The concept of assembloid was first proposed by the group of Dr. Sergiu Pașca from Stanford University [176], and its definition has since been refined to refer to microscale, functional tissue models generated through the self-assembly of multiple cell types using 3D culture/manufacturing techniques [177, 178]. To further advance in vivo-mimicking complex assembloid models, different advanced manufacturing technologies could be combined. The group of Prof. Wei Sun and Prof. Yuan Pang has proposed a spheroid-on-demand manipulation strategy aimed at the construction of staged endothelialized hepatocellular

carcinoma (HCC) assembloids based on a microdroplet jetting 3D bioprinting technology with a microfluidic chip. Homogeneous HCC spheroids were first quickly generated using an oxygen-permeable microwell plate, and the microvascular network was self-assembled in a semi-open microfluidic chip to support subsequent spheroid printing. The alternating viscous and inertial force jetting-driven microdroplets realized the controllable spatiotemporal arrangement of the tumor spheroids within the vascularized substrate. The printed assembloids successfully reproduced microvascular invasion, volume increase, cell migration, and differentiated drug response during the dynamic development of HCC, as well as the spheroid dispersion phenomenon induced by epithelial–mesenchymal transition (EMT) under transforming growth factor-β (TGF-β) induction. These results indicate the potential of the staged HCC models as a reliable experimental platform for the development of antitumor treatment strategies in subsequent clinical trials [179] (Fig. 24a). The Zhuo Xiong team has proposed the construction of an assembloid based on microfluidic droplet technology. In their research, cells from a patient-derived tumor microenvironment (TME) and lung cancer organoids were uniformly encapsulated in microgels through microfluidic chips and produced lung cancer assembloids (LCAs) with a uniform size and cell composition. The LCA model was able to reconstruct the functional heterogeneity of cancer-associated fibroblasts, which reflected the impact of the TME on the drug response. Notably, the LCAs accurately replicated the clinical outcomes of patients, suggesting that the LCA model has the potential for predicting personalized treatments [180] (Fig. 24b).

6 Advances in tissue/organ regeneration strategies in China

In the exploration of tissue-regeneration strategies, Chinese research teams have deployed a comprehensive approach encompassing a wide range of the major systems of the human body. Among them, the musculoskeletal system has received the most attention where a multidimensional strategy is used that covers bioceramic scaffolds, multicellular scaffolds, tissue-engineered bone, bone–cartilage regeneration, and skeletal muscle reconstruction. This is followed by the circulatory system, which primarily focuses on artificial blood vessels, multilevel vascular construction, functionalized vascular structures, and stem cell printing. Subsequently, the nervous system is addressed, including neural regeneration and repair of spinal cord injury. In turn, the research on the respiratory system is primarily centered on bioengineered tracheas, whereas that on the reproductive system involves cavernous tissue repair. Although research on the immune and digestive systems has been reported, it is less extensive and has not touched upon core functionalities, specifically skin repair and vascularized liver tissue construction. It is noteworthy that the urinary and endocrine systems remain

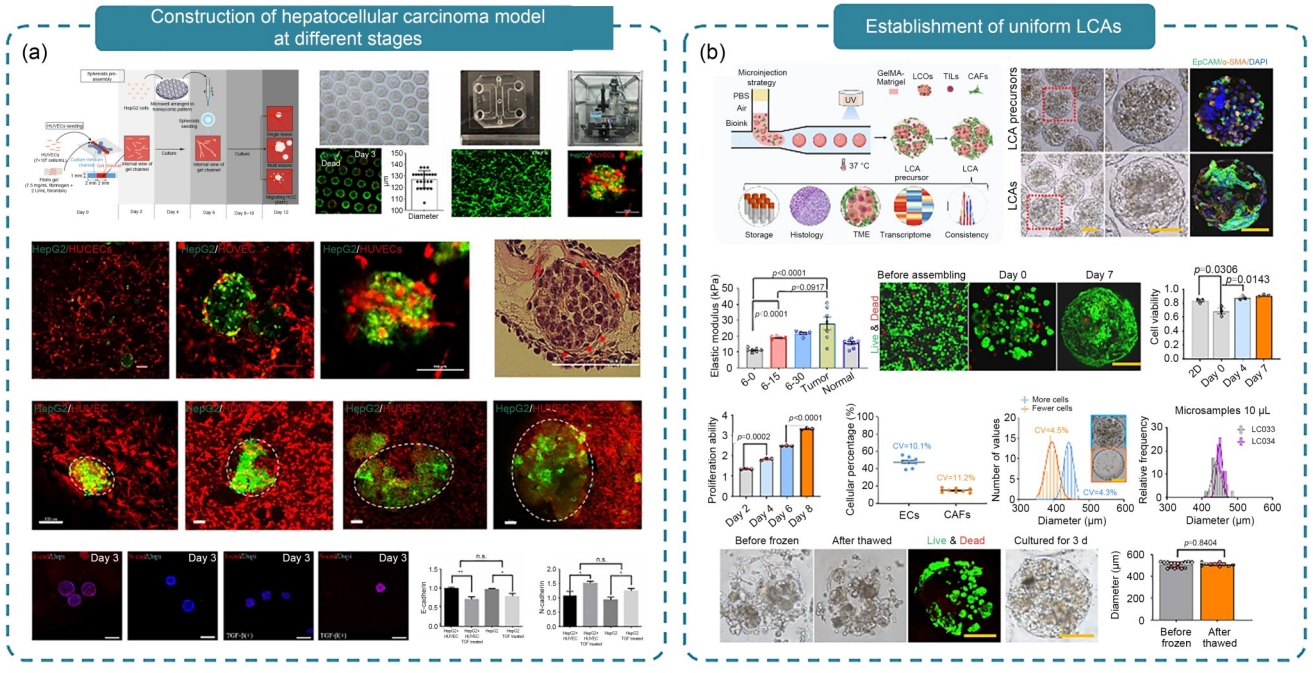

Fig. 24 Three-dimensional bioprinting of assembloids with a heterogeneous microenvironment: (a) assembloid on-demand printing of an endothelialized hepatocellular carcinoma model at different stages; (b) establishment of uniform lung cancer assembloids (LCAs) using a microinjection strategy based droplet microfluidic technology. Part (a) was adapted from [179], Copyright 2023, with permission from IOP Publishing. Part (b) was reproduced from [180], Copyright 2024, with permission from the authors, licensed under CC BY 4.0

unexplored in this context; thus, the research potential in these related fields is enormous, holding promise as "blue ocean" areas for future scientific exploration (Fig. 25).

6.1 Musculoskeletal system

The human musculoskeletal system is a complex network of interwoven bones, muscles, joints, and connective tissues. It not only provides a stable structural support for the body, but also serves as the core engine that drives diverse motor behaviors. The system is centered on the skeleton, which is composed of more than 200 closely arranged bones. This rigid framework not only carries the weight of vital organs, but also firmly anchors muscle tissues and serves as a key lever during movement.

Concomitantly, the muscle system, which consists of more than 600 skeletal muscles, is the source of power for movement. This system is tightly connected to the bones through tendons, is under precise regulation by the nervous system, and achieves the coordinated contraction and relaxation of muscles, thus performing various actions ranging from subtle to powerful.

Joints, as the connecting hub between bones, skillfully achieve a balance between flexibility and stability. Based on their structural characteristics, they are divided into three types, i.e., synovial joints, fibrous joints, and cartilage joints, to adapt to the needs of different movement patterns. Connective tissues such as ligaments, tendons, and cartilage act as the system's ties and protective umbrellas, thus ensuring the precise alignment and efficient operation of each component while promoting an effective transmission of force and robust protection of joints.

6.1.1 Design and manufacturing of bone scaffolds (provided by the Yan'en Wang group)

Bone regeneration consists of a series of carefully orchestrated osteoinductive and transductive biological events involving multiple cell types and intracellular and extracellular molecular signaling pathways with a definable temporal and spatial sequence. In this process, the choice of material for the bone scaffold, the structural design, and the gentle manufacturing process all affect bone regeneration. To address these challenges, the Yan'en Wang group at Northwestern Polytechnical University has conducted systematic research on the design and manufacturing of bone scaffolds. In terms of material, hydroxyapatite (HA) was modified with carboxymethyl chitosan (CMCS). The HA/CMCS scaffold with a CMCS content of 3% (mass fraction) exhibited the best bioactivity (Fig. 26a) [181]. Furthermore, the incorporation of

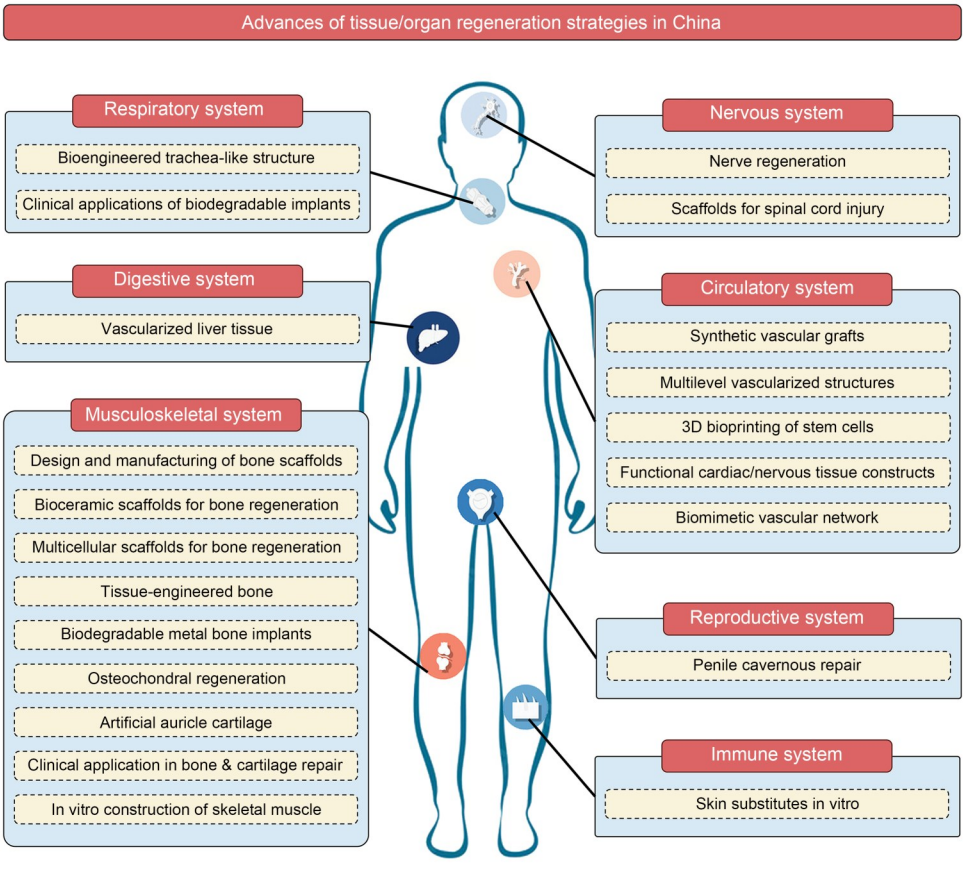

Fig. 25 Advances in tissue/organ regeneration strategies in China

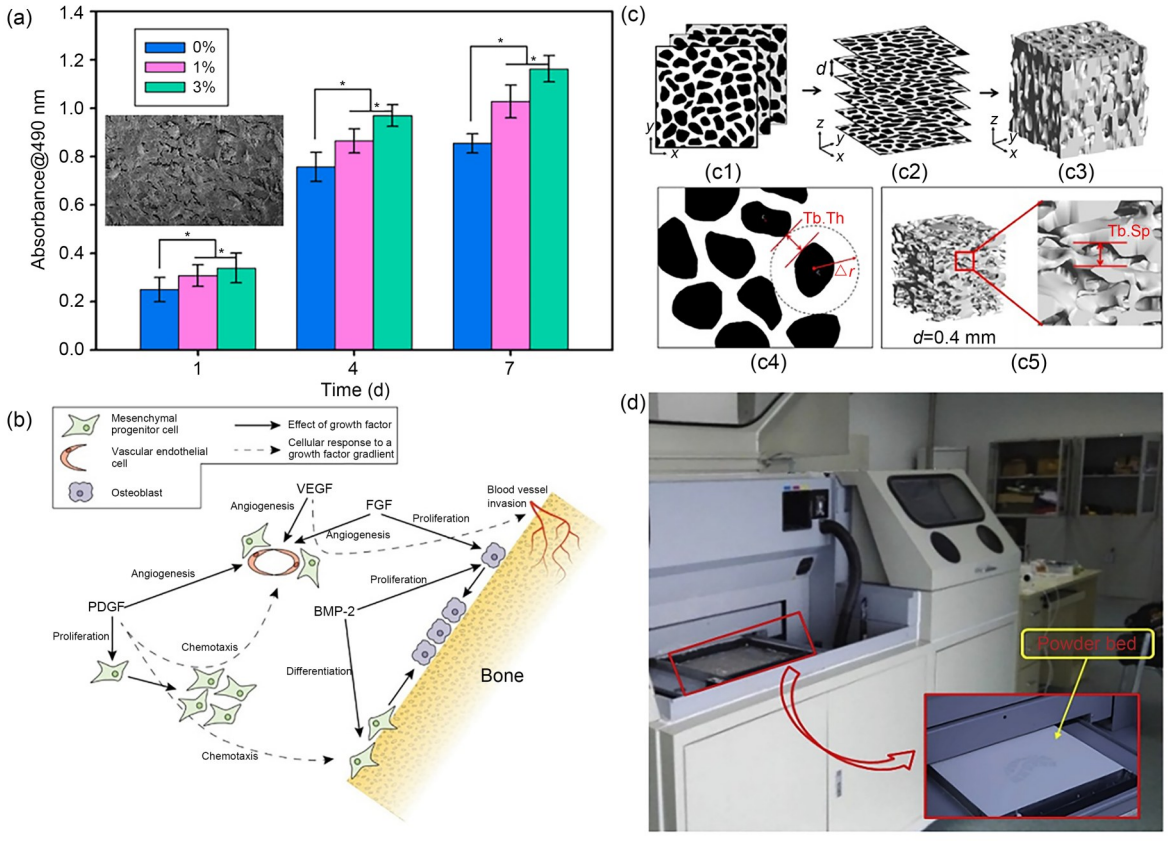

Fig. 26 Improving the bone-regeneration ability of bone scaffolds from multiple angles: (a) effect of the carboxymethyl chitosan (CMCS) content in hydroxyapatite (HA) bone scaffolds on cell proliferation; (b) mechanisms of action of different growth factors on bone regeneration; (c) biomimetic design method for porous bone scaffolds to promote bone regeneration; (d) image of an inkjet printer. Part (a) was reproduced from [181], Copyright 2022, with permission from Elsevier. Part (b) was reproduced from [182], Copyright 2021, with permission from Elsevier. Part (c) was reproduced from [183], Copyright 2022, with permission from Elsevier. Part (d) was reproduced from [186], Copyright 2019, with permission from Elsevier

growth factors into the ceramic bone scaffolds can enhance bone regeneration. The mechanism of the action of the growth factors is depicted in Fig. 26b [182]. Commonly used growth factors include bone morphogenetic proteins (BMPs), platelet-derived growth factor, fibroblast growth factor, TGF-β, insulin-like growth factor-1 (IGF-1), and vascular endothelial growth factor (VEGF) [182]. In terms of design, the group of Yan'en Wang developed a biomimetic design that utilizes computed tomography (CT) scanning, 3D reconstruction, and feature extraction of human cancellous bone (Fig. 26c). The designed structures exhibit permeability and fluid shear stress, which promote bone cell adhesion, migration, and differentiation [183]. In terms of manufacturing, inkjet printing can fabricate bone scaffolds at room temperature that preserve the activity of the incorporated growth factors (Fig. 26d). The Yan'en Wang research group simulated and modeled the key printing processes, studied the penetration behavior of adhesives, and optimized the parameters of the printing process [184–186]. Their research provided a viable solution for the preparation of active bioceramic bone scaffolds.

6.1.2 Bioceramic scaffolds for bone regeneration (provided by the Chengtie Wu group)

The complex compositions, cell types, and multilevel structure of bone tissue give it excellent biological and mechanical properties. Therefore, ideal bone repair materials should be able to mimic the complex structure and physiological microenvironment of the bone tissue to realize the regeneration of bone defects and reconstruction of stress conduction. Inspired by the multilevel structure of natural materials, the Chengtie Wu team has proposed the strategy of 3D printing biomimetic bioceramic scaffolds with a macrostructure, microstructure, and multicellular structure, separately.

6.1.2.1 Biomimetic scaffolds with a macrostructure

Bone regeneration requires not only the reconstruction of the bone matrix, but also the repair of blood vessels, nerves, and other important tissues. Inadequate blood vessels and nerves can lead to delayed bone repair [187]. Therefore, it is very important to achieve adequate vascularization and innervation at the same time as the bone repairs via a biomimetic

structure design. To biomimic the multilevel structure and multicellular distribution of natural bone tissue, Haversian bone-mimicking scaffolds combined with Haversian canals, Volkmann canals, and a cancellous bone structure were designed and fabricated [188]. By culturing MSCs on cancellous bone structure and endothelial cells/Schwann cells (ECs/SCs) on Haversian canals, Haversian bone-mimicking scaffolds promoted the growth of blood vessels and nerves and further promoted bone ECM deposition and osteogenic differentiation. In addition, to specifically regulate the behavior of MSCs, ECs, and SCs, polyhedral scaffolds with different spatial topologies were prepared to promote vascularization, innervation, and bone repair (Fig. 27a) [189]. The results of the computational fluid dynamics simulation analysis showed that the polyhedral scaffolds had a lower average wall pressure than the traditional cross-structure scaffolds, which contributed to an improved cell residence. Moreover, the topology activated the phosphatidylinositol 3-kinase/protein kinase B (PI3K/Akt) signaling pathway to promote osteogenic differentiation and induce vascularization and innervation. In addition to the structure of the bone tissue, the relationship between the function and multilevel structure of natural materials is worth reference and imitation. For example, the multichannel structure of the lotus root not only promotes the exchange of air and water with the external environment, but also maintains a lower flow resistance. Inspired by the multichannel structure, biomimetic lotus root scaffolds were fabricated via a modified 3D printing method with specially designed nozzles (Fig. 27b) [190, 191]. Biomimetic lotus root scaffolds could accelerate the release of bioactive ions and cell migration to promote vascularization and osteogenesis. Moreover, to achieve a better delivery

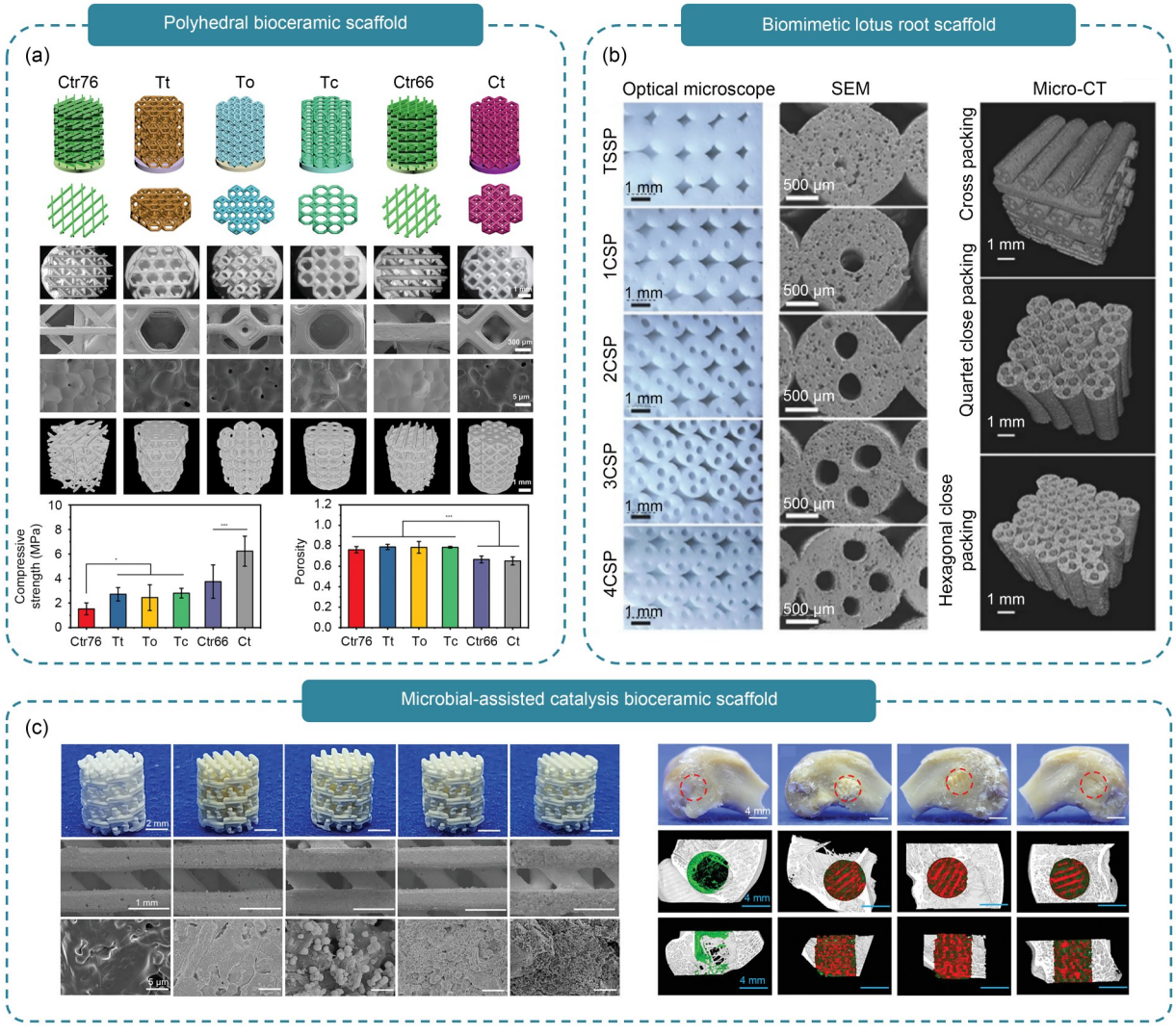

Fig. 27 Biomimetic 3D-printed bioceramic scaffolds for bone regeneration: (a) three-dimensionally printed polyhedral bioceramic scaffolds and cross scaffolds; (b) biomimetic lotus root scaffolds; (c) microbial-assisted catalysis bioceramic scaffold. Part (a) was reproduced from [189], Copyright 2023, with permission from Wiley. Part (b) was adapted from [190], Copyright 2017, with permission from the authors, licensed under CC BY. Part (c) was adapted from [194], Copyright 2021, with permission from Wiley

capacity of ions, drugs, and proteins, bioceramic rods were embedded inside the hollow tube of the scaffolds via bidirectional freezing [192]. The biomimetic hot dog bioceramic scaffolds have an excellent capability of drug loading and releasing, as well as a better capability of delivery and differentiation of MSCs. Moreover, some natural sponge organisms dominated by inorganic components have high flexibility while maintaining strength, which is important for flat bone repair. Their excellent mechanical properties are attributed to the unique concentric layer structure of the sponge organisms. Therefore, inspired by the hexagonal deep-sea sponges, biomimetic sponge bioceramic scaffolds were fabricated via cryogenic hydrothermal mineralization [193]. The high strength and unique flexibility and elasticity of the biomimetic sponge scaffolds exhibited great potential for the regeneration of the skull and orbit bones, as well as other flat bones.

6.1.2.2 Biomimetic scaffolds with a microstructure

Bone is a mineral-rich tissue that is composed of organic and inorganic substances with a high hardness and complex micro-/nano-scale structures. Biomimetic reconstruction of micro-/nano-scale structures can deeply affect cell behavior and bone regeneration through chemical and mechanical signals. Inspired by microbially catalyzed mineralization, the microbial-assisted catalysis concept was proposed to biologically synthesize micro-/nano-scale structures on bioceramic scaffolds (Fig. 27c) [194]. The special biomimetic $CaCO_3$ micro-/nano-scale structures fabricated by microbes have excellent bone-forming bioactivity, which can activate the Wnt signaling pathway and the osteogenic differentiation of MSCs. Moreover, tricalcium phosphate scaffolds with a micro-/nano-scale structure, which were fabricated using a hydrothermal process, promoted the regeneration of cartilage and subchondral bone [195]. In addition, inspired by the gear, scaffolds with a microscale groove structure were fabricated using a modified 3D printing method with specially designed nozzles [196]. The gear-inspired 3D-printed scaffolds displayed good immunoregulatory and osteogenic activity. The scaffolds could regulate early inflammation and macrophage behavior, and then promote the osteogenic differentiation of MSCs and bone regeneration.

6.1.3 Multicellular scaffolds for bone regeneration (provided by the Chengtie Wu group)

The multicellular 3D bioprinting technology can easily and accurately regulate the composition of biomaterials, the distribution of cells, and the release of bioactive factors to achieve the reconstruction of complex tissues. The group of Chengtie Wu has proposed a novel concept of combining inorganic-biomaterial-based bioinks with multicellular 3D bioprinting for the regeneration of multiple complex tissues, such as neural–bone tissue, osteochondral tissue, and bone–tendon interfaces.

Nerves play a very important role in the regeneration of bone tissue and can regulate the repair progress in multiple ways. For example, various neurotransmitters secreted by nerves can affect bone homeostasis and regeneration and can guide skeletal muscle maturation through the formation of neuromuscular joints (NMJs) [187]. A delay in neuralization often blocks the regeneration and maturation of bone tissue [197]. Therefore, the synergistic relationship of the neural-bone system should be taken seriously. Using 3D bioprinting technology, multicellular scaffolds consisting of MSCs, SCs, and silicon-based bioceramics were fabricated for the regeneration of neural-bone tissues [198]. The release of inorganic ions could accelerate the maturation and myelination of SCs and induce the growth of nerve fibers. Moreover, multicellular scaffolds could effectively promote the formation and osseointegration of bone tissue to achieve neural-bone regeneration. Furthermore, neural stem cells were combined with silicon-based bioceramic and multiple types of tissue cells to prepare inorganic-biomaterial/neural-stem-cell constructs (Fig. 28a) [199]. The multicellular constructs led to excellent effects of osteogenesis, angiogenesis, and neuromuscular junction formation, indicating their versatile therapeutic ability for tissue regeneration.

The unique gradient structure of the bone–tendon interface gives it excellent mechanical properties and plays an important role in the kinetic system. However, because of the complexity of this structure, the regeneration of the bone–tendon interface and the construction of stress conduction remain intractable difficulties. To biomimic the gradient structure and cellular composition of the bone–tendon interface, multicellular 3D-bioprinted scaffolds were fabricated by regulating the spatial distribution of the bioceramic inks (Fig. 28b) [200]. The release of molybdenum ions within the multicellular bioceramic scaffolds could promote the differentiation of tendon stem/progenitor cells (TSPCs) into tendons via the TGF-β signaling pathway. Moreover, the biomimetic multilayer structure of the scaffolds could achieve the bidirectional differentiation of the tendon and bone, thus better promoting the regeneration of the bone–tendon interface. Furthermore, by combining manganese silicate nanoparticles with multilayer scaffolds loaded with TSPCs and MSCs, multicellular bioceramic scaffolds with an immune-regulation function were successfully fabricated [201]. The release of manganese ions could stimulate the secretion of prostaglandin E2 (PGE2) by macrophages, followed by the enhancement of the bidirectional differentiation of the tendon and bone. Similarly, the regeneration of osteochondral tissues faces the demand of bidirectional differentiation and the reconstruction of the gradient structure. Using a multicellular 3D bioprinting technology, scaffolds with a multilayer

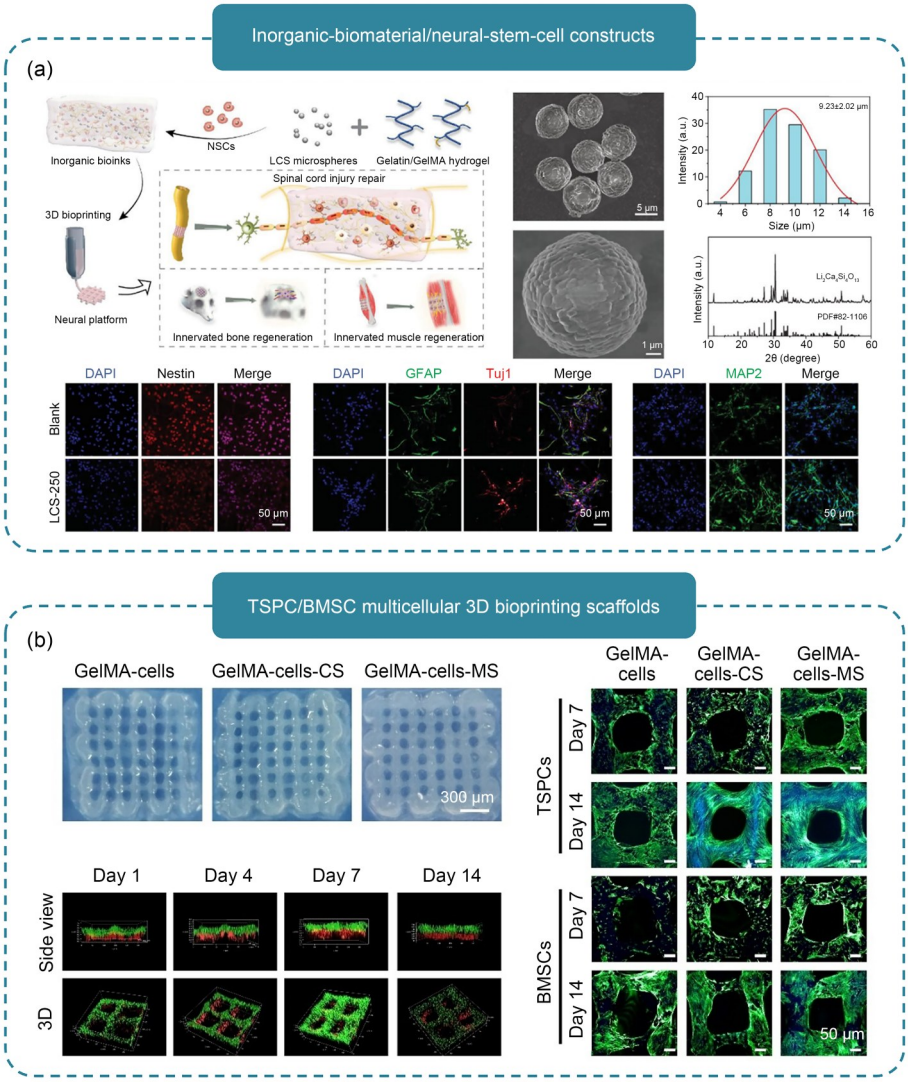

Fig. 28 Multicellular 3D bioprinting scaffolds for bone regeneration: (a) inorganic-biomaterial/neural-stem-cell constructs; (b) multicellular 3D-bioprinted scaffolds containing tendon stem/progenitor cells (TSPCs) and bone marrow mesenchymal stem cells (BMSCs). Part (a) was adapted from [199], Copyright 2024, with permission from the authors, licensed under CC BY 4.0. Part (b) was reproduced from [200], Copyright 2023, with permission from the authors, licensed under CC BY

structure of MSCs were fabricated using bioceramic-based bioinks and successfully achieved the integrated regeneration of osteochondral tissues [202, 203].

6.1.4 Tissue-engineered bone (provided by the Changshun Ruan group)

Bioprinting, which can synchronously deposit cells and biomaterials, provides a robust approach to the fabrication of the new generation of tissue-engineered bone substitutes with a biomimetic structure and precise composition of cells and biomaterials [132, 204]. However, to achieve this applied goal, the following requirements need to be met: a favorable microenvironment for osteogenesis and a high mechanical strength, as well as printability, high fidelity, and good biocompatibility. The Changshun Ruan group has made great efforts to address the challenges of bioprinting for the construction of tissue-engineered bone. First, this team developed suitable bioinks for the creation of tissue-engineered bone that possess superior printability and fidelity, while also ensuring good biocompatibility: a temperature-programable gelatin-based bioink [205] and an alginate-based bioink boosted by a small-molecule polycationic crosslinker [206] (Fig. 29a). The team of Changshun Ruan further demonstrated that the osteogenic capability of 3D-bioprinted tissue-engineered bone was significantly better than that of 3D-printed scaffolds without exogenous cells, suggesting that exogenous bone-related cells can play a key role in the promotion of bone regeneration. In addition, to create a favorable microenvironment to promote osteogenic differentiation, the Changshun Ruan team bioprinted a cell-laden polyethylene glycol

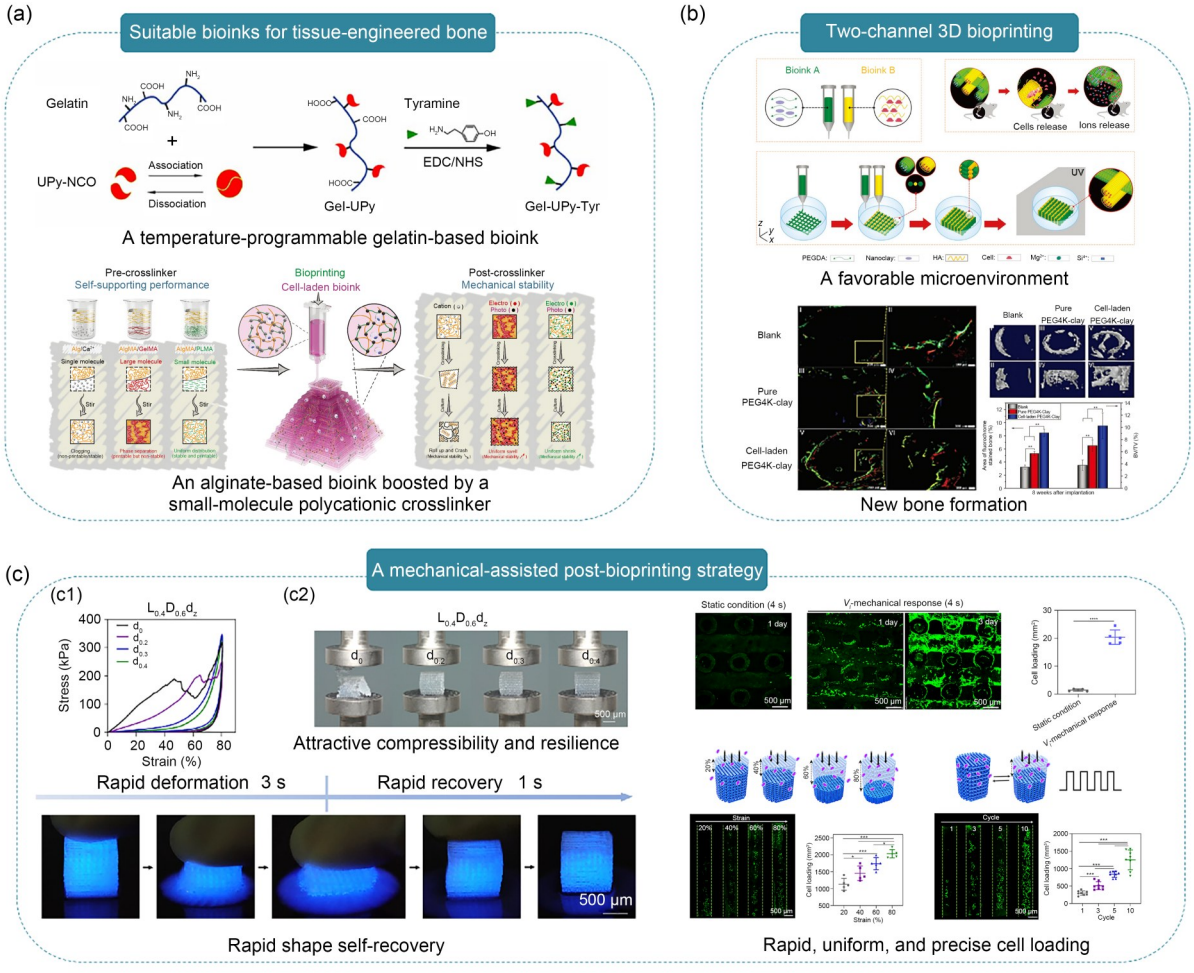

Fig. 29 Bioprinting for tissue-engineered bone: (a) suitable bioinks for tissue-engineered bone that possess superior printability, fidelity, and good biocompatibility; (b) bioprinting a cell-laden polyethylene glycol (PEG)–clay construct using a two-channel 3D bioprinting method, which can create a favorable microenvironment to promote osteogenic differentiation; (c) loading of cells into hollow hydrogel-based scaffolds (HHSs) with superior mechanical properties in a rapid, uniform, precise, and friendly manner using a mechanical-assisted post-bioprinting strategy. Part (a, upper) was reproduced from [205], Copyright 2020, with permission from IOP Publishing. Part (a, lower) was reproduced from [206], Copyright 2023, with permission from Wiley. Part (b) was reproduced from [207], Copyright 2017, with permission from the authors, licensed under CC BY. Part (c) was reproduced from [208], Copyright 2024, with permission from the authors, licensed under CC BY 4.0

(PEG)–clay construct using a two-channel 3D bioprinting method [207] (Fig. 29b). One channel carried bioink A, which was sufficiently viscous to facilitate the 3D bioprinting process and could release bioactive ions, whereas the other channel guided the accurate delivery of cells into the 3D scaffolds, with the cells being able to maintain high viability in bioink B. To address the unavoidable occurrence of cell damage during the fabrication process and the intrinsically poor mechanical strength of the bioprinted cell-laden scaffolds, the Changshun Ruan group proposed a mechanical-assisted post-bioprinting strategy based on heart-inspired hollow hydrogel-based scaffolds (HHSs) [208] (Fig. 29c). This strategy can load cells into HHSs in a rapid, uniform, precise, and friendly manner. HHSs with the loaded cells exhibited an enhanced regenerative capability in the repair of the critical-sized segmental and osteoporotic bone defects in vivo. In summary, this work offers a robust method for the functional assembly of cells and biomaterials for tissue-engineered bone.

6.1.5 Biodegradable metal bone implants (provided by the Peng Wen group)

Annually, millions of patients worldwide suffer from bone defects caused by trauma, infection, tumors, and joint-revision surgeries. These bone defects hinder the bones' ability to self-heal and necessitate the use of bone-graft materials for repair. Biomedical metals are widely used for the treatment of bone defects because of their excellent mechanical properties and biocompatibility. However, they face the following three primary challenges. First, the implant's outline must match the anatomical shape of the bone defect to provide

reliable support for healing. Second, the implant should possess a porous interconnected microstructure to reduce the elastic modulus, avoid stress shielding, provide nutritional channels, and create space for bone ingrowth, thereby promoting osseointegration. Third, the implant's material must be bioactive, which means it would gradually degrade and be absorbed as the bone reconstruction progresses to avoid secondary surgeries. To address these challenges, the group of Peng Wen has focused on magnesium (Mg)-based and zinc (Zn)-based biodegradable metal bone implants, and developed laser additive manufacturing methods, powder materials, digital design, and surface-modification strategies for them [209]. They revealed the interaction mechanisms between the laser and the Mg and Zn metals, established numerical models for the optimization of the energy and gas flow fields [210] (Fig. 30a), overcame the additive manufacturing challenges of highly active and evaporative metals, and successfully printed porous Zn scaffolds for the first time worldwide [211, 212]. Moreover, they developed Mg-based and Zn-based metal powder materials that are suitable for additive manufacturing and biodegradable applications by alloying, which improved the biocompatibility, mechanical strength, degradation behavior, and osteogenic capacity of the implants [213, 214] (Fig. 30b). Moreover, they developed a machine-learning-based metamaterial design method to optimize the mechanical properties of the porous bone implants, with the results showing that the active learning algorithm efficiently endowed the Zn scaffolds with a structure and modulus that were adapted to the bone and exhibited a 20% increase in strength [215] (Fig. 30c). These authors also proposed new surface-modification strategies to enhance the biocompatibility of the metal implants.

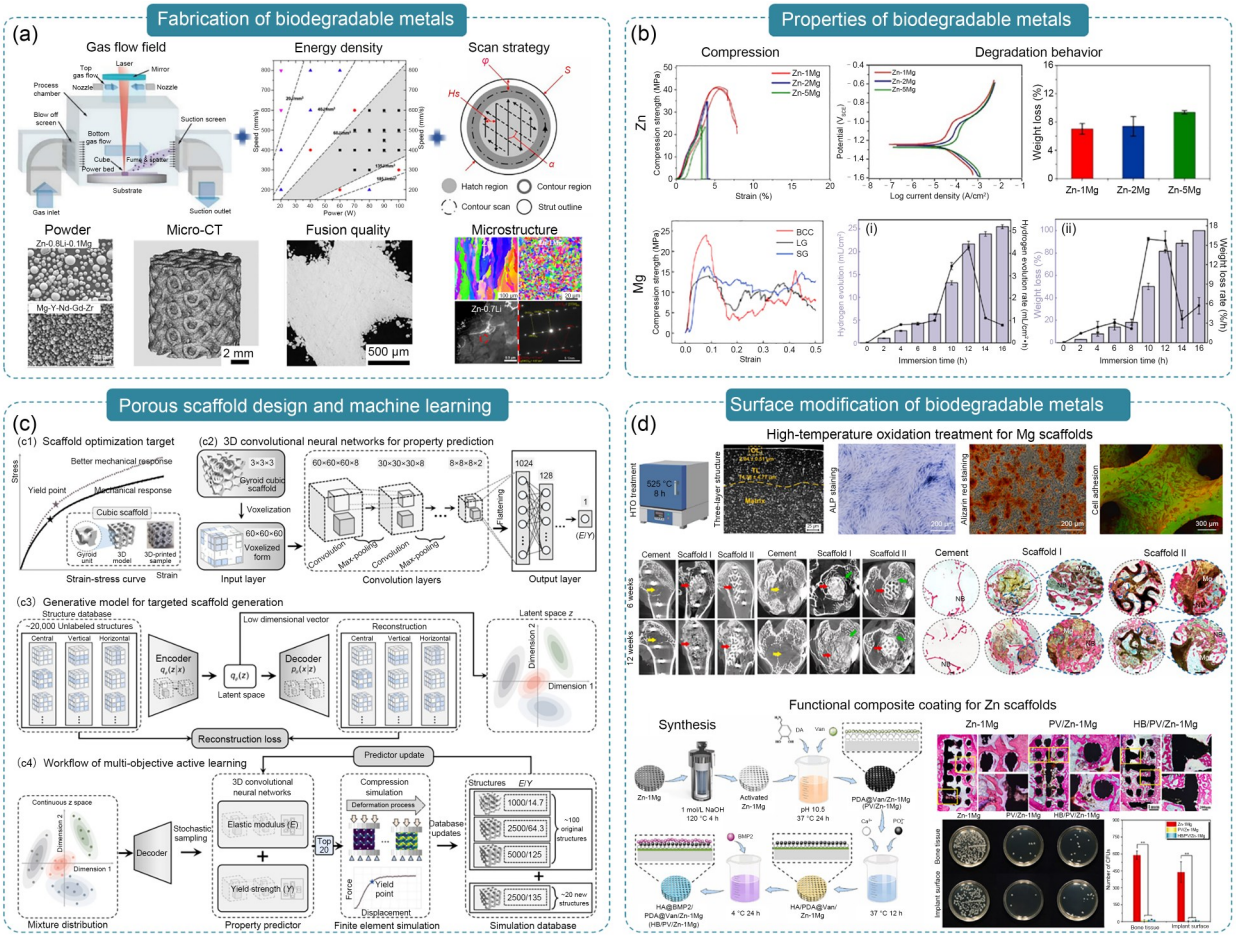

Fig. 30 Laser additive manufacturing of biodegradable metal bone implants: (a) processing, powder, formation quality, and microstructure of biodegradable metals; (b) mechanical properties and biodegradation behavior; (c) machine-learning-enabled multi-objective design of porous scaffolds; (d) surface modification of the biodegradable metal to bolster bone regeneration. Part (a) was adapted from [214] (Copyright 2022, with permission from the authors, licensed under CC BY 4.0) and [219] (Copyright 2022, with permission from the authors, licensed under CC BY-NC-ND 4.0). Part (b, upper) was reproduced from [220], Copyright 2022, with permission from Acta Materialia Inc. Part (b, lower) was reproduced from [214], Copyright 2022, with permission from the authors, licensed under CC BY 4.0. Part (c) was adapted from [215], Copyright 2023, with permission from the authors, licensed under CC BY 4.0. Part (d, upper) was adapted from [216], [221], and [222], Copyright 2022, 2023, and 2023, respectively, with permission from the authors, licensed under CC BY-NC-ND 4.0. Part (d, lower) was reproduced from [218], Copyright 2023, with permission from the authors, licensed under CC BY-NC-ND 4.0

High-temperature oxidation treatment was employed to solve the critical problems of the Mg porous scaffold, i.e., an uneven surface-coating quality and a resultant rapid degradation [216] (Fig. 30d). Electrochemical polishing was adopted to provide a surface pattern with nano-scale roughness, thus facilitating filopodia formation and macrophage spreading and creating a multiscale biodegradable Zn–Li porous scaffold for immunomodulatory osteogenesis [217]. A drug-loaded composite coating was successfully prepared on the surface of Zn – Mg porous scaffolds to inhibit the excessive release of Zn^{2+} and provide an antibacterial surface that was conducive to osseointegration [218]. Eventually, these technologies and findings have greatly promoted the development of laser additively manufactured biodegradable metal bone implants and their clinical applications.

6.1.6 Osteochondral regeneration (provided by the Changshun Ruan group)

Articular cartilage and bone tissue possess distinct biological components and regenerative capacities, leading to tremendous challenges in the repair of osteochondral defects. The use of 3D printing to fabricate bionic constructs, which recapitulate single-to-multiple co-features, holds great promise for promoting osteochondral regeneration. With this in mind, professor Changshun Ruan and his colleagues developed several bionic scaffolds, from material gradient to cell gradient, and comprehensively evaluated their osteochondral regenerative capacities. In early studies, the team spent more effort on printing high-fidelity and mechanically stable scaffolds that precisely matched the gradient structure of the osteochondral unit [223, 224]. Two high-strength hydrogels were synthesized to fulfill this aim, i.e., poly(*N*-acryloyl glycinamide-co-*N*-[tris(hydroxymethyl) methyl] acrylamide) hydrogel (PNT hydrogel) (Fig. 31a) and poly(*N*-acryloyl 2-glycine) (PACG) (Fig. 31b) and GelMA hybrid hydrogel (PACG-GelMA hydrogel). The incorporation of an *N*-[tris (hydroxymethyl) methyl] acrylamide block mitigates the hydrogen bonding interactions among the *N*-acryloyl glycinamide blocks; thus, the printability and mechanical strength of the PNT hydrogel were optimized by adjusting the ratio of the two blocks. Subsequently, the PNT-hydrogel-based gradient scaffold (chondrogenic layers: PNT containing a recombinant transforming growth factor β1 (TGFβ1) protein; osteogenic layers: PNT containing β-tricalcium phosphate (β-TCP)) was prepared via a dual nozzle extrusion printer, and demonstrated the osteochondral-induction ability in a rat osteochondral defect model. In addition, the hydrogen bond strategy was adopted to reinforce the traditional GelMA soft hydrogel. PACG remarkably increased Young's modulus (up to 320 kPa) and compression modulus (up to 837 kPa) of the GelMA hydrogel, thus being able to mimic the mechanical properties of the native cartilage with a compression modulus within 300–800 kPa. By combining this with a chondrogenic Mn ion and an osteogenic bioglass, the PACG-GelMA-stratified scaffold induced neo-osteochondral tissue in vivo. During the research rolling out, the team realized that cells are obligated to further enhance the scaffold osteochondral regeneration performance. Thereafter, bone-marrow mesenchymal stromal cells (BMSCs) were introduced into the bone region of the osteochondral scaffold [225] (Fig. 31c). Although the scaffold yielded positive results, the coordinated effects of an anti-inflammatory drug (diclofenac sodium) and a chondrogenic molecule (Kartogenin) shadowed the function of the BMSCs, and it was difficult to identify the role(s) of the exogenously implanted cells. Thus, in a recently published work, inspired by the articular cartilage and bone cellular features, chondrocyte progenitor cells and BMSCs containing a gradient scaffold were bioprinted, and were termed anisotropic bicellular living hydrogels (ABLHs) [226] (Fig. 31d). Interestingly, the ABLHs not only regenerated cartilage and subchondral bone, but also formed an interface that was similar to the native calcified cartilage zone (CCZ). The CCZ is a chimerical region of the cartilage and bone that is critical for maintaining the integrity of the osteochondral unit. In turn, its nanoporotic structure enables the crosstalk between small molecules while avoiding the invasion of catabolic proteins, neurons, and blood vessels into the cartilage from the subchondral bone. ABLHs, which are the 3rd generation of the 3D-printed osteochondral scaffolds stemming from the team of Prof. Ruan, proved that mimicking the natural tissue-specific cell features is an approach to regenerating the multizonal structure of the osteochondral unit.

6.1.7 Artificial auricle cartilage (provided by the Changchun Zhou group)

Traditional dense bulk hydrogels cannot fulfill the requirements of cartilage regeneration. The 3D-printed hydrogel scaffold has demonstrated tremendous potential for regulating cytological behavior during cartilage repair because of its highly controllable interlayer pore structure. The reported sodium alginate scaffolds, collagen hydrogel scaffolds, and GelMA/silk fibroin methacryloyl (SilMA) fabricated using the 3D printing technology have all successfully yielded good repair effects. The functional GelMA/SilMA composite hydrogel was studied, which proved that this hydrogel exhibited good mechanical strength and bioactivity and can be utilized for high-precision 3D printing via photocrosslinking. Compared with the load-bearing cartilage, some cartilage tissues with personalized shapes but without excessive mechanical requirements, such as the auricle and nose, have shown promising application potential. It is exciting to note that the Changchun Zhou group has reported satisfactory results in the bioprinting of non-load-bearing artificial auricle cartilage

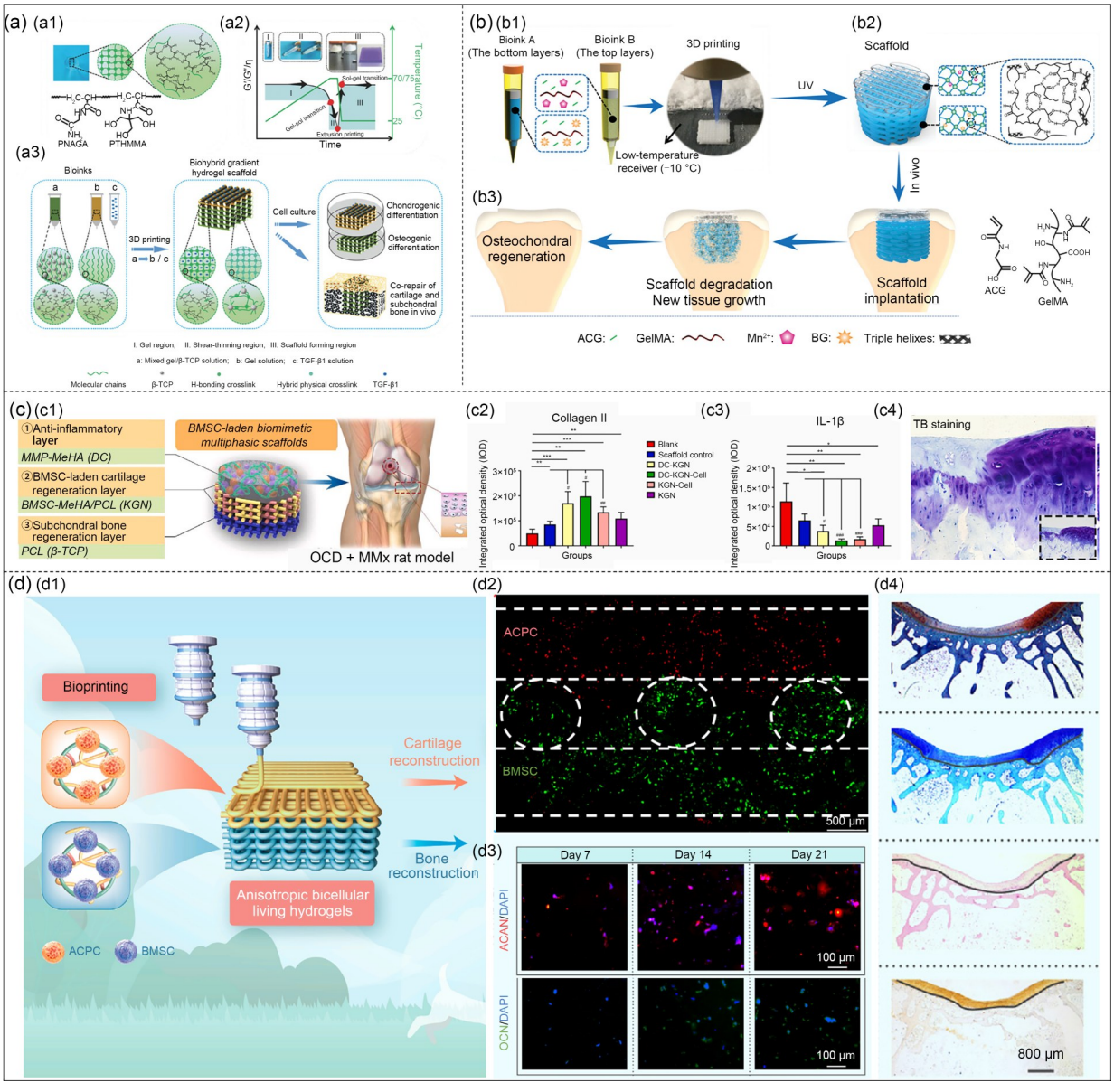

Fig. 31 Bioprinting of anisotropic scaffolds guides osteochondral regeneration. (a, b) Three-dimensional printing of mechanically stable gradient scaffolds with high-strength poly(*N*-acryloyl glycinamide-co-*N*-[tris(hydroxymethyl) methyl] acrylamide) (PNT) (a) and poly(*N*-acryloyl 2-glycine) and gelatin methacryloyl (PACG-GelMA) (b) hydrogels for the efficient repair of osteochondral defects. (c) Bone marrow-derived mesenchymal stem cell (BMSC)-laden biomimetic multiphasic scaffolds for osteoarthritic osteochondral regeneration. (d) Bicellular living hydrogels boost osteochondral regeneration via the reconstruction of the cartilage–bone interface. Part (a) was adapted from [223], Copyright 2018, with permission from Wiley. Part (b) was adapted from [224], Copyright 2019, with permission from the authors, licensed under CC BY. Part (c) was adapted from [225], Copyright 2021, with permission from Elsevier. Part (d) was adapted from [226], Copyright 2023, with permission from the authors, licensed under CC BY-NC-ND 4.0

tissue. These personalized cartilage tissues show potential for clinical application (Figs. 32a–32c) [227, 228].

6.1.8 Clinical application in bone and cartilage repair (provided by the Yongqiang Hao group)

The repair and reconstruction of bone and cartilage defects remain major unresolved issues in the field of orthopedics. Compared with traditional implant materials, 3D-bioprinted personalized active bone and cartilage offer advantages, including bioactivity, osteo/chondrogenic inducibility, and personalized design, thus exhibiting significant clinical application prospects. The team of Prof. Yongqiang Hao has been dedicated to exploring the application of 3D bioprinting to the repair of bone and cartilage injuries. They are investigating how to achieve effective treatment while ensuring safety, with the ultimate goal of translating this technology from the laboratory to clinical practice. The team members have

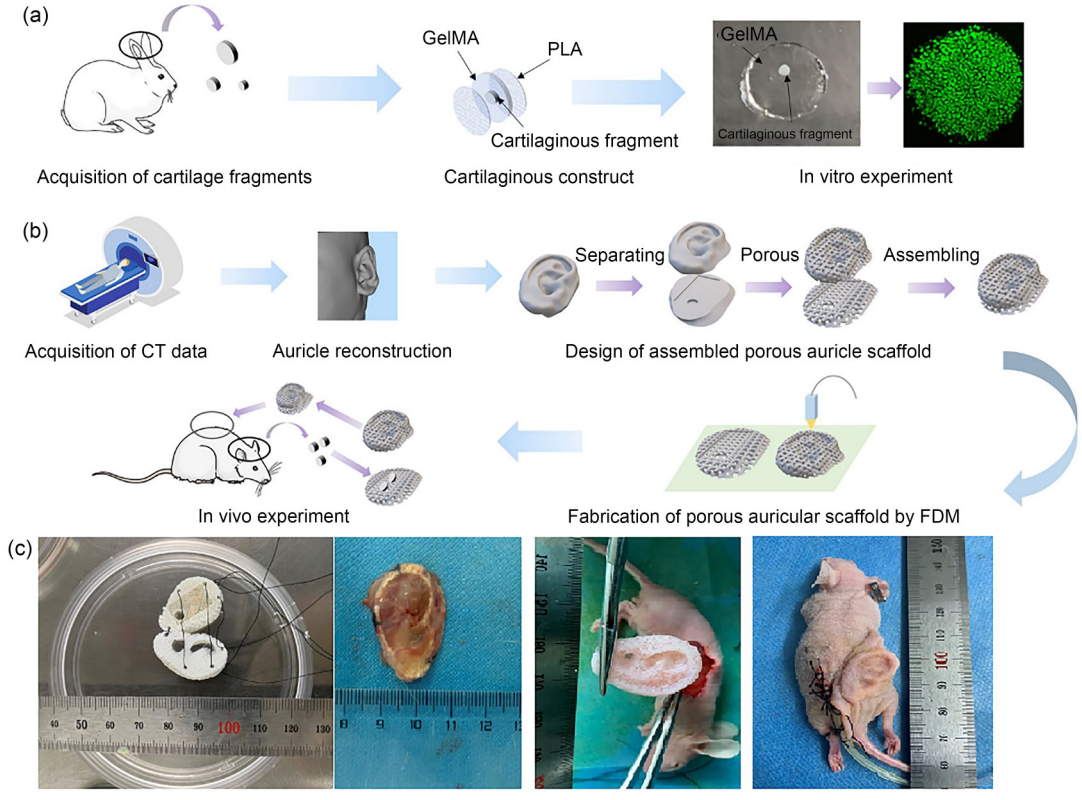

Fig. 32 Three-dimensional printing of the auricle tissue scaffold: the ear cartilage fragments were combined with a porous auricle scaffold and tested in vivo and in vitro. (a) Activity evaluation of rabbit ear cartilage fragments in vitro. (b, c) In vivo cartilage fragments combined with a 3D-printed poly(lactic acid) (PLA) scaffold to reconstruct the auricle. Parts (a), (b), and (c, left) were reproduced from [227], Copyright 2023, with permission from Zhejiang University Press. Part (c, right) was reproduced from [228], Copyright 2021, with permission from Elsevier

explored molding conditions based on melt electro-writing (MEW) printing inks [229], and have utilized MEW and inkjet-printing technologies to establish composite scaffolds for cartilage repair. These scaffolds contain multiple layers of growth factors, thereby offering high precision and excellent mechanical and biological properties [230]. They further developed hybrid cell-laden hydrogel inks based on PEGDA and ECM to construct composite scaffolds loaded with BMSCs [231]. Inspired by natural bone and cartilage tissues, the team designed and manufactured a three-layered scaffold (superficial cartilage, deep cartilage, and subchondral bone) (Fig. 33a). This scaffold combines a GelMA hydrogel loaded with region-specific growth factors and a poly(ε-caprolactone) and poly(ethylene glycol) (PCEC) network to achieve the simultaneous regeneration of cartilage and subchondral bone [232]. The team utilized computer-aided design and manufacturing (CAD/CAM) technology to construct in vitro a biphasic scaffold resembling the shape and structure of a goat femoral head (Fig. 33b). After seeded with chondrocytes and BMSCs, these scaffolds were implanted subcutaneously into nude mice, thus achieving an integrated structure of both cartilage and bone [233].

Furthermore, the team explored the feasibility of using engineered exosomes derived from TGFβ3-preconditioned BMSCs for cartilage repair and osteoarthritis treatment. The TGFβ3-extracellular vesicle (T3-EV) hydrogel designed in this study exhibited significant potential for the treatment of cartilage defects [234]. Considering the development of bioprinting for repairing bone defects, one of the primary technological challenges consists in the creation of bioinks with a rapid internal vascularization capability and sustained osteoinductive bioactivity. The team addressed this challenge by employing low-temperature printing to create graded porous sponge-like scaffolds. These scaffolds promoted interactions between cells and materials while regulating the paracrine activity of BMSCs for vascularization and bone-regeneration purposes [235]. Moreover, the team incorporated rat platelet-rich plasma (PRP) into a GelMA/methacrylate alginate (AlgMA) system and utilized polycaprolactone (PCL) for the layer-by-layer printing of hydrogel bioinks to create active bone-repair scaffolds. In vivo experiments demonstrated that the PRP-GelMA/AlgMA system scaffold significantly promoted vascular ingrowth and bone regeneration at the defect site [236]. Moreover, the team clinically applied patient-derived PRP-based bioinks combined with PCL/β-TCP composite scaffolds for the first time. They used 3D bioprinting to layer-by-layer print personalized PCL/β-TCP/PRP active scaffolds for repairing

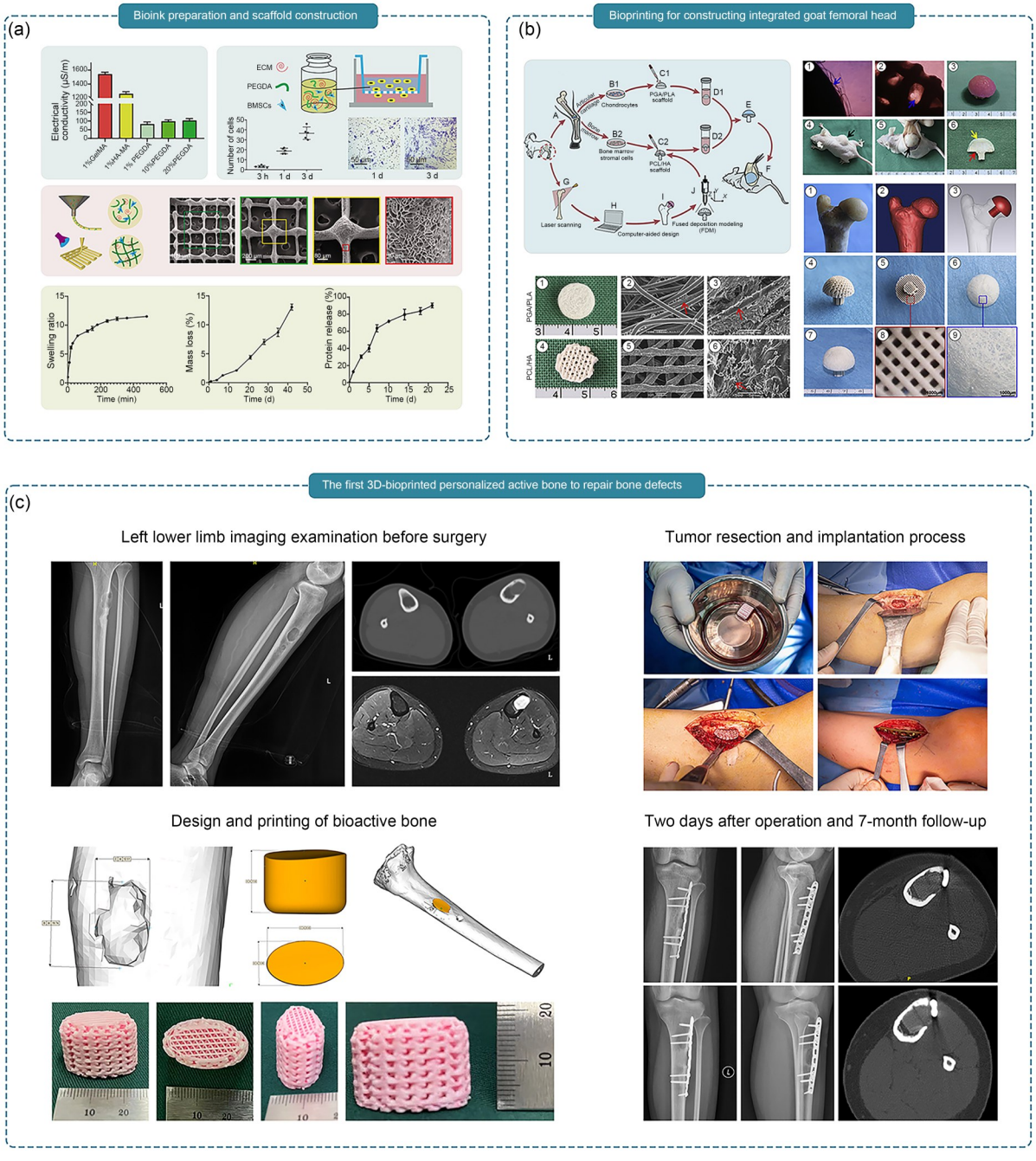

Fig. 33 Three-dimensional bioprinting for repairing bone and cartilage injuries: (a) preparation of bioinks and construction of multilayer scaffolds; (b) 3D bioprinting to construct integrated bone–cartilage goat femoral heads; (c) clinical application for bone repair after tibial tumor resection. Part (a) was reproduced from [231], Copyright 2022, with permission from the authors, licensed under CC BY-NC-ND 4.0. Part (b) was adapted from [233], Copyright 2013, with permission from Elsevier. Part (c) was reproduced from [237], Copyright 2022, with permission from the authors, licensed under CC BY 4.0

and reconstructing bone defects after tibial tumor resection in patients [237] (Fig. 33c). This is the first example worldwide of the clinical application of a 3D-bioprinting-based bioactive scaffold for the repair and reconstruction of bone and cartilage defects. This work is of great clinical significance and paves the way for the future development of orthopedic regenerative medicine.

6.1.9 In vitro construction of skeletal muscle (provided by the Shuo Bai group)

Skeletal muscle injury is a leading cause of pain and morbidity worldwide. Tissue engineering has emerged as a promising and effective approach to addressing the regeneration of skeletal muscle injuries. By combining scaffolds, muscle

cells, and growth factors, tissue engineering aims to construct functional muscle tissues for the replacement or repair of damaged tissues. The skeletal muscle is a highly organized tissue with a stiffness of 10–12 kPa and is responsive to electrical signals. Therefore, it is crucial to develop a tissue-engineered scaffold that mimics these characteristics for effective muscle repair. Taking this into consideration, Bai's group employed the directional freezing technique to fabricate an anisotropic conductive scaffold for skeletal muscle repair. The scaffold consisted of GelMA as the matrix hydrogel and silver nanowire (AgNW) as the conductive dopant. It was characterized by a directional longitudinal section and a honeycomb cross-section, with a mechanical strength of 10.5 kPa and an excellent conductivity of 0.26 $S \cdot m^{-1}$. These properties perfectly mimic the native muscle ECM. Through contact cues and electrical stimulation, the scaffold effectively guided the formation of arrayed myotubes in vitro and promoted muscle reconstruction in vivo.

In muscle tissue engineering, the implantation of self-renewing cells poses significant challenges. Three-dimensional bioprinting has emerged as a leading trend for fabricating anisotropic scaffolds to recreate skeletal muscle tissue in vitro [238] (Fig. 34a). Gu's group utilized the 3D bioprinting technology to construct skeletal-muscle-like bundles of different widths, such as 0.6, 2, and 5 mm [239] (Fig. 34b). They found that the differentiation and maturity of the myotubes were highest in the 0.6-mm group. This phenomenon can be attributed to the fact that cells in wider muscle-like bundles experience less stress because of their larger cross-section. Remote magnetic field technology has also been employed for anisotropic scaffold fabrication. Wu's group demonstrated the encapsulation of magnetically controlled short nanofibers into a photocurable GelMA hydrogel to fabricate an anisotropic scaffold using a remote magnetic control approach [240] (Fig. 34c). By guiding the 3D cellular alignment and organization using a remote magnetic field to mimic the anatomical locations of the native muscle tissue, the scaffold significantly enhanced the aligned myofiber formation in vivo and improved the functional recovery of the injured muscles in the animal volumetric muscle loss (VML) models. Despite the significant progress in muscle tissue engineering, the integration of innervation remains a challenge. Native muscle tissue is innervated through the peripheral nerve system via the formation of NMJs. Effective nerve integration into bioengineered skeletal muscle tissues is crucial for restoring muscle function and should be the focus of future research.

6.2 Digestive system

The human digestive system, comprising the alimentary canal and digestive glands, is responsible for converting ingested

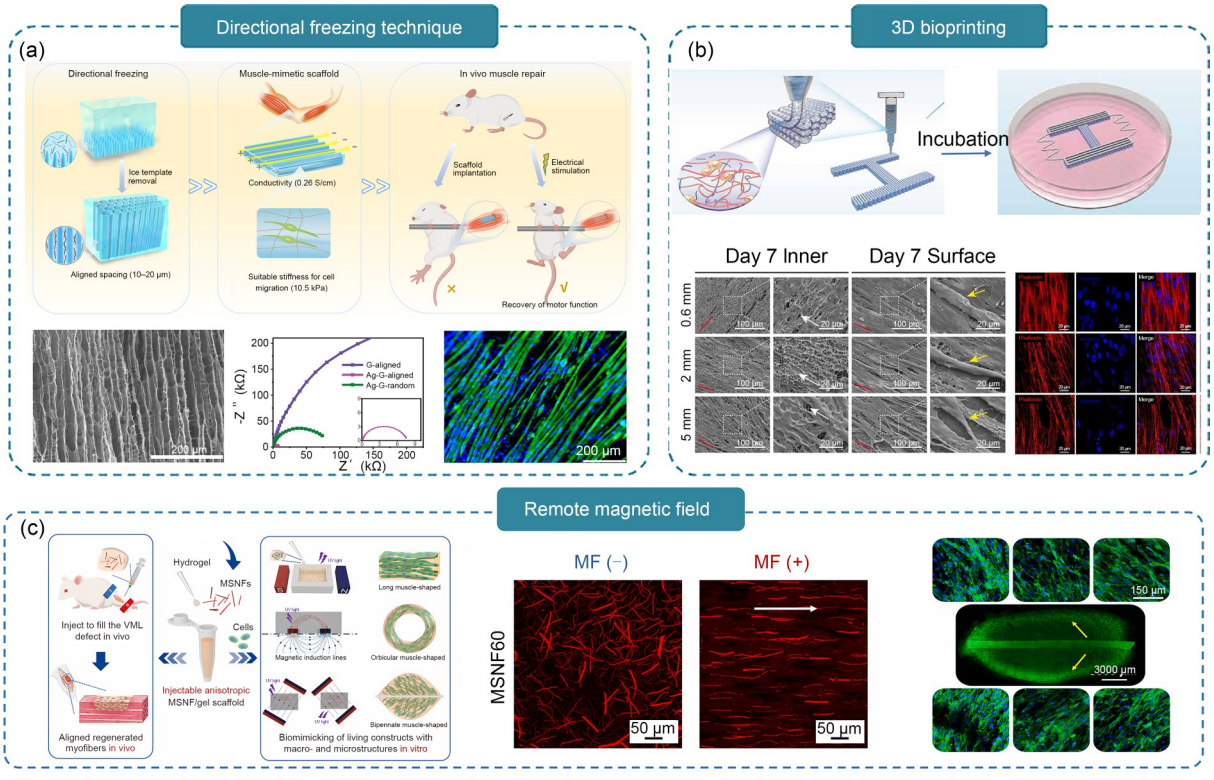

Fig. 34 Anisotropic scaffold fabrication method: (a) directional freezing technique; (b) 3D bioprinting; (c) remote magnetic field control. Part (a) was adapted from [238], Copyright 2023, with permission from Wiley. Part (b) was adapted from [239], Copyright 2021, with permission from the authors, licensed under CC BY 4.0. Part (c) was adapted from [240], Copyright 2022, with permission from Elsevier

food into energy and nutrients that are essential for life activities. Throughout this process, food undergoes intricate physical breakdown and chemical decomposition, gradually transforming into small molecules, which facilitates their absorption and utilization by the body.

Specifically, the mouth serves as the initial point of the alimentary canal, where food undergoes preliminary physical processing through chewing and crushing. Subsequently, food travels down the esophagus and enters the stomach, where it is further broken down into chyme under the combined action of gastric juice and hydrochloric acid. Next, in the small intestine—the primary site of nutrient absorption—nutrients are efficiently absorbed because of the increased surface area provided by the villi and microvilli that line the intestinal wall. In turn, the large intestine is primarily responsible for reclaiming water and electrolytes while facilitating the formation of feces from food residues, which are ultimately expelled from the body through the anus.

The digestive glands contribute to the chemical breakdown of food by secreting fluids that are rich in various digestive enzymes, thereby facilitating the smooth progression of the digestive process. The salivary glands secrete saliva containing amylase, which initiates the breakdown of starch in food. The gastric glands in the stomach secrete gastric juice containing pepsin, hydrochloric acid, and other enzymes, initiating the digestion of proteins and fats. The pancreas secretes pancreatic juice, which is abundant in multiple digestive enzymes that are capable of further breaking down carbohydrates, fats, and proteins. The gallbladder stores and concentrates bile, which is secreted by the liver, to aid the digestion and absorption of fats. Finally, the intestinal glands secrete intestinal juice, which continues to digest the residual food components within the small intestine.

6.2.1 Vascularized liver tissue (provided by the Qi Gu group)

Orthotopic liver transplantation is the most common treatment for patients with end-stage liver failure. The absolute liver shortage highlights the need for alternative liver sources for regenerative medicine. Currently, bioprinted liver tissues have demonstrated a certain level of liver functions, such as the synthesis of albumin and urea, glycogen accumulation, and drug metabolism [241]. The establishment of perfusable, multiscale vascular networks has allowed the size of printed tissues to surpass the limits of nutrient and oxygen diffusion, successfully constructing vascularized liver tissues that are larger than 1 cm [242, 243]. Moreover, engineered tissues have a functional and multiscale vasculature that could be immediately perfused upon implantation and efficiently supply oxygen and nutrients. However, the production of implantable and vascularized liver tissue remains a challenge. The Qi Gu team has proposed a multimaterial extrusion bioprinting method to fabricate soft, vascularized tissue at the centimeter scale [244] (Fig. 35a). This vascularized liver tissue supported the formation of capillary networks and mimicked the mature and functional liver tissue. Moreover, the printed vascularized liver tissue with an internal and external pressure-bearing layer was successfully implanted via direct vascular anastomosis to achieve immediate blood perfusion. Subsequently, the authors designed microgels crosslinked in cell-laden bioinks (Fig. 35b), which support angiogenesis to form spontaneous microvascular networks in vitro and enhance the mechanical stability of the tissue to withstand the shear stress from the physiological blood perfusion that occurs in vivo [245]. Furthermore, they proposed a paradigm of vascularized organ bioprinting and the

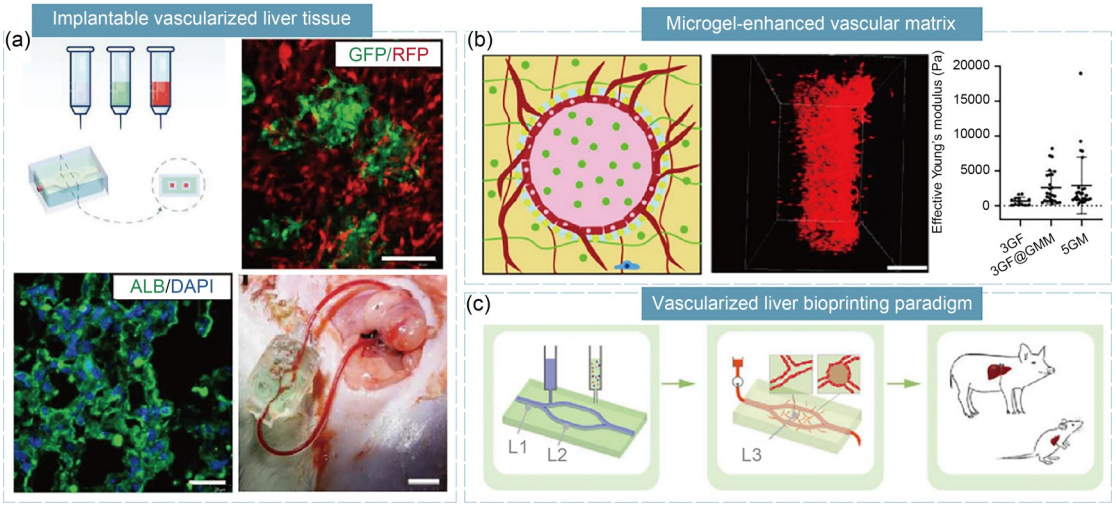

Fig. 35 Three-dimensional bioprinting of implantable vascularized liver tissue: (a) construction of the implantable vascularized liver tissue; (b) microgel-enhanced vascular matrix; (c) vascularized liver bioprinting paradigm. Part (a) was adapted from [249], Copyright 2021, with permission from Wiley. Part (b) was adapted from [245], Copyright 2023, with permission from the authors, licensed under CC BY. Part (c) was reproduced from [250], Copyright 2023, with permission from the authors, licensed under CC BY

math-model-based batch insight generator for future use [246]. The Dufva Martin team presented a method for the fabrication of thick and densely populated (e.g., 1×10^7 cells/mL) liver tissue constructs with a 3D four-arm branch network, which can be directly perfused on a fluidic platform for long periods (>14 days) [247] (Fig. 35c). In addition, millimetric vessel-like scaffolds and 3D-bioprinted vascularized tissues are interconnected, creating fully engineered hierarchical vascular constructs for implantation [248]. In conclusion, this work represents a significant step toward the fabrication and implantation of thick perfusable vascularized liver tissue, which lays the foundation for the transformation of engineered tissues in the future.

6.3 Respiratory system

The respiratory system, which encompasses the respiratory tract and lungs, is responsible for inhaling oxygen and exhaling carbon dioxide and other waste products. The respiratory tract, comprising the nasal cavity, throat, trachea, bronchi, and bronchioles, ensures the smooth passage of air into and out of the lungs, with each component performing specific functions, such as filtration, connection, airway support, and further subdivision of the airways. The lungs, as the core organ of gas exchange, consist of alveoli, lobes, pulmonary bronchi, and connective tissue. Among these, the alveoli serve as the basic units for gas exchange, the lobes form the structural basis of the lungs, the pulmonary bronchi subdivide and connect to the alveoli, and the connective tissue supports the lung structure and is rich in blood vessels and nerves, thus collectively maintaining respiratory function.

6.3.1 Bioengineered trachea-like structure

Tracheal stenosis caused by tumors, trauma, or congenital anomalies disrupts airway function. Tracheal resection with end-to-end anastomosis represents the gold-standard treatment for such stenosis. However, in patients necessitating extended resections, tension at the anastomosis site frequently leads to life-threatening complications, including anastomotic fistula and tracheal rupture. Therefore, the development of a practical strategy for tracheal reconstruction is urgently needed to improve patient outcomes. To address these challenges, the team of Yong He has proposed two innovative approaches: the design of "bio-concrete" composite materials (Fig. 36a) and the utilization of coaxial printing for the construction of multilevel vascular networks [251] (Fig. 36b). Bio-composites refer to the synchronous manipulation of cells and a biomimetic ECM by employing a combination of extrusion printing and near-field direct writing techniques. The latter technique allows the deposition of degradable fibers, mimicking collagen fibers, which provide sufficient mechanical support for biomimetic tissues [252]. These fibers also act as prefabricated templates that facilitate rapid cell growth [31, 253]. This design achieves localized softness to promote cell growth while maintaining the overall

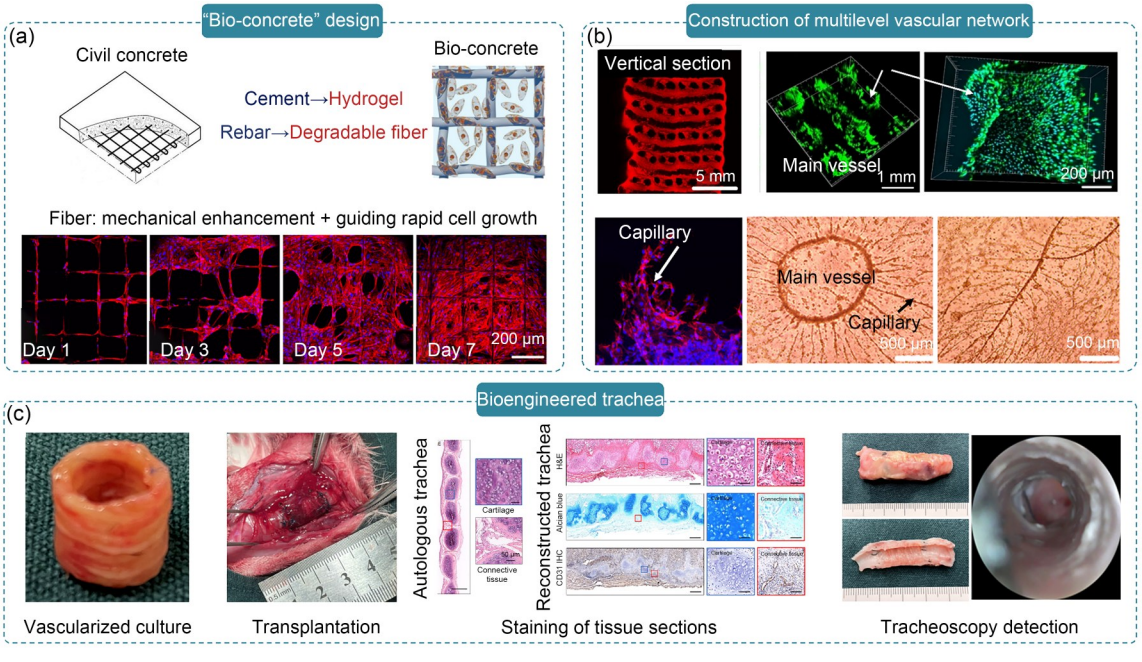

Fig. 36 Bioengineered trachea-like structure: (a) bio-concrete design; (b) construction of a multilevel vascular network; (c) implantation and repair effects of the bioengineered trachea. Part (a, lower) was reproduced from [31], Copyright 2019, with permission from Elsevier. Part (b, upper) was reproduced from [39], Copyright 2020, with permission from IOP Publishing. Part (b, lower) was reproduced from [26], Copyright 2022, with permission from the authors, licensed under CC BY 4.0. Part (c) was adapted from [27], Copyright 2023, with permission from the authors and exclusive licensee American Association for the Advancement of Science

toughness to fulfill the mechanical requirements. Furthermore, those authors proposed a coaxial bioprinting method that utilizes hollow fibers as the fundamental printing unit [254]. This approach effectively addresses the challenge of nutrient supply for the in vitro culture of centimeter-scale tissues [39, 255]. Building upon this foundation, they induced capillary growth through growth factor perfusion [256] and in vivo ectopic implantation, ultimately forming a multilevel vascular network. By leveraging these advancements, they designed a biomimetic trachea composed of a high-strength cartilage ring and a vascularized connective tissue ring [27]. This construct was subsequently transplanted into rabbits with tracheal defects. The bioengineered tracheal constructs exhibited mechanical properties that were comparable to those of the native rabbit trachea and displayed transmural vascularization between the rings. The eight-week survival rate in the transplanted rabbits was 83.3%, and the respiratory rate of these animals was similar to the preoperative levels (Fig. 36c).

6.3.2 Clinical applications of biodegradable implants (provided by the Jiankang He group)

Biodegradable implants are pivotal in tissue engineering by serving as temporary structural supports for tissue regeneration and holding great potential to become the next generation of clinically used medical implants [257]. Achieving optimal therapeutic outcomes requires a harmonious balance of biocompatibility, macro/microscale structures, mechanical properties, and the degradation–regeneration speed of these implants [258]. Significant strides have been made by Jiankang He's team regarding the additive manufacturing of patient-specific scaffolds with complex architectures, which greatly advanced their clinical applications, particularly in soft tissue engineering. The primary challenge of this approach lies in the accurate replication of the complex, multiscale architecture of natural soft tissues. To address this issue, He's team has refined their additive manufacturing techniques, including fused filament fabrication, selective laser sintering, and high-resolution electrohydrodynamic printing, to produce biodegradable tissue-engineered scaffolds with meticulously controlled macro/microarchitectures [259–263]. Upon in vivo implantation, these implants conform to the anatomical contours of the defect regions and provide a conducive microenvironment for cellular residence, thus promoting proper cell proliferation and differentiation [264, 265]. The second critical challenge of this technique lies in ensuring that the mechanical properties of the scaffolds mimic those of the native tissues. The team has addressed this issue by designing and fabricating scaffolds with highly tunable mechanical properties by utilizing designed porous structures (Fig. 37a) [266, 267]. This approach allows the creation of

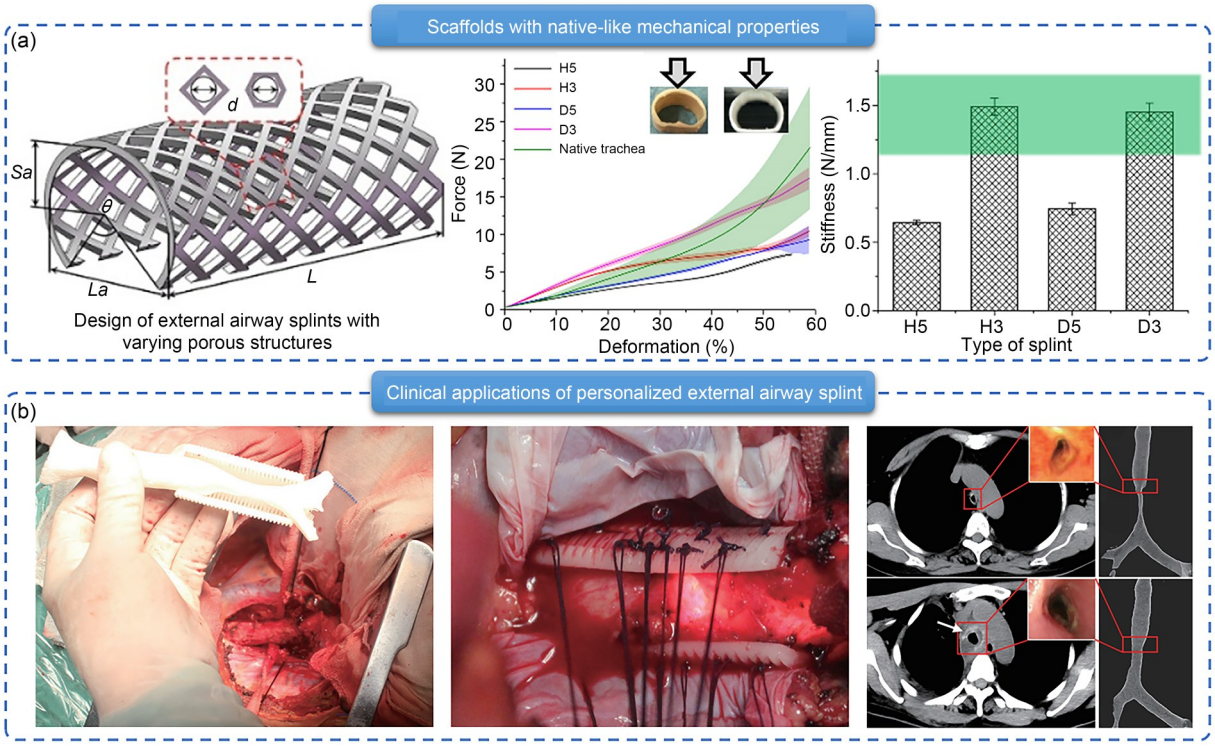

Fig. 37 Design, fabrication, and clinical applications of biodegradable implants: (a) design of biodegradable external airway splints with native-like mechanical properties; (b) clinical application of personalized biodegradable external airway splints. Part (a) was reproduced from [267], Copyright 2021, with permission from the authors, licensed under CC BY-NC-ND 4.0. Part (b) was reproduced from [272], Copyright 2016, with permission from Journal of Thoracic Disease

morphologically controlled scaffolds with an adjustable initial elastic modulus ranging from several tens of MPa to tens of kPa, which meets the mechanical requirements of various soft tissues, from cartilage to muscle and adipose tissues [268]. These design and manufacturing systems have exhibited efficacy in promoting breast tissue reconstruction and treating tracheomalacia in animal models [258, 269]. Building on this foundation, the team collaborated with the Xijing Hospital of the Air Force Medical University to conduct the first international clinical trial of customized flexible biodegradable breast implants. The outcomes of the implementation in 31 clinical cases showed that the biodegradable breast implants effectively integrated with the host tissues and supported tissue ingrowth [270, 271]. In addition, in collaboration with the Tangdu Hospital of the Air Force Medical University, the team proposed a tracheal suspension surgery using biodegradable airway splints, which represented the first clinical application of this material in China (Fig. 37b) [272]. The performance of this trial has shown promise, with the completion of 22 clinical cases to date [273–275]. Moreover, these clinical trials have garnered significant recognition and positive social responses, thereby highlighting the potential of addictively manufactured biodegradable implants for various clinical applications.

6.4 Nervous system

The nervous system serves as the core regulatory system of physiological functions within the organism; it is composed of neural tissues and is subdivided into the central nervous system and the peripheral nervous system. The central nervous system, which encapsulates the majority of the neural tissues, comprises the brain (including the cerebrum, cerebellum, and brainstem) and the spinal cord. It is responsible for information integration, command issuance, and advanced brain functions, such as consciousness, movement, sensation, and memory. Notably, the cerebrum plays a pivotal role and is also involved in endocrine regulation. The cerebellum modulates fine motor movements, whereas the brainstem harbors vital life-sustaining centers. In contrast, the peripheral nervous system encompasses cranial and spinal nerves, which are extensively distributed throughout the head, face, trunk, and limbs and are responsible for information transmission and feedback. These two systems work in close coordination to maintain normal physiological activities and environmental homeostasis in the human body.

6.4.1 Nerve regeneration (provided by the Mengfei Yu group)

Nerve injury, resulting in severe neurological damage and dysfunction both at the peripheral and central sites, has become a severe public health problem worldwide because of its physical, psychosocial, and economic burden. The peripheral nervous system has the intrinsic capacity for spontaneous regeneration and axon regrowth, to some extent, in contrast with the central nervous system (CNS) [276]. Presently, autograft surgery, which represents the mainstream therapeutic modality in peripheral nerve repair, remains problematic because of high morbidity at the donor site and regenerative fiber size mismatch. In detail, because of the extension difficulty of Büngner's bands and constant damaged environmental insults, peripheral nerve regeneration still faces various problems, including the low velocity and inaccurate direction of the peripheral nerve after injury. To tackle these problems, the group of Mengfei Yu established a multiresponsive dynamic repair system as an advanced strategy to promote peripheral nerve regeneration and functional recovery. First, using an updated bibliometric analysis, these researchers systematically reviewed and visually represented the three potential elements and four sequential phases of the development of a nerve guidance conduit (NGC) (Fig. 38a). They found that advanced NGCs should be manufactured as more-stimulus-responsive NGCs to comprehensively address long-distance peripheral nerve injury and multifunctional therapeutic needs [277]. Therefore, they fabricated a bilayer comprising a shaped memory polymer (SMP) and a hydrogel using 4D printing (Fig. 38b). This dynamic multilayer membrane can switch from a flat to a micropillar topography to enhance cell adhesion and proliferation and the differentiation of these behaviors [278]. Immediately afterward, they designed a 4D-oriented dynamic scaffold to repair the peripheral nerve (Fig. 38c). Subsequently, these stimulus-responsive NGCs can regulate early neuronal proliferation and promote axonal formation. Furthermore, 15 mm of significant segmental nerve defects in rats can be effectively repaired, and robust, functional, regenerating nerve bundles can be formed [279]. In contrast with its peripheral counterpart, the CNS exhibits a lower regenerative capability and faces even more complex pathological settings with inadequate axon-guiding and vascular signals. However, the repair of spinal cord injury, which is a severe traumatic CNS disorder, was also explored in their attempt. In addition, they fabricated dental pulp stem cell (DPSC)-loaded microspheres to repair spinal cord injury in rats (Fig. 38d). As transport vehicles produced by digital light processing printing, the microspheres provide a natural ECM environment to enhance excellent stemness as well as angiogenic and neurogenic potential [280]. In summary, the team of Mengfei Yu proposed a novel multi-stimulus-responsive NGC theory for nerve regeneration. Subsequently, they successfully constructed a multiresponsive dynamic repair system using 4D printing for peripheral nerve regeneration and functional recovery in vitro and in vivo. In conclusion, this work bridges the knowledge gap in multiresponse nerve regeneration, thus paving the way for the acceleration and functionalization of nerve regeneration.

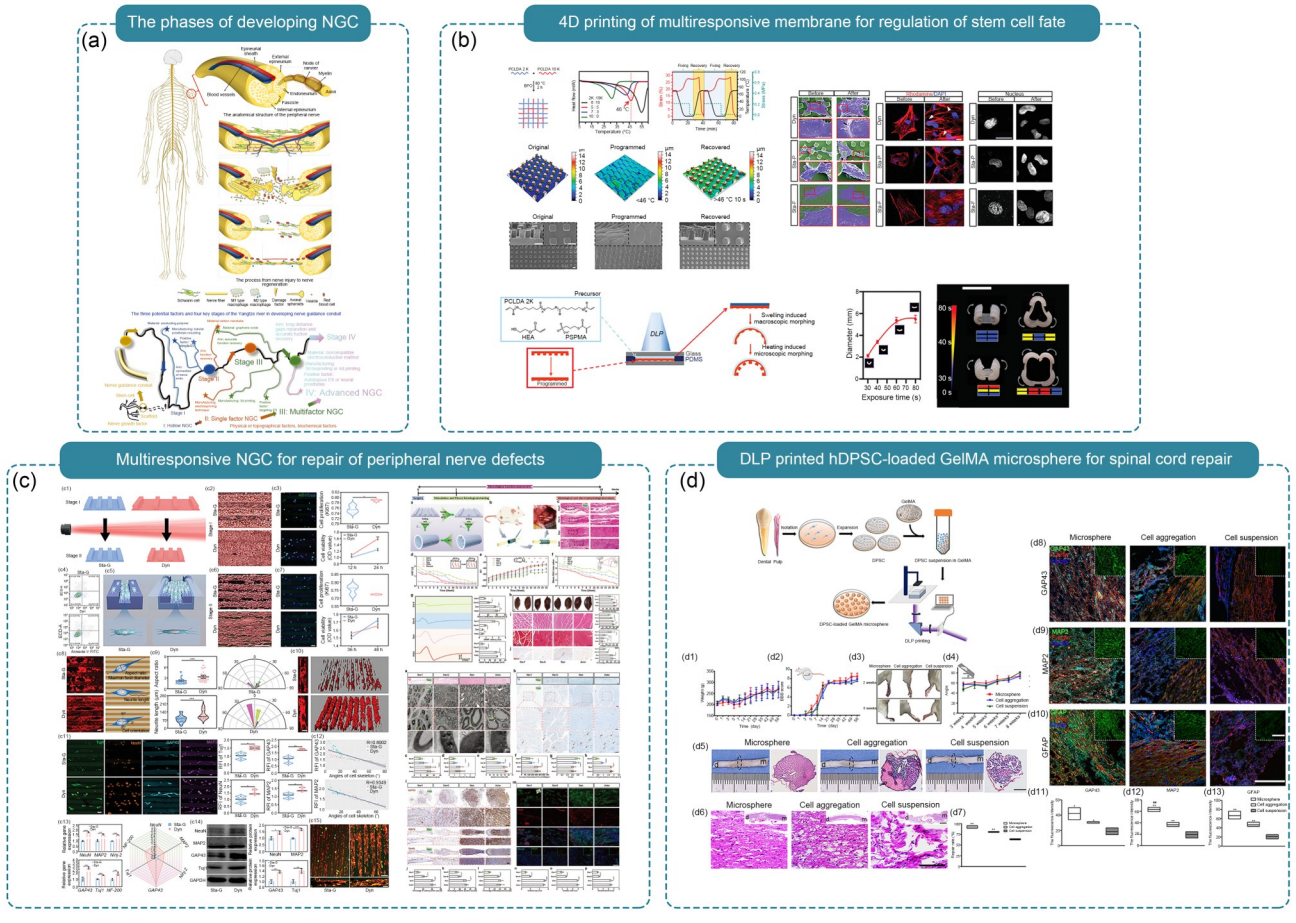

Fig. 38 Acceleration and functionalization of nerve regeneration: (a) the three potential elements and four stages of the development of nerve guidance conduit (NGC) are visually represented; (b) the dynamic regulation of surface topography by the shaped memory polymer (SMP); (c) a 4D dynamic scaffold is fabricated for peripheral nerve regeneration, showing the remarkable ability of neurological functional recovery; (d) dental pulp stem cell (DPSC)-loaded microspheres have a better recovery effect in locomotor function and tissue morphology compared with the groups of cell suspension and cell aggregation. Part (a) was reproduced from [277], Copyright 2023, with permission from Wiley. Part (b) was adapted from [278], Copyright 2021, with permission from Wiley. Part (c) was reproduced from [279], Copyright 2023, with permission from Wiley. Part (d) was adapted from [280], Copyright 2023, with permission from Elsevier

6.4.2 Scaffolds for spinal cord injury

Spinal cord injury (SCI) is a serious condition with over half a million new cases recorded annually. Recovery is hindered by a nonpermissive microenvironment and insufficient cell replenishment. Despite advances in the understanding of the pathology of SCI, no clinical therapy effectively balances neuroinflammation inhibition or neural circuit restoration. Human amniotic epithelial stem cells (hAESCs), which are derived from the placenta, are safe, hypoimmunogenic, and secrete anti-inflammatory and neurotrophic factors, which render them suitable for SCI treatment. However, scaffold-based cell-delivery systems face challenges such as insufficient cell loading and complex operation. A high flow resistance in scaffolds results in poor surface utilization and nonhomogeneous cell distribution. Cell-laden bioprinting offers customized implants with a dense cell arrangement, but compromises cell viability because of mechanical stress and free radicals. Improvements in the techniques are needed to mitigate cellular damage during fabrication (Fig. 39a).

The Yong He group developed a hyperexpansion scaffold (HES) with high cell loading via self-promoted absorption [281]. This system, which was termed HES–hAESCs, was tested in SCI models. GelMA scaffolds were dehydrated through super-absorption and adhesion postprocessing, which facilitated efficient cell absorption via macroscopic swelling and microscopic features. HES loaded 2.6 million uniformly distributed cells within 2 min in an hAESC suspension, rendering it an effective delivery tool for SCI repair. In rat SCI models, HES–hAESC treatment significantly improved hindlimb locomotion and motor-evoked potential signals. The treatment promoted axonal projections and myelination preservation, which were mediated by the hAESC-mediated inhibition of the immune response and increased neurotrophic factors. HES–hAESCs improved the tissue microenvironment and ameliorated motor deficits in rats with SCI.

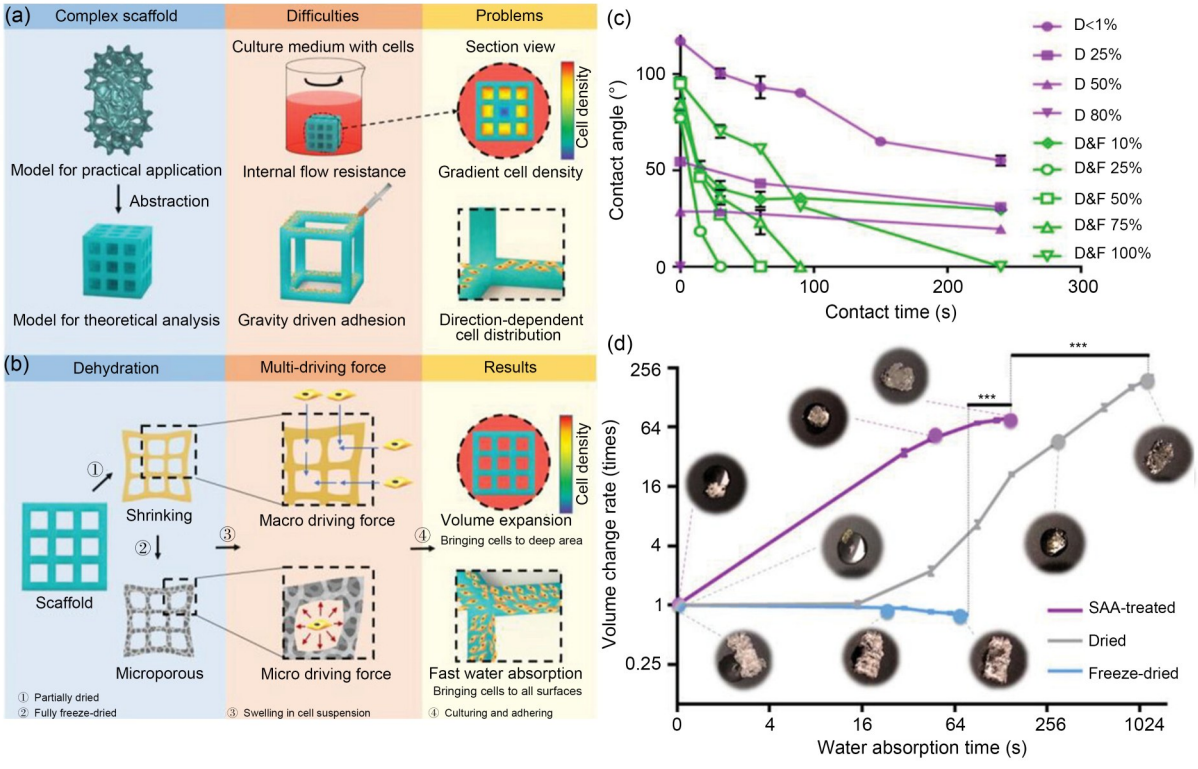

Fig. 39 Three-dimensionally printed cell absorption scaffold for spinal injury repair: (a) challenges of stem-cell-involved therapeutics in spinal cord injury (SCI) repair; (b) schematic diagram of the 3D-printed dual driving force scaffold; (c) contact angle changing over time during water absorbing; (d) the water absorbing rate and swelling volume of three-periodic minimal surface (TPMS) scaffolds with different postprocessing. Reproduced from [281], Copyright 2023, with permission from the authors, licensed under CC BY

The dual driving force model enables the self-promoted cell uptake by the hydrogel scaffolds. HES can efficiently load multiple cell types and can be manufactured for long-term storage and clinical use. hAESCs could be developed into a cellular agent that is compliant with good manufacturing practices. This work provides a clinically translatable approach with potential for treating SCI (Fig. 39b).

6.5 Circulatory system

The circulatory system, which is the cornerstone that sustains human physiological activities, comprises two major subsystems: the cardiovascular system and the lymphatic system. The cardiovascular system relies on the heart as its power source, via the intricate interplay of arteries, capillaries, and veins, to facilitate the circulation of blood throughout the body. This process ensures the delivery of oxygen and nutrients to all tissues and organs while simultaneously collecting metabolic waste and carbon dioxide for excretion. Conversely, the lymphatic system acts as an auxiliary to blood circulation, leveraging the lymphatic vessels, lymphatic organs, and lymphatic tissues to promote lymph circulation. It participates in vital physiological processes, such as fluid balance, immune defense, and waste removal. These two systems are intricately interconnected and complementary, and jointly ensure the accomplishment of material transportation, fluid regulation, internal environment stability, and defense mechanisms, thereby sustaining the normal physiological functions of the human body.

6.5.1 Synthetic vascular grafts (provided by the Jiayin Fu group)

Three-dimensional printing techniques can also be used for the fabrication of vascular graft templates using the geometries of the blood vessels and external or internal scaffolds for the blood vessels. For example, a polyvinyl alcohol (PVA) solution was extruded using a 3D printer to fabricate graft templates. Then, the graft templates were coated with thermoplastic polyurethane (TPU) to fabricate the vascular graft per se. After the removal of the PVA templates by immersion in water, the tubular constructs of TPU were obtained. Because the printing path can be controlled precisely using a digital apparatus, graft templates with complicated structures, such as bifurcate structures, can be generated [282]. Conversely, two additional groups demonstrated the feasibility of the fabrication of external scaffolds for blood vessels via 3D printing. One group printed a PCL solution helically on the outside of the vascular grafts using a microextruder. The fiber diameter of the 3D-printed material was around

100 μm and the 3D-printed helical PCL structures efficiently protected the vascular graft against dilation [283]. The other group directly printed the melt PCL onto a rotational mandrel using a fused deposition modeling 3D printer [76]. They first heated the PCL to 200 °C to completely melt the PCL, and then extruded the melted PCL into fibers with a size of 200 μm, which were deposited on a rotational mandrel. After cooling in air, the PCL external scaffolds were obtained by removing them from the mandrel. The external scaffolds efficiently prevented the dilation of vein grafts that were implanted in an arterial circulating system. The 3D-printed scaffolds can also be used as internal scaffolds of blood vessels. Zhi et al. fabricated PCL scaffolds with a fiber diameter of 60 μm via 3D-printing melting PCL, and then embedded them subcutaneously to induce the infiltration of host cells and the deposition of the ECM onto the PCL scaffolds. The host tissue-filled PCL scaffolds can then be used for vascular implantation without concerns about the occurrence of blood leakage [284].

However, because of its limited resolution (60–200 μm), 3D printing still cannot be used for the fabrication of vascular grafts per se, as large pores between the fibers can also cause serious blood leakage after arterial implantation. To solve this problem, an external electric field is added to the 3D printer to develop a high-resolution 3D printing technology—melt electrowetting, which can further diminish the diameter of the extruded fibers (800 nm to 150 μm). Using this new technology, Chen et al. developed a truly implantable and 3D-printed vascular graft [24] (Fig. 40a). The vascular graft contains two layers, the inner layer and the outer layer. The inner layer has fiber diameters of (35±2.8) μm and pore sizes of 200 μm, which allows rapid infiltration of the host cells and guided alignment. The outer layer, which mimics the adventitia of the arteries, has thinner fibers ((16.79±6.3) μm) and smaller pores ((25.84±6.7) μm), which can prevent over dilation and blood leakage from vascular grafts (Fig. 40b). After implantation in vivo for one month, the grafts regenerate the intima, media, and adventitia of the blood vessels and exhibit a pulsation that is similar to that of the native arteries, with a compliance (8.9%) that is quite close to that of the native ones (11.36%) (Figs. 40c and 40d).

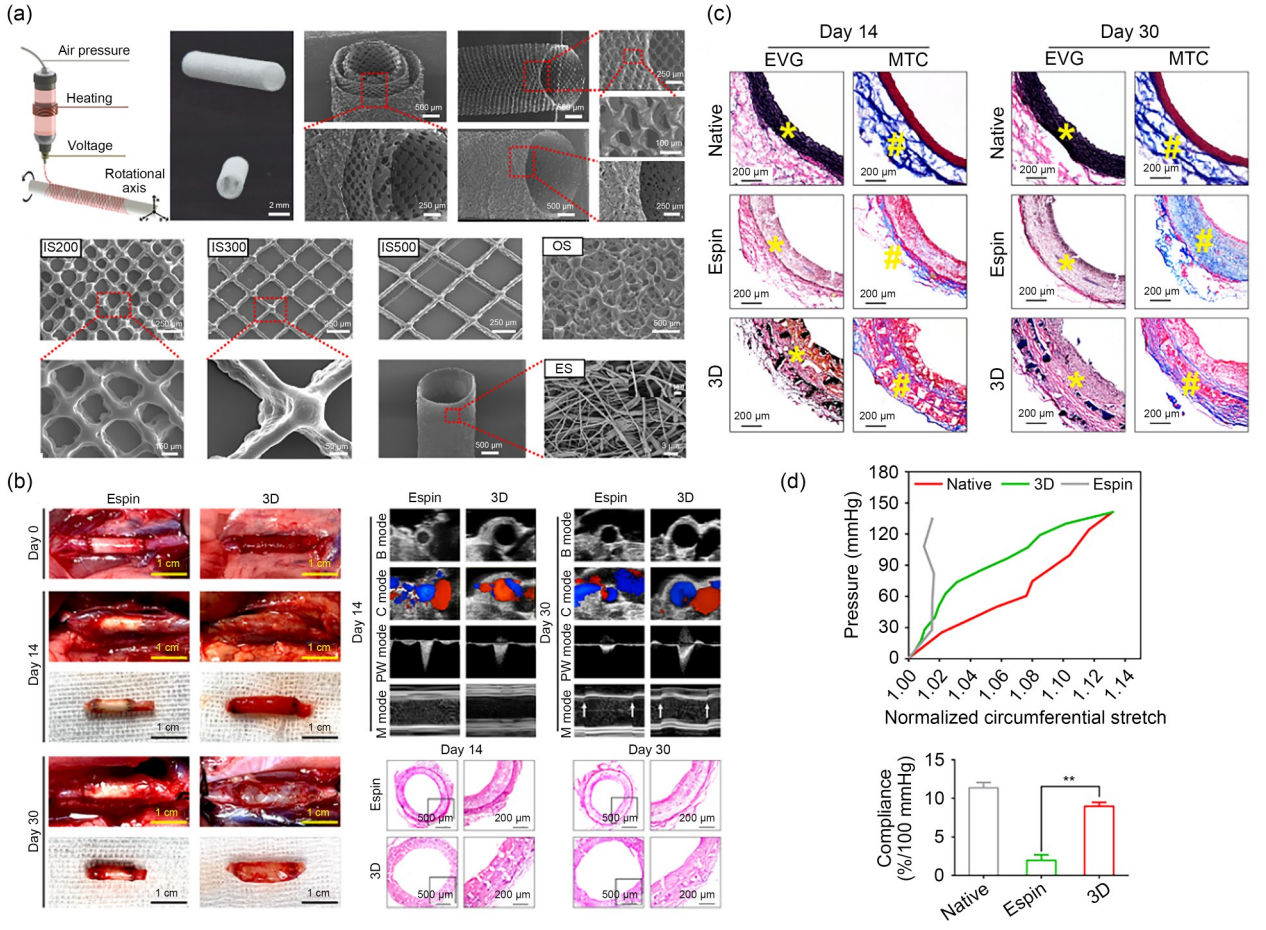

Fig. 40 Synthetic vascular grafts: (a) manufacturing method based on high-resolution melt electro-writing; (b) animal experiments of vascular graft implantation in vivo; (c) elastin and collagen staining of vascular grafts after 14 and 30 days of implantation in vivo; (d) compliance of vascular grafts after 30 days of implantation in vivo. Adapted from [24], Copyright 2024, with permission from the authors, licensed under CC BY 4.0

6.5.2 Multilevel vascularized structures (provided by the Lei Shao group)

The macro/micromultilevel vascular network system is very important for adequate nutrient/oxygen supply to every corner of the whole tissues/organs. Consequently, the 3D bioprinting of multilevel vascular systems within artificial tissues, ranging from macroscopic to microscopic vessels, is crucial for constructing large-volume artificial tissues and even complete organs. Moreover, the multilevel artificial vessels offer the possibility of a direct connection with the host's vessels upon transplantation, and the timely integration of the channels with the host's vessels can prevent the apoptosis of cells within the tissues and further promote the development of cells and tissues. The 3D bioprinting technologies that are used currently for creating vasculature include coaxial, sacrificial, embedded, and DLP-based bioprinting. For vascular structures, Yong He's team first proposed a coaxial 3D bioprinting method that utilizes hollow fibers as the fundamental printing unit [251, 254] (Fig. 41a). This approach effectively addresses the challenge of adequate nutrient supply for the in vitro culture of centimeter-scale tissues. Building upon this foundation, they induce capillary growth through growth factor perfusion and in vivo ectopic implantation, ultimately forming a multilevel vascular network [285, 286]. For sacrificial 3D bioprinting, the team of Lei Shao printed 3D sacrificial templates to engineer interconnected 3D vascular networks in hydrogels [287] (Fig. 41b). For embedded 3D bioprinting, the Tiantian Kong team constructed a freeform 3D network of interconnected tubular channels via interfacial coacervation by aqueous-in-aqueous embedded 3D bioprinting [288]. In turn, Zhuo Xiong's team developed expanding embedded 3D bioprinting to engineer complex organs with freeform vascular networks [131] (Fig. 41c). For

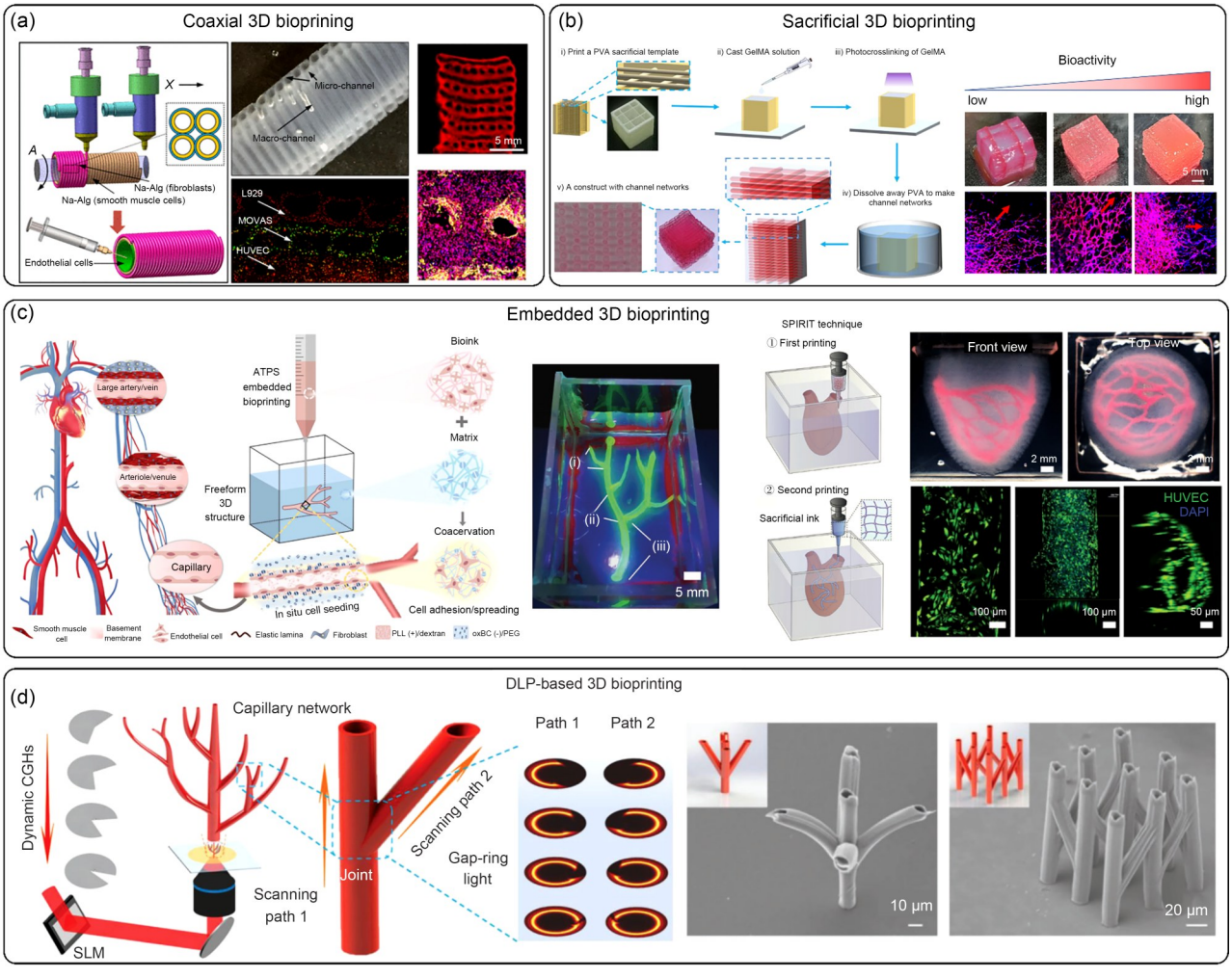

Fig. 41 Three-dimensional bioprinting of multilevel vascularized structures: (a) coaxial 3D bioprinting; (b) sacrificial 3D bioprinting; (c) embedded 3D bioprinting; (d) DLP-based 3D bioprinting. Part (a) was reproduced from [251], Copyright 2017, with permission from the American Chemical Society. Part (b) was reproduced from [287], Copyright 2022, with permission from the authors, licensed under CC BY-NC-ND 4.0. Part (c, left) was reproduced from [288], Copyright 2022, with permission from Wiley. Part (c, right) was reproduced from [131], Copyright 2023, with permission from Wiley. Part (d) was reproduced from [289], Copyright 2023, with permission from Wiley

DLP-based 3D bioprinting, the team of Jiawen Li achieved the rapid construction of 3D biomimetic capillary networks with a complex morphology using dynamic holographic processing [289] (Fig. 41d). Although there are many 3D bioprinting technologies that can construct multilevel vascular network structures, the construction of high-density vascular networks remains difficult. To construct high-density multilevel functional vascular networks, it is necessary to promote vasculogenesis and angiogenesis through perfusion culture.

6.5.3 3D bioprinting of stem cells (provided by the Qi Gu group)

The current bioprinting technology still has a limited capability to fully resemble the tissues/organs, and fails to mimic their biological functions and activities. It should be noted that the intrinsic potency of stem cells addresses the limitations of the current bioprinting technology. Numerous studies have demonstrated that stem cells can self-assemble or induce other cells to form heterogeneous and topologically complex organoids, among which the micron-scaled structures and the well-organized multiple cell lineages are beyond the highest bioprinting resolution [290, 291]. In this regard, through the regulation of endogenous genes or the induction of multiple factors (such as exogenous growth factors, biochemical signals, and mechanical signals), it is possible to construct complex tissues and organs using adult or pluripotent stem cells. Because of their functionality, robustness, and ease of acquisition, MSCs were one of the model cell types that were used in the early stage of bioprinting stem cells. Fedorovich et al. 3D-printed MSC/chondrocyte-containing hydrogel scaffolds to biologically fabricate biphasic osteochondral tissue equivalents, which provided a strategy for building highly reproducible structures and demonstrated the feasibility of bone repair [292].

Tissue-specific stem cells are also valuable tools for biofabrication. For example, Gu et al. developed a multimaterial bioink system that is suitable for printing human neural stem cells, in which the stem cells were expanded and differentiated in situ. The functionality of the printed neural tissue was demonstrated by the formation of synaptic contacts, neural networks, and a drug-responsive behavior [293] (Fig. 42a). In another study, Fan et al. bioprinted C2C12 cells to construct muscle tissues with highly aligned muscle-like bundles. The cells experienced proliferation and differentiation periods, followed by a well-observed self-assembly process of the muscle cells, which yielded highly aligned muscle fibers and enhanced mechanical performances [294] (Fig. 42c). Moreover, pluripotent stem cells are of higher interest to provide an ultimate solution for bioprinting. It is difficult to manipulate the cell fates of pluripotent stem cells (PSCs) in vitro; however, several pioneering studies have clearly demonstrated the potential of bioprinting PSCs. Ouyang et al. demonstrated the feasibility of bioprinting embryonic stem cells with hydrogels onto 3D macroporous structures that maintained viability, pluripotency, cell growth, and directed embryoid body formation [295]. Gu et al. extruded iPSC-laden, polysaccharide-based bioinks that allowed the differentiation of iPSCs into three germ lineages or more homogeneous functional neural tissues in situ [296] (Fig. 42b). In addition to the bioink material, the topological cues are crucial for manipulating the embryo fates [297]. As mentioned previously, the regulation of endogenous genes could be a powerful tool to manipulate bioprinted stem cells. In a recent study, Skylar-Scott et al. [106] engineered patterned tissues comprising neural stem cells, endothelium, and neurons in a one-pot manner, which was achieved by utilizing multimaterial co-extrusion and genetically programmed iPSCs. By overexpressing certain transcription factors, programmed iPSCs differentiated into desired cell types independent of the culture media, which indicated the potential of the use of synthetic biology approaches in stem cell bioprinting.

6.5.4 Functional cardiac/nervous tissue constructs (provided by the Jiankang He group)

The recapitulation of the complex structures and highly vascularized architectures of the native myocardium and nervous tissue is crucial for engineering functional cardiac and nervous tissue constructs, which are valuable for investigating their physiological activities, developing drugs, and treating injuries [298–300]. The group of Jiankang He fabricated layer-specifically-oriented, multiscale conductive scaffolds for cardiac regeneration, which were designed to mimic the complex architecture and electrical properties of the native myocardium [301] (Fig. 43a). The PCL microfibers and conductive submicrofibers were deposited with gradual angular rotation to guide multiple-layer cellular alignment. The primary cardiomyocytes (CMs) seeded in the multiscale conductive scaffolds exhibited an improved synchronous beating behavior and increased CM-specific gene expression compared with those in the pure microfibrous scaffolds. The same group further developed a novel strategy to direct 3D cellular alignment by embedding cell/hydrogel (collagen or fibrin) suspensions into the predefined microlattice scaffolds without any external stimuli [121, 122] (Fig. 43b). The cells/hydrogel gradually reorganized to form multidirectional cardiac bands along the orientations of the printed microfibers. The resultant 3D cardiac constructs expressed mature CM-specific phenotypes and exhibited improved electrophysiological activity. With the addition of endothelial cells, the prevascularized engineered cardiac constructs effectively realized functional repair of the infarcted myocardium in vivo, as evidenced by the reduced infarcted area and enhanced neovascularization.

As an exploration, human induced pluripotent stem cell-derived CMs were employed in a similar strategy to produce

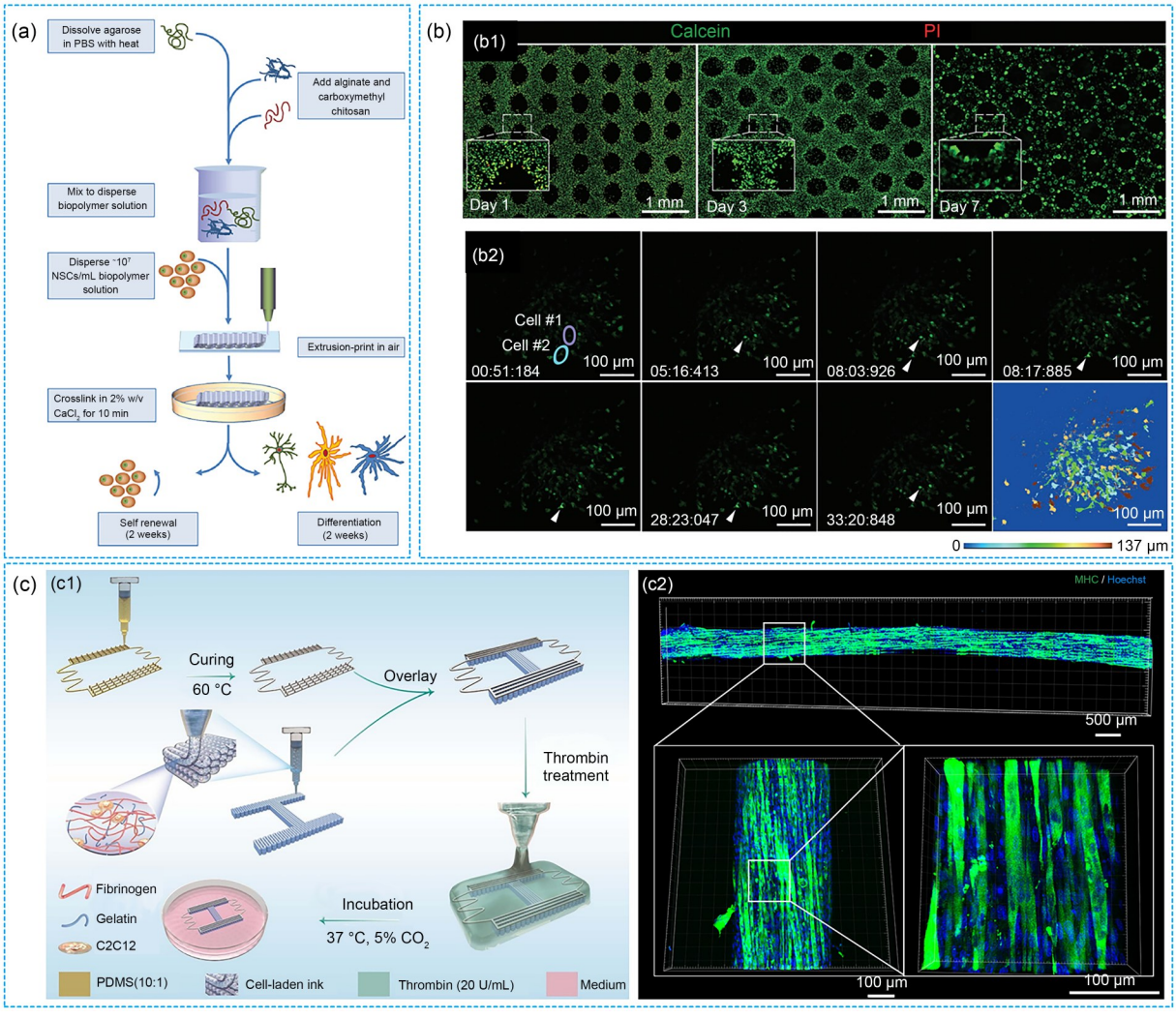

Fig. 42 Three-dimensional bioprinting of adult and pluripotent stem cells to fabricate tissue-specific constructs. (a) Schematics of the bioprinting neural tissues using neural stem cells followed by in situ differentiation. (b1) Live/dead staining of bioprinted iPSCs postprinting and (b2) time course of bicuculline-induced calcium flux for individual neurons 1–2 within the bioprinted porous construct, demonstrating neural function and cell migration. (c1) Schematics of the bioprinting of muscle-like bundles and (b2) immunofluorescent images of mature and highly aligned muscle fibers. Part (a) was reproduced from [293], Copyright 2016, with permission from Wiley. Part (b) was reproduced from [296], Copyright 2017, with permission from Wiley. Part (c) was reproduced from [294], Copyright 2021, with permission from the authors, licensed under CC BY 4.0

leaf-venation cardiac constructs [302, 303] (Fig. 43c). These constructs, consisting of a hierarchical structure for high-efficiency action potential transmission, exhibited an evident structural and functional improvement as the culture time increased. Supported by PCL microfibers, the 3D constructs demonstrated programable mechanical properties and shape recovery after injection, without compromising cellular viability, which illustrated their potential for minimally invasive clinical implantation. In addition, the Ling Wang group produced a 3D hollowed coaxial neurovascular model using a two-stage methodology consisting of embedding printed endothelial layers and casting to construct astrocyte layers [304] (Fig. 43d). The dynamic regulation of the concentration of the hydrogel enabled high stiffness for printability during the shaping stage, followed by targeted lysis, to reduce the hydrogel modulus, thus ensuring cellular functionalization during the culturing stage. As a result, the endothelial cells in the engineered neurovascular constructs exhibited tight junction proteins and selective permeability, whereas the astrocytes spread out with branches and interacted directly with the endothelial cells. These engineered cardiac and neurovascular constructs provide a promising modeling method for a better understanding of tissue functions and damage repair.

6.5.5 Biomimetic vascular network (provided by the Huixia Xuan group)

Vascular networks are vital for sustaining tissue function by concurrently supplying cells with adequate oxygen and

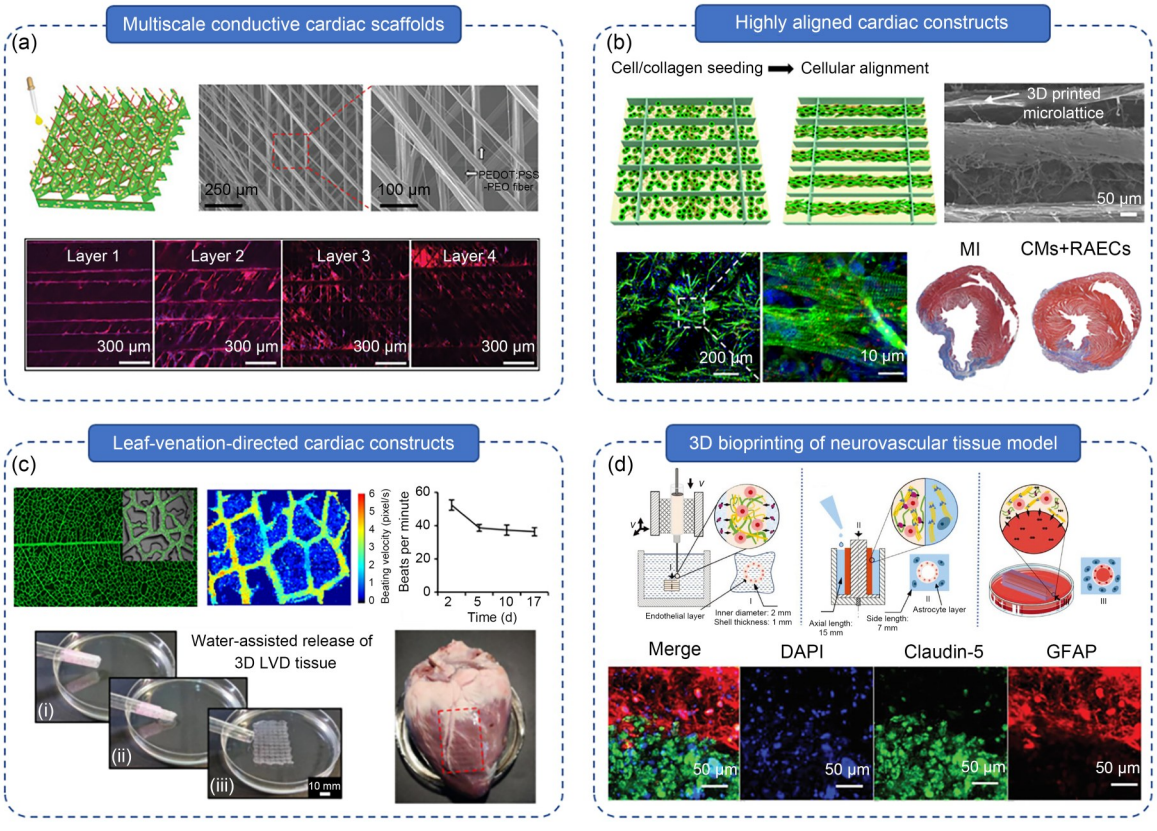

Fig. 43 Bioprinting of functional cardiac/nervous tissue constructs: (a) multiscale conductive cardiac scaffolds for directing cell-layer-specific alignment; (b) engineering of highly aligned cardiac constructs for infarcted myocardium repair; (c) leaf-venation-directed engineered cardiac constructs for injectable delivery; (d) 3D bioprinting of the neurovascular tissue model. Part (a) was reproduced from [301], Copyright 2019, with permission from the Royal Society of Chemistry. Part (b) was reproduced from [121] (Copyright 2019, with permission from Acta Materialia Inc.) and [122] (Copyright 2022, with permission from IOP Publishing). Part (c) was reproduced from [302], Copyright 2023, with permission from the authors, licensed under CC BY 4.0. Part (d) was reproduced from [304], Copyright 2023, with permission from the authors, licensed under CC BY

nutrients while facilitating the effective elimination of metabolites. However, mimicking natural microvascular networks to establish a long-range, functional mass exchange and transport system remains a challenge. Some strategies, such as laser microablation and micromolding, have been utilized to construct vascular tissues; nevertheless, it is difficult to prepare 3D constructs using these approaches, and multiple complex steps are often required. Three-dimensional printing has facile, customizable, and controllable features and has been widely utilized in tissue engineering. The You group at Donghua University presented a novel strategy inspired by the Chinese traditional caramel painting art to create biodegradable perfusable and permeable hierarchical microchannel-networks (PHMs) via the combination of one-pot 3D-printed sacrificial caramel templates and polymer coating with integrated phase separation [305] (Fig. 44a). The PHMs are similar to natural vascular networks in different length scales with well-organized structural features, including a custom-made scalable 3D framework, interconnected microchannels, and permeable walls with controllable micropores. This strategy can be adapted to various polymers and integrated with diverse technologies to create a series of composite scaffolds, including hydrogels, porous scaffolds, and electrospun nanofibers with a built-in hierarchical transport system. PHMs are capable of promoting cell attachment, proliferation, osteogenesis, and angiogenesis compared with the normal non-hollow-pipe-structured scaffolds, as well as enhancing bone regeneration and vascularization in rabbit bone defects [306]. Using this strategy, He's team developed a microchannel-network-enriched nanofibrous scaffold to sequentially release dimethyloxalylglycine and bone-forming peptide-1 to treat a skull defect [307] (Fig. 44c). Furthermore, You and coworkers created a perfusable and multifunctional epicardial device consisting of a biodegradable elastic patch, PHMs, and a system that enabled the delivery of therapeutic agents from a subcutaneously implanted pump [308] (Fig. 44b). The device yielded promising results in the treatment of myocardial infarction. The feasibility of minimally invasive surgical device implantation in pigs was verified, demonstrating its promise for clinical translation to treat heart disease. Recently, this fabrication strategy was also used to customize multilevel epi-/peri-/endoneurium-mimetic branched nerve

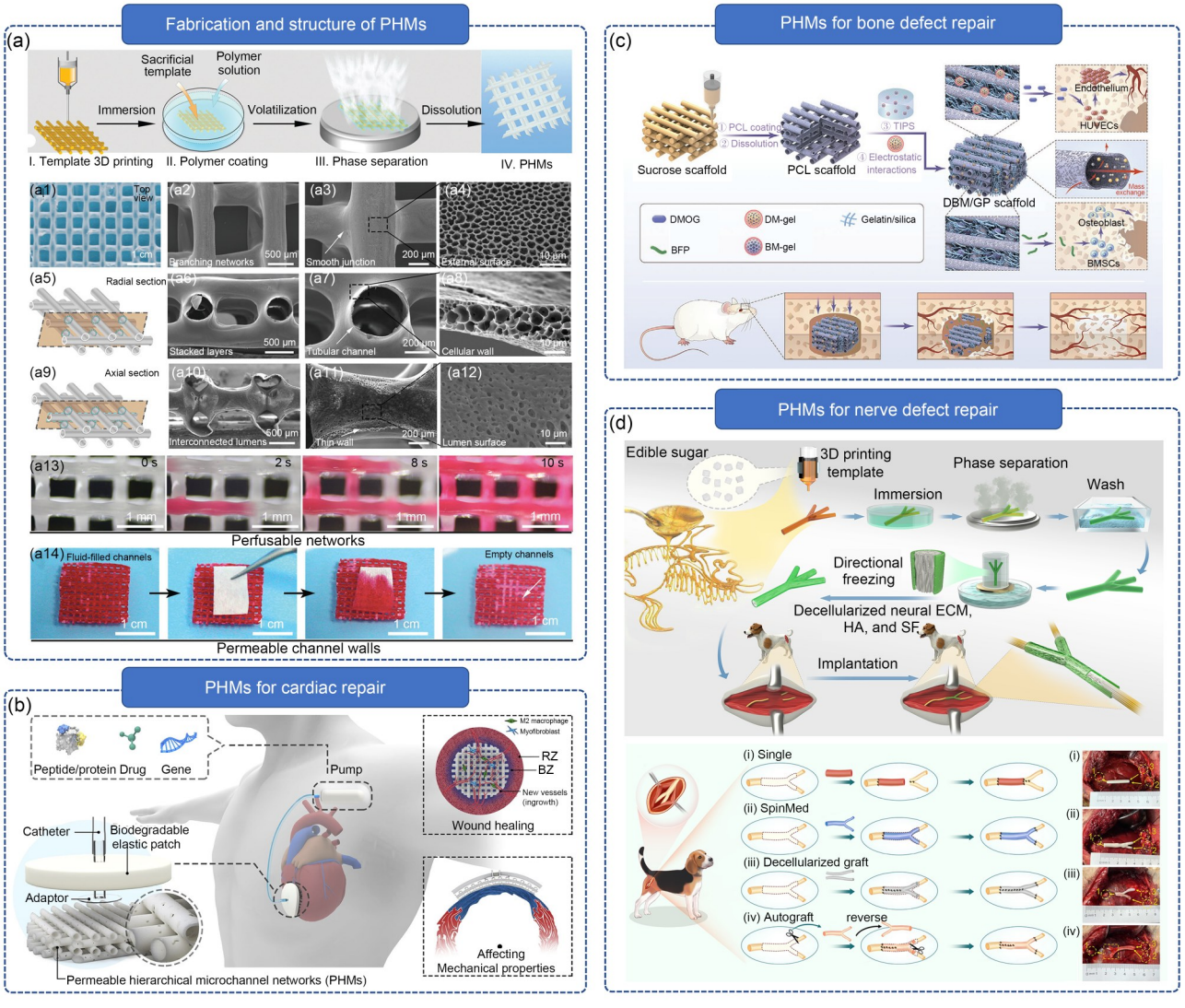

Fig. 44 Design and application of biomimetic vascular networks using 3D printing: (a) schematic diagram of the preparation, morphology, and mass exchange ability of the perfusable and permeable hierarchical microchannel networks (PHMs) with hierarchical architectures; (b) schematic diagram of the application of a PHM-based multifunctional epicardial device for treating myocardial infarction; (c) schematic diagram of a microchannel-network-enriched nanofibrous scaffold for skull defect treatment; (d) illustration of multilevel epi-/peri-/endoneurium-mimetic device for the repair of complicated sciatic nerve defects and surgical procedures. Part (a) was reproduced from [305], Copyright 2019, with permission from the Royal Society of Chemistry. Part (b) was reproduced from [308], Copyright 2021, with permission from the authors, under exclusive licence to Springer Nature America. Part (c) was adapted from [307], Copyright 2022, with permission from Wiley. Part (d) was reproduced from [309], Copyright 2024, with permission from the authors, licensed under CC BY 4.0

grafts to support rapid vascular reconstruction and consequent efficient repair of the nerve trunk, especially branches, superior to that achieved by decellularized grafts and even autografts in an animal nerve defect model [309] (Fig. 44d). Overall, this caramel painting-inspired 3D-printing strategy provides a simple and versatile way to fabricate sophisticated 3D constructs, which are difficult to achieve using the existing methods. This innovative concept and the corresponding design are suitable for a wide range of applications, such as the treatment of irregular injuries, massive defects, and bulky disease models, and provide powerful tools for diverse fields, including tissue regeneration and organ chips.

6.6 Reproductive system

The reproductive system is a pivotal system for sustaining human reproduction and reproductive health and is categorized into male and female systems. The male reproductive system encompasses internal genitalia (testes, epididymis, vas deferens, etc.) and external genitalia (penis and scrotum), which are primarily responsible for sperm production, maturation, and transportation, as well as sexual-behavior execution. The testes, as the core organ, not only produce sperm, but also secrete testosterone, which is crucial for the development of male reproductive organs and the maintenance of

secondary sexual characteristics. Conversely, the female reproductive system consists of internal genitalia (ovaries, fallopian tubes, uterus, and vagina) and external genitalia (mons pubis, labia majora, etc.), which oversee oogenesis, fertilization, pregnancy, and parturition. The ovaries, which are the central organ of the female reproductive system, secrete estrogen and progesterone to promote the development of reproductive organs and maintain female characteristics.

6.6.1 Penile cavernous repair (provided by the Xuetao Shi group)

The penis is a critical external genital organ in males that is susceptible to a range of health challenges, including trauma, senescence, and surgical interventions, which may result in the impairment of standing urination and varying levels of erectile dysfunction [310]. In cases of partial penile injury, penile reconstruction surgery is commonly utilized to restore penile morphology; however, the restoration of erectile function remains a formidable challenge. The current research in this area is limited, predominantly focusing on acellular matrices or stem cell therapies, with outcomes that have yet to meet the desired efficacy [311, 312]. By recognizing the pivotal role of porous cavernous tissue in penile erection, in 2020, Shi and colleagues pioneered the use of a 3D-printed hydrogel scaffold to replicate the sinusoidal architecture, thereby facilitating the repair of penile damage [313]. Utilizing a 3D-printed hybrid GelMA and HAMA hydrogel scaffold, they seeded muscle-derived stem cells with a hypoxia-inducible factor-1α (HIF-1α) mutation, which, upon implantation in a rabbit model, led to microvascular regeneration in the injured cavernous tissue and subsequent recovery of erectile function [313] (Fig. 45a). Despite these advancements, the dynamic microenvironment of penile tissue poses a risk of mechanical incompatibility and scaffold damage post-implantation, which could adversely impact the efficacy of cavernous tissue repair. To mitigate this problem, the Shi group developed a novel diffusion-induced phase separation (DIPS) 3D-printed hydrogel system that was characterized by strain-hardening properties and was further reinforced via hydrogen bonding and chemical crosslinking [314]. By combining this mechanically robust hydrogel scaffold with the previously developed biomimetic artificial tunica albuginea [315], those authors successfully repaired extensive penile defects and restored erectile, copulatory, and ejaculatory functions in male rabbits [314] (Fig. 45b). Although the integration of 3D printing technology into penile tissue engineering is a relatively recent development, and the field remains nascent, with significant strides yet to be made before clinical translation [316], the ongoing evolution of 3D printing holds promise for the precise replication of penile tissue at the macroscopic and microscopic scales, as well as in terms of cellular distribution. It is anticipated that these advancements will enable the repair of more complex tissue injuries, ultimately benefiting the patients affected by them.

6.7 Immune system

The immune system constitutes a complex and intricate network within the human body that is tasked with safeguarding the organism against invasion by external pathogens (such

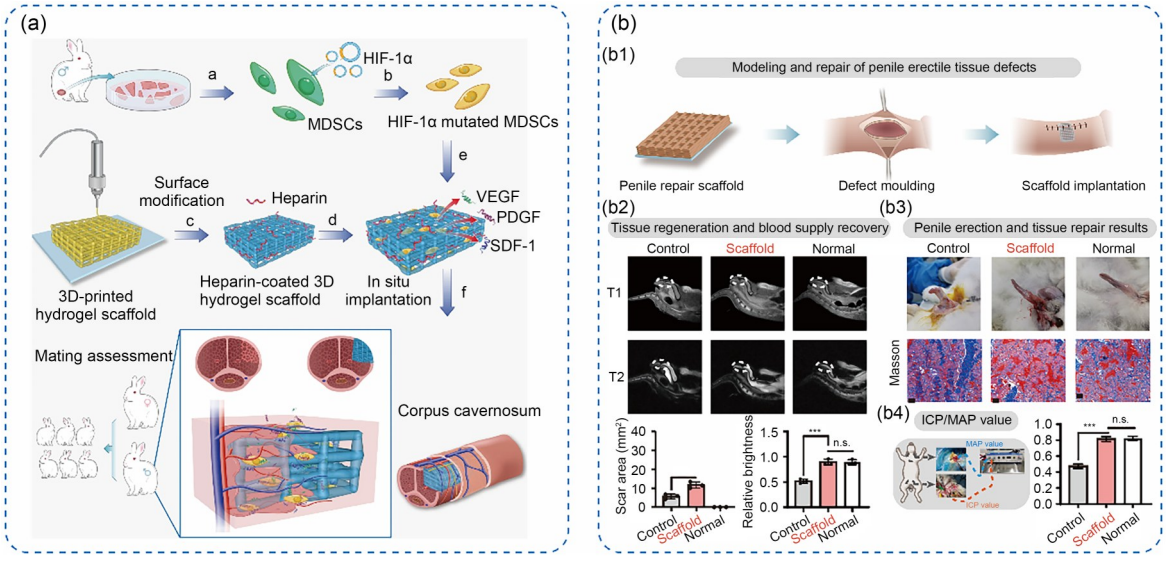

Fig. 45 Three-dimensionally printed hydrogel scaffolds for corpus cavernosum repair: (a) schematic illustration of the repair of an injured corpus cavernosum using 3D-printed hydrogel scaffolds seeded with hypoxia-inducible factor-1α (HIF-1α)-expressing stem cells in rabbits; (b) dynamically adapted penile repair scaffolds for the treatment of penile erectile tissue defects. Part (a) was reproduced from [313], Copyright 2020, with permission from the authors, licensed under CC BY 4.0. Part (b) was adapted from [314], Copyright 2024, with permission from the authors, licensed under CC BY

as bacteria and viruses) and maintaining the stability of the internal environment. This system comprises three primary components: immune organs, immune cells, and immune molecules. The immune organs encompass both the central and peripheral immune organs and serve as the cornerstone of the immune system.

Central immune organs, as exemplified by the thymus and bone marrow, are the sites at which immune cells are generated, differentiated, and matured. Specifically, the bone marrow serves as the birthplace of various blood cells and immune cells, whereas the thymus provides a crucial environment for the development and maturation of T cells. Peripheral immune organs, including the spleen, lymph nodes, and tonsils, serve as the habitats for mature immune cells and the venues where immune responses are initiated. These organs capture, process, and present antigens to immune cells, thereby triggering immune responses.

Furthermore, additional immune organs or tissues, such as the appendix and the skin, play significant roles in the immune system. Although the skin is primarily recognized for its protective, sensory, thermoregulatory, secretory, and excretory functions, it possesses robust immunological capabilities, acting as a vital immune barrier.

6.7.1 Skin substitutes in vitro (provided by the Qi Gu group)

In recent years, 3D bioprinting has emerged as a transformative technology in tissue engineering and regenerative medicine. One of its exciting applications is the development of skin substitutes in vitro, aiming to mimic the complex structure and function of native human skin. Recent studies have highlighted the potential of bioprinting techniques for fabricating skin substitutes containing keratinocytes, fibroblasts, and epidermal stem cells [317, 318]. The team of Haochen Liu constructed a dermis with fibroblasts and layered laminin and keratinocytes over it [317]. They used a sterile wire mesh for the air–liquid interface (ALI) culture used to prepare full-thickness skin tissue. In recent years, the remodeling of sweat glands and hair follicles has been shown to be important in skin substitutes [319, 320]. Xiaoping Fu's team bioprinted a sweat gland (SG)-like matrix to guide the transformation of mesenchymal stem cells into functional sweat glands and promote sweat gland recovery in mice (Fig. 46a) [320]. In addition, efforts have been made to incorporate vascular networks within bioprinted skin substitutes to facilitate nutrient transport and waste removal, which

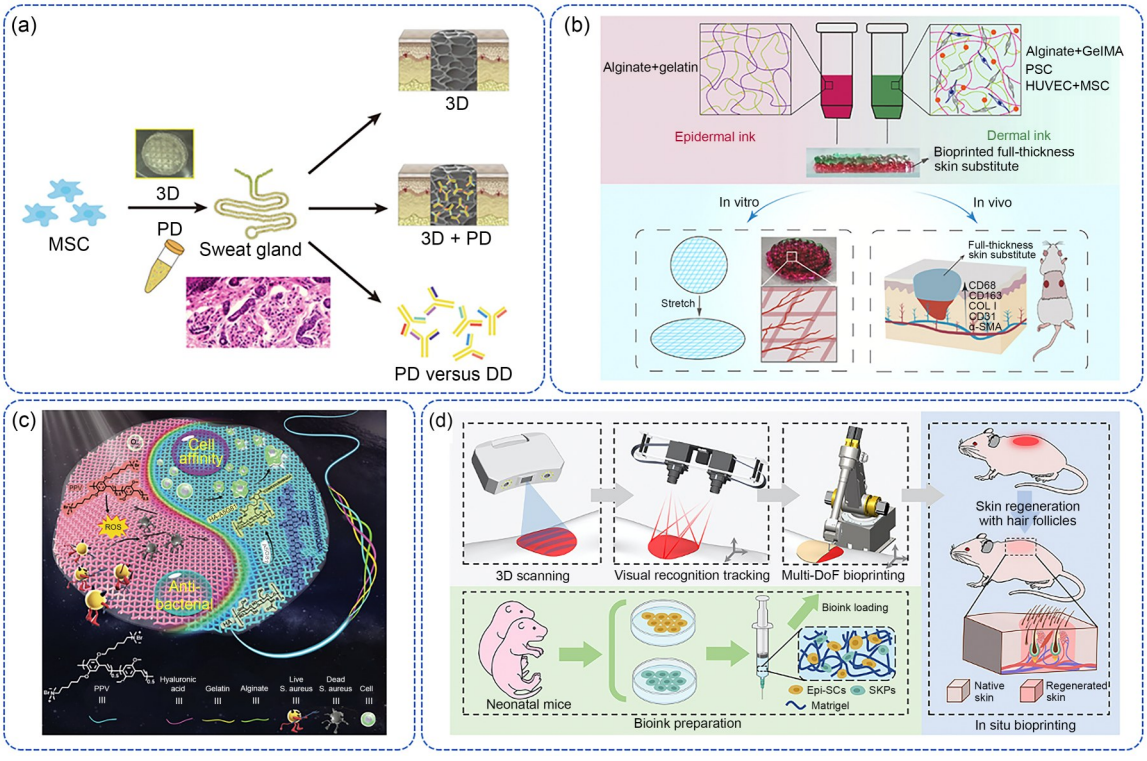

Fig. 46 Three-dimensional bioprinting of skin substitutes in vitro: (a) three-dimensional bioprinting of a skin substitute containing a sweat gland (SG)-like matrix; (b) 3D bioprinting of a vascularized full-thickness skin substitute; (c) 3D bioprinting of an antibacterial artificial skin patch containing poly(phenylene vinylene) derivative (PPV); (d) in situ bioprinting of the skin in mice. Part (a) was reproduced from [320], Copyright 2020, with permission from the authors and exclusive licensee American Association for the Advancement of Science. Part (b) was reproduced from [321], Copyright 2023, with permission from the authors, licensed under CC BY-NC-ND 4.0. Part (c) was adapted from [325], Copyright 2022, with permission from the Royal Society of Chemistry. Part (d) was reproduced from [327], Copyright 2022, with permission from the authors, licensed under CC BY

are essential for the long-term viability and functionality of the constructs [321–323]. To address these challenges, Qi Gu's team has proposed a vascularized full-thickness skin substitute (Fig. 46b) [321]. The bioprinted skin was composed of an epidermal layer with toughness and mechanical properties, and the dermal layer exhibited suitable mechanical properties, biocompatibility, and induced vascularized bioactivity. In terms of application, skin grafts should not only promote wound healing and protect the body from microorganism invasion, but also reduce the need for secondary surgeries and mitigate potential scarring risks. In Huang Sha's study, a 3D functional human hypertrophic scar model consisting of preformed cellular aggregates (PCA) was described to study its therapeutic interventions [324]. The human hypertrophic scar model was developed from the scar decellularized ECM to mimic the microenvironmental factors. The team of Qi Gu developed a 3D-printed artificial skin patch containing a photoactive cationic conjugated poly(phenylene vinylene) derivative (PPV), which exhibited excellent photodynamic therapy (PDT)-based anti-infection superiority against *Staphylococcus aureus* (Fig. 46c) [325, 326]. In recent years, with the advancement of 3D printing technology, in situ printing of skin has also been developed. Tao Xu's team developed an adaptive bioprinting robot that afforded rapid in situ bioprinting [327]. In combination with robotics, epidermal stem cells and skin-derived precursors isolated from neonatal mice were mixed with Matrigel and printed directly onto the injured site to replicate the skin structures (Fig. 46d). In conclusion, these developments hold promise for applications in wound healing, disease modeling, and personalized medicine.

7 Outlook

Breaking the shackles of time and space has always been a great dream held by humanity. In the spatial dimension, we aspire to explore the mysteries of the universe and achieve the feat of interstellar migration; in the temporal dimension, we hope to prolong the journey of life and replace aging organs. In fact, in the early stages, researchers envisioned utilizing the 3D bioprinting technology to manufacture transplantable organs. However, as research progressed, scientists discovered that the task of creating artificial organs was exceedingly arduous. Thus, the topic of "organ printing" gradually faded from public view after 2010. However, in recent years, with the rapid advancement of 3D printing technology, we believe that it is time to reconsider the issue of transplantable-organ manufacturing. Although the journey toward achieving this goal remains long and arduous, it is no longer purely in the realm of science fiction.

To advance toward this goal, our primary focus should be the achievement of more biomimetic designs, more precise printing, and more bioactive inks (Fig. 47a). Given the limitations in the current manufacturing capabilities, biomimetic designs need to be aligned with engineering implementation

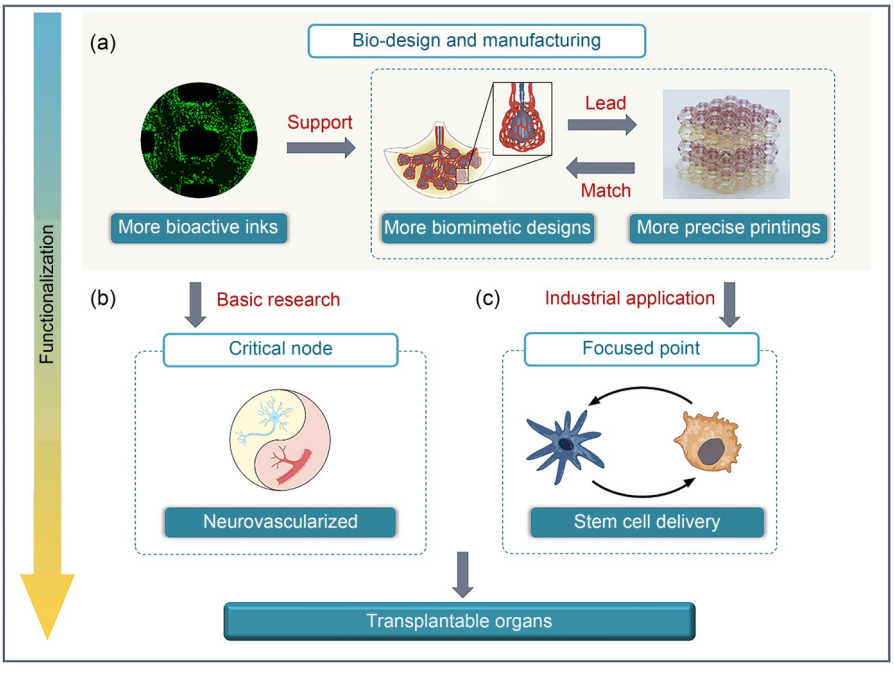

Fig. 47 Outlook of transplantable organ manufacturing: (a) development directions in 3D bioprinting; (b) critical node in foundational research—neurovascularization; (c) focus point of industrial applications—stem cell delivery. Part (a, first panel) was reproduced from [328], Copyright 2019, with permission from IOP Publishing. Part (a, second panel) was adapted from [12], Copyright 2020, with permission from Elsevier. Part (b) was adapted from [329], Copyright 2023, with permission from Springer Nature

capabilities; in turn, the pursuit of higher-level biomimicry will continually drive advancements in manufacturing technology, thus enabling more precise printing. Furthermore, as the cornerstone of the entire system, the performance of the bioinks must be continuously optimized. Future research should focus on leveraging artificial intelligence to accelerate the iteration of bioinks, thereby designing smart-responsive bioinks that match the developmental processes of different tissues and organs.

In basic research on organ reconstruction, the successful establishment of neuralization and vascularization represents a critical node (Fig. 47b), which is vital for ensuring the viability of large-scale engineered tissues and serves as a fundamental prerequisite for the functionalization of biological tissues. However, the capillary networks and nerve endings within natural tissues are typically on the micrometer scale, whereas the overall size of the organs reaches decimeter scales and above. This process of precise construction from micro-scales to macro-scales poses extremely high demands on manufacturing technology.

In the path of the industrial application of 3D printing, serving cell therapy will become a focus point in the future (Fig. 47c). Currently, stem cell therapy primarily involves the direct injection of cells or cell microspheres; however, this approach presents cells in a state that significantly differs from their true environment within biological organisms. In contrast, using biological scaffolds as carriers for the precise delivery of stem cells and regulating cell behavior through structural design can prompt cells to form "mini-tissues" that resemble their real state more closely. This strategy holds promise for achieving a paradigm shift from cell therapy to "mini-tissue" therapy, thus providing new perspectives and pathways for clinical treatment.

The manufacturing of transplantable organs is one of the most challenging frontier areas in the current scientific research, as it requires deep integration and collaborative innovation across multiple disciplines, such as manufacturing technology, materials science, and biomedicine, to jointly drive breakthrough progress in this field. Specifically, the exploration of next-generation 3D bioprinting technologies and tissue regeneration strategies will contribute to the acceleration of this process.

7.1 Prospects of 3D bioprinting

7.1.1 Bioink optimization

Bioinks, the material precursors used in 3D bioprinting, play a critical role in the success of bioprinting processes. Developing bioinks that possess desired properties, including good printability, biocompatibility, tunable mechanical properties, and compatibility with high cell density, is essential for creating bioprinted constructs that closely mimic native tissues. The quest for the perfect bioink is an ongoing endeavor. Researchers are constantly innovating and exploring novel bioink formulations. This includes incorporating natural biomaterials, such as collagen, hyaluronic acid, and decellularized ECM, to mimic the native cellular environment. Furthermore, the integration of bioactive molecules, growth factors, and nano-reinforcements within the bioink is being explored to enhance the cell attachment, differentiation, and overall functionality of the bioprinted construct.

7.1.2 Multimaterial and multicell bioprinting

Accurately replicating the intricate composition and architecture of natural tissues is essential for creating functional bioprinted organs. This requires the development of multimaterial and multicell bioprinting techniques. By incorporating diverse biomaterials and cell types, researchers can mimic the heterogeneity of native tissues, leading to the fabrication of bioprinted constructs with enhanced functionality and improved biocompatibility.

7.1.3 High-cell-density bioprinting with vascularization

Achieving high cell density in bioprinted constructs is crucial for recapitulating the physiological environment of natural tissues and promoting tissue function. However, high cell density can hinder oxygen and nutrient diffusion, leading to cell death. To overcome this obstacle, strategies aimed at incorporating interconnected vascular networks within bioprinted constructs are essential. These vascular networks are crucial for ensuring the long-term survival and function of the engineered tissues, thereby providing essential pathways for nutrient and oxygen delivery, removing waste products, and supporting cell–cell interactions. The development of strategies for the bioprinting complex vascular networks with precise control over their architecture and connectivity remains a significant challenge.

7.1.4 Stem cell printing

Despite the achievement of the bioprinting of pluripotent stem cells, which hold great promise as the panacea for the construction of solid functional organs, challenges remain that need to be addressed. The bioprinting of functional solid organs requires trillions of cells. The first obstacle is obtaining sufficient high-quality cells at an affordable cost; moreover, the genetic background of the different cells needs to be strictly controlled. The following step involves the manipulation of the cell fate, in which cell morphology, stage, and differentiation need to be controlled. In addition to manipulating the cells, the microenvironment in which the cells reside is a crucial factor. This may primarily depend on the properties of the bioink materials, for which the contradiction between bioactivity and mechanical strength warrants

resolution. The vascularization, neuralization, and immunization of the bioprinted organ are also important, and have been hot spots in biofabrication and tissue engineering. Nevertheless, as a multidisciplinary field, progress in biology, chemistry, material science, and mechanical engineering is boosting the bioprinting technology to realize its potential. In particular, the rapid advance in artificial intelligence technology witnessed in recent years is expected to drive the evolution of bioprinting technology in an unprecedented manner.

7.2 Explorations in tissue regeneration

7.2.1 Bone and cartilage

Natural bone has a high mechanical strength, which enables it to provide support and maintain the proper microenvironment for bone-related cells. The high mechanical strength of the tissue-engineered bone is essential for reconstructing tissue functionality. Although the significant advantages of bioprinted tissue-engineered bone in repairing bone defects have been demonstrated, the achievement of high mechanical strength in bioprinted tissue-engineered bone remains a formidable challenge. Currently, the conflict between the mechanical strength of bioinks and cell activity has yet to be resolved: high mechanical strength endows constructs with excellent self-supporting properties, which are beneficial for shape fidelity and large-sized fabrication; conversely, a low mechanical strength supports the proliferation and migration of the embedded cells. A multichannel 3D bioprinting method can utilize bioinks with cells and bioinks with high mechanical strength in separate channels, thus achieving high-strength tissue-engineered bone. However, the loaded cells are unable to sense the high-mechanical-strength microenvironment, which is not conducive to their osteogenic differentiation. The mechanical-assisted post-bioprinting strategy proposed by the Changshun Ruan group offers a promising outlook for addressing the intrinsically poor mechanical strength and cell activity of bioprinted tissue-engineered bone. However, this strategy is still in its infancy and many issues remain to be resolved. In addition, enhancing the adaptive capacity of cells to a high-mechanical-strength matrix microenvironment may be another approach to the construction of tissue-engineered bone with high mechanical strength and cell activity simultaneously. Overall, addressing this inherent contradiction remains a crucial but challenging task.

The osteochondral regeneration research field has developed various strategies aimed at triggering or accelerating the regeneration process. Cells, bioactive factors, biomaterials/inks, scaffold structures/topographies, and the corresponding 3D printing technologies are being intensively studied. Many possibilities have been proposed. For instance, Camarero-Espinosa et al. prepared a gradient scaffold in which the bone region was hollowed and filled with a BMSC-containing alginate hydrogel [330]. This structure was designed to sequester BMSCs at the cartilage–bone interface to mimic the native process in which subchondral bone BMSCs flow over into the cartilage defect and initiate tissue repair. This cell-niche strategy will be more convincing in the case of a scaffold containing evenly loaded BMSCs as the control. In addition to using BMSCs directly, discovering subpopulations that are involved in the repair process via single-cell sequencing may guide the selection of more specific seed cells or inspire ECM (i.e., bioprinting ink) design to facilitate BMSC functionalization [331]. It is well accepted that mimicking the zonal structure of the osteochondral unit benefits osteochondral regeneration. From the cell type and density to the ECM component and porosity, the natural osteochondral unit has complicated gradient features. Even the advanced 3D printing technology is unable to recapitulate all of these features. Using an in vitro dynamic culture device, letting the printed constructs mature, and forming osteochondral organoids may represent an alternative method [332]. Thousands of publications focus on osteochondral regeneration, and all of the aforementioned variables seem to have beneficial effects.

Conversely, the study of the biomimetic mechanical properties of cartilage is also crucial. Therefore, the development of high-strength hydrogels for the 3D printing of osteochondral tissue scaffolds is an important research direction. At present, the 3D-printed PEG/sodium alginate hydrogel has a fracture toughness as high as 1500 $J \cdot m^{-2}$, which is higher than that of articular cartilage. In addition, bioprinting of inks with seed cells and growth factors can further promote cartilage regeneration. Chondrocytes are usually selected as the seed cells; however, the extraction method is rather complex and has certain immunogenicity. In contrast, the extraction and source of stem cells are more convenient, and have the potential for multidirectional differentiation. Mesenchymal stem cells can also suppress the inflammation of the scaffold implanted in the body and reduce the damage caused by the foreign body reaction. In turn, it is exciting to note that several researchers have achieved satisfactory results in the bioprinting of non-load-bearing cartilage tissue. For example, personalized cartilage tissues, such as artificial auricles and noses, show significant potential for clinical application [227, 228].

The challenges in the application of 3D bioprinting to bone and cartilage repair include significant technical hurdles related to nerve and blood vessel regeneration within the bioprinted constructs. The methods used for stimulating their growth and seamlessly integrating them require further development. Moreover, discrepancies between laboratory conditions and in vivo environments impact the behavior and functionality of bioprinted tissues, warranting the refinement

of bioprinting techniques and the optimization of biological products for reliable performance in clinical settings. The transition of 3D bioprinting technologies from the laboratory to the clinic necessitates strict adherence to technical standards and safety protocols. Rigorous validation of efficacy and safety parameters through comprehensive testing, including studies involving large animals prior to human trials, is essential. These challenges highlight the interdisciplinary nature of the advancement of bioprinting for effective bone and cartilage repair, thus emphasizing the continuous need for innovation and collaboration across engineering, biological, and medical disciplines.

7.2.2 Nerve

Composite tissue defects caused by trauma, tumors, or congenital deformations lead to severe dysfunction and even irreversible damage. The existing clinical treatment modalities for composite nerve tissue defects include autologous tissue flap transplantation. Furthermore, the observation that nerve composite tissue transplantation is more beneficial for restoring blood supply, improving the survival rate of the transplanted tissue flap, and promoting the functional recovery of the innervated tissue is of concern. However, autologous nerve tissue flap transplantation is limited by restricted donor sources, donor-site morbidity, and inefficient attention to the regenerative roles of the nerve in the defect area. Because this situation exists, it is necessary to construct composite nerve functional units for systematically repairing the nerve and innervated tissues. Three-dimensional bioprinting appears promising for the construction of biomimetic composite nerve functional units. However, several issues still need to be solved and require elaboration: the complex responses of multitissue structures, insufficient blood vessel formation and oxygen supply, inaccurate matching of the functional neural connections, and challenging integrated printing with extra electrical stimulation. Multilevel, multiphase processes of multitissue structures require the universal compatibility of bioinks and the adaptability of printing nozzles forcing on cells. In addition to developing bioinks with the characteristics mentioned above, the thickness of the printed composite tissues deserves attention because of the regenerative requirement for adequate delivery of nutrients and oxygen. The precise and functional neural connection interface for the localization, proliferation, and promotion of the differentiation of multiple cells requires an appropriate microenvironment created by thickness for functional repair. However, the complex interface clues and communication of 3D bioprinting for multitissue structures remain challenging. A noteworthy issue that differs from other composite tissues could be that composite nerve functional units must restore the physiological nerve conduction and innervated tissue movement by loading electrical stimulation. However, because of the unclear bionic environment, designing a self-discharge scaffold using 3D bioprinting in vivo remains a subject of research.

7.2.3 Liver

The development of tissues is supported by a complex network of blood vessels, which provides oxygen, nutrients, and waste exchange and mediates paracrine interactions via growth and differentiation factors [333]. Because of the diffusion limits, the generation of liver tissue in vitro requires both vascularization and flow to maintain cell viability in the entire construct. Therefore, the lack of vascularization in the engineered liver tissue prevents oxygen and nutrient exchange, which is thought to be the main reason for the occurrence of apoptosis within the engineered tissues. Several hurdles impede the achievement of vascularization in engineered liver tissue using bioprinting. The minimal diameter of the engineered vessels that have been integrated into a perfusion system to date has been limited to 150 μm; the size of the generated tissues, particularly those requiring extensive blood flow (e.g., brain, liver, and heart), has been limited to 400 − 500 μm in at least one dimension. In addition, most of the bioprinted channels in the tissue are typically lined with only a single layer of endothelial cells. Although the channels could be surgically anastomosed to host vasculatures to achieve instantaneous perfusion within engineered tissues, the tortuous geometries of these vessels can render them prone to premature thrombosis. Such vessels may ultimately fail to perform the physiological function of either arteries or capillaries. Furthermore, hepatocytes often interact with vascular cells to influence the vascular structure and tissue functions. Defining and obtaining appropriate perivascular and hepatocyte cells will be necessary to capture the complete cellular diversity of the liver tissue. Most importantly, the engineered liver tissues that have been implemented to date do not preserve a physiologically relevant signaling context within the tissue, and do not develop to a level of complexity that is comparable to that of organs in vivo.

7.2.4 Skin

All technologies, including 3D bioprinting, present specific limitations and challenges for skin regeneration. Foremost among these challenges is the creation of fully functional skin substitutes using bioprinting. Although bioprinted skin can replicate most native skin functions by incorporating various types and quantities of cells (such as keratinocytes, fibroblasts, melanocytes, Langerhans cells, and even hair follicle cells), the development of functional hair follicles and sweat glands in engineered tissues remains unclear. Stem cell use is a potential solution, but ethical concerns, costs, and technical demands restrict its full application. Another

significant obstacle is the inability of current 3D-bioprinted skin tissue structures to accurately replicate the intricate architecture of natural skin, including blood vessels, nerves, and skin appendages. Achieving highly complex vascular systems in printed skin structures remains a formidable challenge. Nerve regeneration from 3D-printed skin poses an equally complex and intriguing challenge. The formation of new tissue induced by 3D-printed skin relies heavily on the establishment of new blood vessels for nerve regeneration. Without adequate blood supply, nerve regeneration is severely impeded. Lastly, human skin exhibits unique physical and mechanical properties, which leads to a need to carefully select biomaterials that match the characteristics of the skin tissue during the 3D bioprinting process.

7.2.5 Urinary system, endocrine system, immune system, and digestive system

Currently, there is a notable research gap in 3D bioprinting for tissue repair in the context of the urinary, endocrine, immune, and digestive systems. This phenomenon can be primarily attributed to the following three major challenges.

1. The intricate complexity of the organ structure and function. Specifically, organs within these systems, such as the kidney, possess sophisticated filtration and regulatory mechanisms, whereas the immune system encompasses a diverse array of immune cells and intricate signaling networks. These complexities significantly increase the difficulty of the construction of functional tissue-engineered models that can mimic genuine physiological functions.

2. The diversity and specificity of the cell types. These systems harbor a rich variety of cell types, each endowed with unique physiological roles and functions. For instance, the kidney comprises renal tubular epithelial cells, interstitial cells, and immune cells, whereas the immune system encompasses T cells, B cells, macrophages, and numerous other cell types. Consequently, the challenge of constructing tissue-engineered models that comprehensively represent all functional cell types is formidable.

3. The intricacy of microenvironment regulation. The microenvironments of these systems are crucial for maintaining their normal functions. For example, the kidney microenvironment necessitates precise regulation to maintain osmotic balance and ion homeostasis, whereas the immune system microenvironment modulates the inflammatory and immune responses. Crafting tissue-engineered models that can accurately mimic the in vivo microenvironmental characteristics necessitates a profound understanding of the physiological mechanisms of these microenvironments, coupled with sophisticated techniques and methodologies for their in vitro recreation and manipulation.

Future research must focus on these challenges to facilitate the widespread application of 3D bioprinting technology in the field of medical repair. The success of 3D bioprinting in tissue regeneration within these complex systems will critically hinge on interdisciplinary collaborations among researchers from various fields, including bioengineering, materials science, cell biology, immunology, and regenerative medicine. By confronting these challenges head-on and harnessing the latest advancements in technological and scientific understanding, we can pave the way for the extensive utilization of 3D bioprinting in the development of innovative therapeutic strategies targeting a wide spectrum of diseases.

Acknowledgements This work was supported by the National Natural Science Foundation of China (Nos. 52325504, 52235007, and T2121004).

Author contributions Writing—original draft: all authors; writing—review & editing: CFH, HYY, and YH; funding acquisition: YH; supervision: HYY and YH.

Declarations

Conflict of interest HYY is an editor-in-chief for *Bio-Design and Manufacturing* (*BDM*); JKH, CSR, YW, SB, JY, CJS, CCZ, XZ, XTS, MFY, YP, YEW, and YH are associate editors for *BDM*; HZZ and LM are academic editors for *BDM*. They were not involved in the editorial review or the decision to publish this article. The authors declare that they have no conflict of interest.

Ethical approval This article does not contain any studies with human or animal subjects performed by any of the authors.

References

1. Drucker CB (2008) Ambroise Paré and the birth of the gentle art of surgery. Yale J Biol Med 81(4):199–202
2. Keeling C, Davies S, Goddard J et al (2024) The clinical significance of sub-total surgical resection in childhood medulloblastoma: a multi-cohort analysis of 1100 patients. eClinicalMedicine 69: 102469. https://doi.org/10.1016/j.eclinm.2024.102469
3. Jo SH, Kang SH, Seo WS et al (2021) Psychiatric understanding and treatment of patients with amputations. Yeungnam Univ J Med 38(3):194–201. https://doi.org/10.12701/yujm.2021.00990
4. Gurrado A, Faillace G, Bottero L et al (2009) Laparoscopic appendectomies: experience of a surgical unit. Minim Invasiv Ther Allied Technol 18(4):242–247. https://doi.org/10.1080/13645700903053840
5. Lin ZY, Zhang XL, Chen YJ et al (2023) Negative pressure wound therapy for flap closed-incisions after 3D-printed prosthesis implantation in patients with chronic osteomyelitis with soft tissue defects. BMC Musculoskelet Disord 24(1):827. https://doi.org/10.1186/s12891-023-06970-1
6. The Lancet Editors (2018) Retraction-Tracheobronchial transplantation with a stem-cell-seeded bioartificial nanocomposite: a proof-of-concept study. Lancet 392(10141):11. https://doi.org/10.1016/S0140-6736(18)31558-7
7. Mazzoni E, Iaquinta MR, Lanzillotti C et al (2021) Bioactive

materials for soft tissue repair. Front Bioeng Biotechnol 9:613787. https://doi.org/10.3389/fbioe.2021.613787
8. Chan BP, Leong KW (2008) Scaffolding in tissue engineering: general approaches and tissue-specific considerations. Eur Spine J 17(Suppl 4):467–479. https://doi.org/10.1007/s00586-008-0745-3
9. Song L, Xu B, Chen YD et al (2021) Thinner strut sirolimus-eluting BRS versus EES in patients with coronary artery disease. JACC Cardiovasc Interve 14(13):1450–1462. https://doi.org/10.1016/j.jcin.2021.04.048
10. Webber MJ, Khan OF, Sydlik SA et al (2015) A perspective on the clinical translation of scaffolds for tissue engineering. Ann Biomed Eng 43(3):641–656. https://doi.org/10.1007/s10439-014-1104-7
11. Bajaj P, Schweller RM, Khademhosseini A et al (2014) 3D biofabrication strategies for tissue engineering and regenerative medicine. Annu Rev Biomed Eng 16(1):247–276. https://doi.org/10.1146/annurev-bioeng-071813-105155
12. Daly AC, Prendergast ME, Hughes AJ et al (2021) Bioprinting for the biologist. Cell 184(1):18–32. https://doi.org/10.1016/j.cell.2020.12.002
13. Richards DJ, Tan Y, Jia J et al (2013) 3D printing for tissue engineering. Isr J Chem 53(9–10):805–814. https://doi.org/10.1002/ijch.201300086
14. Moroni L, Boland T, Burdick JA et al (2018) Biofabrication: a guide to technology and terminology. Trends Biotechnol 36(4): 384–402. https://doi.org/10.1016/j.tibtech.2017.10.015
15. He CF, Qiao TH, Wang GH et al (2025) High-resolution projection-based 3D bioprinting. Nat Rev Bioeng 3:143–158. https://doi.org/10.1038/s44222-024-00218-w
16. Wang PJ, Sun YZ, Shi XQ et al (2021) 3D printing of tissue engineering scaffolds: a focus on vascular regeneration. Bio-Des Manuf 4(2):344–378. https://doi.org/10.1007/s42242-020-00109-0
17. Gao G, Ahn M, Cho WW et al (2021) 3D printing of pharmaceutical application: drug screening and drug delivery. Pharmaceutics 13(9):1373. https://doi.org/10.3390/pharmaceutics13091373
18. Sun W, Starly B, Daly AC et al (2020) The bioprinting roadmap. Biofabrication 12(2):022002. https://doi.org/10.1088/1758-5090/ab5158
19. Fang YC, Wang CJ, Liu ZB et al (2023) 3D printed conductive multiscale nerve guidance conduit with hierarchical fibers for peripheral nerve regeneration. Adv Sci 10(12):e2205744. https://doi.org/10.1002/advs.202205744
20. Sun Y, Yu K, Gao Q et al (2022) Projection-based 3D bioprinting for hydrogel scaffold manufacturing. Bio-Des Manuf 5(3): 633–639. https://doi.org/10.1007/s42242-022-00189-0
21. He CF, Chen XC, Sun Y et al (2022) Rapid and mass manufacturing of soft hydrogel microstructures for cell patterns assisted by 3D printing. Bio-Des Manuf 5(4):641–659. https://doi.org/10.1007/s42242-022-00207-1
22. Yuan XM, Zhu Z, Xia PC et al (2023) Tough gelatin hydrogel for tissue engineering. Adv Sci 10(24):2301665. https://doi.org/10.1002/advs.202301665
23. Wang ZL, Zheng Y, Qiao L et al (2024) 4D-printed MXene-based artificial nerve guidance conduit for enhanced regeneration of peripheral nerve injuries. Adv Healthc Mater 13(23):e2401093. https://doi.org/10.1002/adhm.202401093
24. Chen YW, Zou ZF, Fu T et al (2024) 3D printed grafts with gradient structures for organized vascular regeneration. Int J Extrem Manuf 6(3):035503. https://doi.org/10.1088/2631-7990/ad2f50
25. Shi Y, Shi J, Sun Y et al (2023) A hierarchical 3D graft printed with nanoink for functional craniofacial bone restoration. Adv Funct Mater 33(40):2301099. https://doi.org/10.1002/adfm.202301099
26. Xie MJ, Sun Y, Wang J et al (2022) Thermo-sensitive sacrificial microsphere-based bioink for centimeter-scale tissue with angiogenesis. Int J Bioprint 8(4):599. https://doi.org/10.18063/ijb.v8i4.599
27. Tang H, Sun WY, Liu XC et al (2023) A bioengineered trachea-like structure improves survival in a rabbit tracheal defect model. Sci Transl Med 15(714):eabo4272. https://doi.org/10.1126/scitranslmed.abo4272
28. He J, Sun Y, Gao Q et al (2023) Gelatin methacryloyl hydrogel, from standardization, performance, to biomedical application. Adv Healthc Mater 12(23):e2300395. https://doi.org/10.1002/adhm.202300395
29. Chia HN, Wu BM (2015) Recent advances in 3D printing of biomaterials. J Biol Eng 9(1):4. https://doi.org/10.1186/s13036-015-0001-4
30. Murphy CA, Lim KS, Woodfield TBF (2022) Next evolution in organ-scale biofabrication: bioresin design for rapid high-resolution vat polymerization. Adv Mater 34(20):e2107759. https://doi.org/10.1002/adma.202107759
31. Gao Q, Xie CQ, Wang P et al (2020) 3D printed multi-scale scaffolds with ultrafine fibers for providing excellent biocompatibility. Mater Sci Eng C Mater Biol Appl 107:110269. https://doi.org/10.1016/j.msec.2019.110269
32. Yu K, Zhang XJ, Sun Y et al (2022) Printability during projection-based 3D bioprinting. Bioact Mater 11:254–267. https://doi.org/10.1016/j.bioactmat.2021.09.021
33. Sun Y, Yu K, Nie J et al (2021) Modeling the printability of photocuring and strength adjustable hydrogel bioink during projection based 3D bioprinting. Biofabrication 13(3):035032. https://doi.org/10.1088/1758-5090/aba413
34. Yao K, Hong GY, Yuan XM et al (2024) 3D printing of tough hydrogel scaffolds with functional surface structures for tissue regeneration. Nano-Micro Lett 17(1):27. https://doi.org/10.1007/s40820-024-01524-z
35. Tuan RS, Boland G, Tuli R (2003) Adult mesenchymal stem cells and cell-based tissue engineering. Arthritis Res Ther 5(1): 32–45. https://doi.org/10.1186/ar614
36. Landers R, Hübner U, Schmelzeisen R et al (2002) Rapid prototyping of scaffolds derived from thermoreversible hydrogels and tailored for applications in tissue engineering. Biomaterials 23(23): 4437–4447. https://doi.org/10.1016/s0142-9612(02)00139-4
37. Dhariwala B, Hunt E, Boland T (2004) Rapid prototyping of tissue-engineering constructs, using photopolymerizable hydrogels and stereolithography. Tissue Eng 10(9-10):1316–1322. https://doi.org/10.1089/ten.2004.10.1316
38. Groll J, Burdick JA, Cho DW et al (2018) A definition of bioinks and their distinction from biomaterial inks. Biofabrication 11(1):013001. https://doi.org/10.1088/1758-5090/aaec52
39. Shao L, Gao Q, Xie CQ et al (2020) Directly coaxial 3D bioprinting of large-scale vascularized tissue constructs. Biofabrication 12(3):035014. https://doi.org/10.1088/1758-5090/ab7e76
40. Zhou LY, Fu JZ, He Y (2020) A review of 3D printing technologies for soft polymer materials. Adv Funct Mater 30(28):2000187.

https://doi.org/10.1002/adfm.202000187
41. Zheng K, Chai MY, Luo BP et al (2024) Recent progress of 3D printed vascularized tissues and organs. Smart Mater Med 5(2): 183–195. https://doi.org/10.1016/j.smaim.2024.01.001
42. He CF, Sun Y, Liu NA et al (2023) Formation theory and printability of photocurable hydrogel for 3D bioprinting. Adv Funct Mater 33(29):2301209. https://doi.org/10.1002/adfm.202301209
43. Jin ZBY, He CF, Fu JZ et al (2022) Balancing the customization and standardization: exploration and layout surrounding the regulation of the growing field of 3D-printed medical devices in China. Bio-Des Manuf 5(3):580–606. https://doi.org/10.1007/s42242-022-00187-2
44. Xia MY, Wu MX, Li YR et al (2023) Varying mechanical forces drive sensory epithelium formation. Sci Adv 9(44):eadf2664. https://doi.org/doi:10.1126/sciadv.adf2664
45. He CF, Sun Y, Liu NA et al (2023) Formation theory and printability of photocurable hydrogel for 3D bioprinting. Adv Funct Mater 33(29):2301209. https://doi.org/10.1002/adfm.202301209
46. Jakus AE, Rutz AL, Jordan SW et al (2016) Hyperelastic "bone": a highly versatile, growth factor-free, osteoregenerative, scalable, and surgically friendly biomaterial. Sci Transl Med 8(358): 358ra127. https://doi.org/10.1126/scitranslmed.aaf7704
47. Trombetta R, Inzana JA, Schwarz EM et al (2017) 3D printing of calcium phosphate ceramics for bone tissue engineering and drug delivery. Ann Biomed Eng 45(1):23–44. https://doi.org/10.1007/s10439-016-1678-3
48. Yang YH, Xu TP, Bei HP et al (2022) Gaussian curvature-driven direction of cell fate toward osteogenesis with triply periodic minimal surface scaffolds. Proc Natl Acad Sci USA 119(41): e2206684119. https://doi.org/10.1073/pnas.2206684119
49. Yang YH, Zhang Q, Xu TP et al (2020) Photocrosslinkable nanocomposite ink for printing strong, biodegradable and bioactive bone graft. Biomaterials 263:120378. https://doi.org/10.1016/j.biomaterials.2020.120378
50. Yang YH, Xu TP, Bei HP et al (2021) Sculpting bio-inspired surface textures: an adhesive Janus periosteum. Adv Funct Mater 31(37):2104636. https://doi.org/10.1002/adfm.202104636
51. Fang JH, Liu HQ, Qiao W et al (2023) Biomimicking leaf-vein engraved soft and elastic membrane promotes vascular reconstruction. Adv Healthc Mater 12(2):2201220. https://doi.org/10.1002/adhm.202201220
52. Xu TP, Yang YH, Yeung EHL et al (2023) Injectable, self-contained, subaqueously cross-linking laminous adhesives for biophysical-chemical modulation of osteochondral microenvironment. Adv Funct Mater 33(23):2213428. https://doi.org/10.1002/adfm.202213428
53. Lyu S, Liu Q, Yuen HY et al (2024) A differential-targeting core-shell microneedle patch with coordinated and prolonged release of mangiferin and MSC-derived exosomes for scarless skin regeneration. Mater Horiz 11:2667–2684. https://doi.org/10.1039/d3mh01910a
54. Ravanbakhsh H, Karamzadeh V, Bao G et al (2021) Emerging technologies in multi-material bioprinting. Adv Mater 33(49): e2104730. https://doi.org/10.1002/adma.202104730
55. Zhang YN, O'Mahony A, He Y et al (2024) Hydrodynamic shear stress' impact on mammalian cell properties and its applications in 3D bioprinting. Biofabrication 16(2):22003. https://doi.org/10.1088/1758-5090/ad22ee
56. Song JC, Chen S, Sun LJ et al (2020) Mechanically and electronically robust transparent organohydrogel fibers. Adv Mater 32(8):1906994. https://doi.org/10.1002/adma.201906994
57. Jiang SH, Deng JJ, Jin YH et al (2023) Breathable, antifreezing, mechanically skin-like hydrogel textile wound dressings with dual antibacterial mechanisms. Bioact Mater 21:313–323. https://doi.org/10.1016/j.bioactmat.2022.08.014
58. Chen S, Jiang SH, Qiao D et al (2023) Chinese tofu-inspired biomimetic conductive and transparent fibers for biomedical applications. Small Methods 7(4):e2201604. https://doi.org/10.1002/smtd.202201604
59. Liu ML, Jiang SH, Witman N et al (2023) Intrinsically cryopreservable, bacteriostatic, durable glycerohydrogel inks for 3D bioprinting. Matter 6(3):983–999. https://doi.org/10.1016/j.matt.2022.12.013
60. Chen S, Wang YH, Yang L et al (2023) Biodegradable elastomers for biomedical applications. Prog Polym Sci 147:101763. https://doi.org/10.1016/j.progpolymsci.2023.101763
61. Chen S, Wu ZK, Chu CZ et al (2022) Biodegradable elastomers and gels for elastic electronics. Adv Sci 9(13):e2105146. https://doi.org/10.1002/advs.202105146
62. Zhang LZ, Chen S, You ZW (2023) Hybrid cross-linking to construct functional elastomers. Acc Chem Res 56(21):2907–2920. https://doi.org/10.1021/acs.accounts.3c00391
63. Lei D, Yang Y, Liu ZH et al (2019) A general strategy of 3D printing thermosets for diverse applications. Mater Horiz 6(2): 394–404. https://doi.org/10.1039/c8mh00937f
64. Chen S, Sun LJ, Zhou XJ et al (2020) Mechanically and biologically skin-like elastomers for bio-integrated electronics. Nat Commun 11(1):1107. https://doi.org/10.1038/s41467-020-14446-2
65. Gong Z, Lei D, Wang CG et al (2020) Bioactive elastic scaffolds loaded with neural stem cells promote rapid spinal cord regeneration. ACS Biomater Sci Eng 6(11):6331–6343. https://doi.org/10.1021/acsbiomaterials.0c01057
66. Xu Y, Guo YF, Li YQ et al (2020) Biomimetic trachea regeneration using a modular ring strategy based on poly(sebacoyl diglyceride)/polycaprolactone for segmental trachea defect repair. Adv Funct Mater 30(42):2004276. https://doi.org/10.1002/adfm.202004276
67. Xuan HX, Hu HR, Geng CY et al (2020) Biofunctionalized chondrogenic shape-memory ternary scaffolds for efficient cell-free cartilage regeneration. Acta Biomater 105:97–110. https://doi.org/10.1016/j.actbio.2020.01.015
68. Xiao B, Yang WJ, Lei D et al (2019) PGS scaffolds promote the in vivo survival and directional differentiation of bone marrow mesenchymal stem cells restoring the morphology and function of wounded rat uterus. Adv Healthc Mater 8(5):1801455. https://doi.org/10.1002/adhm.201801455
69. Wang SN, Luo B, Bai BS et al (2023) 3D printed chondrogenic functionalized PGS bioactive scaffold for cartilage regeneration. Adv Healthc Mater 12(27):e2301006. https://doi.org/10.1002/adhm.202301006
70. Yang Y, Lei D, Huang SX et al (2019) Elastic 3D-printed hybrid polymeric scaffold improves cardiac remodeling after myocardial infarction. Adv Healthc Mater 8(10):e1900065. https://doi.org/10.1002/adhm.201900065
71. Chen S, Huang T, Zuo H et al (2018) A single integrated 3D-printing process customizes elastic and sustainable triboelec-

tric nanogenerators for wearable electronics. Adv Funct Mater 28(46):1805108.
https://doi.org/10.1002/adfm.201805108
72. Luo B, Wang SN, Song XQ et al (2024) An encapsulation-free and hierarchical porous triboelectric scaffold with dynamic hydrophilicity for efficient cartilage regeneration. Adv Mater 36(27): e2401009.
https://doi.org/10.1002/adma.202401009
73. Luo B, Zhou QQ, Chen WY et al (2023) Nonadjacent wireless electrotherapy for tissue repair by a 3D-printed bioresorbable fully soft triboelectric nanogenerator. Nano Lett 23(7):2927–2937.
https://doi.org/10.1021/acs.nanolett.3c00300
74. Qian B, Shen A, Huang SX et al (2023) An intrinsically magnetic epicardial patch for rapid vascular reconstruction and drug delivery. Adv Sci 10(36):e2303033.
https://doi.org/10.1002/advs.202303033
75. Lei D, Luo B, Guo YF et al (2019) 4-Axis printing microfibrous tubular scaffold and tracheal cartilage application. Sci China Mater 62(12):1910–1920.
https://doi.org/10.1007/s40843-019-9498-5
76. Yang Q, Lei D, Huang SX et al (2020) A novel biodegradable external stent regulates vein graft remodeling via the Hippo-YAP and mTOR signaling pathways. Biomaterials 258:120254.
https://doi.org/10.1016/j.biomaterials.2020.120254
77. Xiao WW, Chen WL, Wang YG et al (2022) Recombinant DTβ4-inspired porous 3D vascular graft enhanced antithrombogenicity and recruited circulating $CD93^{+}$/$CD34^{+}$ cells for endothelialization. Sci Adv 8(28):eabn1958.
https://doi.org/10.1126/sciadv.abn1958
78. Wang Y, Pan JZ, Han XX et al (2008) A phenomenological model for the degradation of biodegradable polymers. Biomaterials 29(23):3393–3401.
https://doi.org/10.1016/j.biomaterials.2008.04.042
79. Han XX, Pan JZ (2011) Polymer chain scission, oligomer production and diffusion: a two-scale model for degradation of bioresorbable polyesters. Acta Biomater 7(2):538–547.
https://doi.org/10.1016/j.actbio.2010.09.005
80. Han XX, Pan JZ (2009) A model for simultaneous crystallisation and biodegradation of biodegradable polymers. Biomaterials 30(3): 423–430.
https://doi.org/10.1016/j.biomaterials.2008.10.001
81. Chen F, Ekinci A, Li L et al (2021) How do the printing parameters of fused filament fabrication and structural voids influence the degradation of biodegradable devices? Acta Biomater 136: 254–265.
https://doi.org/10.1016/j.actbio.2021.09.020
82. Zhu XL, Chen F, Cao H et al (2023) Design and fused deposition modeling of triply periodic minimal surface scaffolds with channels and hydrogel for breast reconstruction. Int J Bioprint 9(2): 407–421.
https://doi.org/10.18063/ijb.685
83. Li J, Chen F, Wang MX et al (2024) Design and optimization of 3D-bioprinted cell-laden scaffolds in dynamic culture. Int J Bioprint 10(3):1838.
https://doi.org/10.36922/ijb.1838
84. He N, Wang XN, Shi LY et al (2023) Photoinhibiting via simultaneous photoabsorption and free-radical reaction for high-fidelity light-based bioprinting. Nat Commun 14(1):3063.
https://doi.org/10.1038/s41467-023-38838-2
85. He N, Wang XN, Shi LY et al (2023) Photoinhibiting via simultaneous photoabsorption and free-radical reaction for high-fidelity light-based bioprinting. Nat Commun 14(1):3063.
https://doi.org/10.1038/s41467-023-38838-2
86. Li Y, Mao QJ, Yin J et al (2021) Theoretical prediction and experimental validation of the digital light processing (DLP) working curve for photocurable materials. Addit Manuf 37:101716.
https://doi.org/10.1016/j.addma.2020.101716
87. Li Y, Mao QJ, Li XK et al (2019) High-fidelity and high-efficiency additive manufacturing using tunable pre-curing digital light processing. Addit Manuf 30:100889.
https://doi.org/10.1016/j.addma.2019.100889
88. Wu Y, Su H, Li M et al (2023) Digital light processing-based multi-material bioprinting: processes, applications, and perspectives. J Biomed Mater Res Part A 111(4):527–542.
https://doi.org/10.1002/jbm.a.37473
89. Ma XY, Qu X, Zhu W et al (2016) Deterministically patterned biomimetic human iPSC-derived hepatic model via rapid 3D bioprinting. Proc Natl Acad Sci USA 113(8):2206–2211.
https://doi.org/10.1073/pnas.1524510113
90. Wang M, Li WL, Mille LS et al (2022) Digital light processing based bioprinting with composable gradients. Adv Mater 34(1): e2107038.
https://doi.org/10.1002/adma.202107038
91. Su H, Lu BX, Li M et al (2023) Development of digital light processing-based multi-material bioprinting for fabrication of heterogeneous tissue constructs. Biomater Sci 11(19):6663–6673.
https://doi.org/10.1039/d3bm01054f
92. Yang M, Chu L, Zhuang YF et al (2024) Multi-material digital light processing (DLP) bioprinting of heterogeneous hydrogel constructs with perfusable networks. Adv Funct Mater 34(32): 2316456.
https://doi.org/10.1002/adfm.202316456
93. Shi HM, Li Y, Xu KL et al (2023) Advantages of photo-curable collagen-based cell-laden bioinks compared to methacrylated gelatin (GelMA) in digital light processing (DLP) and extrusion bioprinting. Mater Today Bio 23:100799.
https://doi.org/10.1016/j.mtbio.2023.100799
94. Fang HM, Ju JY, Chen LF et al (2024) Clay sculpture-inspired 3D printed microcage module using bioadhesion assembly for specific-shaped tissue vascularization and regeneration. Adv Sci 11(21):e2308381.
https://doi.org/10.1002/advs.202308381
95. Ouyang LL (2022) Pushing the rheological and mechanical boundaries of extrusion-based 3D bioprinting. Trends Biotechnol 40(7): 891–902.
https://doi.org/10.1016/j.tibtech.2022.01.001
96. Ouyang LL, Armstrong JPK, Lin YY et al (2020) Expanding and optimizing 3D bioprinting capabilities using complementary network bioinks. Sci Adv 6(38):eabc5529.
https://doi.org/10.1126/sciadv.abc5529
97. Wang M, Li WL, Hao J et al (2022) Molecularly cleavable bioinks facilitate high-performance digital light processing-based bioprinting of functional volumetric soft tissues. Nat Commun 13(1): 3317.
https://doi.org/10.1038/s41467-022-31002-2
98. Ouyang L, Highley CB, Sun W et al (2017) A generalizable strategy for the 3D bioprinting of hydrogels from nonviscous photo-crosslinkable inks. Adv Mater 29(8):1604983.
https://doi.org/10.1002/adma.201604983
99. McCormack A, Highley CB, Leslie NR et al (2020) 3D printing in suspension baths: keeping the promises of bioprinting afloat. Trends Biotechnol 38(6):584–593.
https://doi.org/10.1016/j.tibtech.2019.12.020
100. Xin SJ, Deo KA, Dai J et al (2021) Generalizing hydrogel microparticles into a new class of bioinks for extrusion bioprinting. Sci Adv 7(42):eabk3087.

https://doi.org/10.1126/sciadv.abk3087
101. Zhou DZ, Dou BH, Kroh F et al (2023) Biofabrication strategies with single-cell resolution: a review. Int J Extrem Maunf 5(4): 42005. https://doi.org/10.1088/2631-7990/ace863
102. You ST, Xiang Y, Hwang HH et al (2023) High cell density and high-resolution 3D bioprinting for fabricating vascularized tissues. Sci Adv 9(8):eade7923. https://doi.org/10.1126/sciadv.ade7923
103. Almeida-Pinto J, Moura BS, Gaspar VM et al (2024) Advances in cell-rich inks for biofabricating living architectures. Adv Mater 36(27):e2313776. https://doi.org/10.1002/adma.202313776
104. Norotte C, Marga FS, Niklason LE et al (2009) Scaffold-free vascular tissue engineering using bioprinting. Biomaterials 30(30): 5910–5917. https://doi.org/10.1016/j.biomaterials.2009.06.034
105. Grogan SP, Dorthé EW, Glembotski NE et al (2020) Cartilage tissue engineering combining microspheroid building blocks and microneedle arrays. Connect Tissue Res 61(2):229–243. https://doi.org/10.1080/03008207.2019.1617280
106. Skylar-Scott MA, Uzel SGM, Nam LL et al (2019) Biomanufacturing of organ-specific tissues with high cellular density and embedded vascular channels. Sci Adv 5(9):eaaw2459. https://doi.org/10.1126/sciadv.aaw2459
107. Machino R, Matsumoto K, Taniguchi D et al (2019) Replacement of rat tracheas by layered, trachea-like, scaffold-free structures of human cells using a bio-3D printing system. Adv Healthc Mater 8(7):e1800983. https://doi.org/10.1002/adhm.201800983
108. Ayan B, Heo DN, Zhang ZF et al (2020) Aspiration-assisted bioprinting for precise positioning of biologics. Sci Adv 6(10): eaaw5111. https://doi.org/10.1126/sciadv.aaw5111
109. Zhang JH, Xin W, Qin YC et al (2022) "All-in-one" zwitterionic granular hydrogel bioink for stem cell spheroids production and 3D bioprinting. Chem Eng J 430:132713. https://doi.org/10.1016/j.cej.2021.132713
110. Wu Y, Ayan B, Moncal KK et al (2020) Hybrid bioprinting of zonally stratified human articular cartilage using scaffold-free tissue strands as building blocks. Adv Healthc Mater 9(22):e2001657. https://doi.org/10.1002/adhm.202001657
111. Ayan B, Wu Y, Karuppagounder V et al (2020) Aspiration-assisted bioprinting of the osteochondral interface. Sci Rep 10(1): 13148. https://doi.org/10.1038/s41598-020-69960-6
112. Li M, Wu Y, Yuan T et al (2023) Biofabrication of composite tendon constructs with the fibrous arrangement, high cell density, and enhanced cell alignment. ACS Appl Mater Interfaces 15(41): 47989–48000. https://doi.org/10.1021/acsami.3c10697
113. Wu Y, Hospodiuk M, Peng WJ et al (2018) Porous tissue strands: avascular building blocks for scalable tissue fabrication. Biofabrication 11(1):015009. https://doi.org/10.1088/1758-5090/aaec22
114. Jing SB, Lian LM, Hou YY et al (2024) Advances in volumetric bioprinting. Biofabrication 16(1):12004. https://doi.org/10.1088/1758-5090/ad0978
115. Xie MB, Lian LM, Mu X et al (2023) Volumetric additive manufacturing of pristine silk-based (bio)inks. Nat Commun 14(1):210. https://doi.org/10.1038/s41467-023-35807-7
116. Kelly BE, Bhattacharya I, Heidari H et al (2019) Volumetric additive manufacturing via tomographic reconstruction. Science 363(6431):1075–1079. https://doi.org/10.1126/science.aau7114
117. Zheng ZH, Lian LM, Xie MB (2024) Ultrasound volumetric bioprinting: opportunities and challenges. Innov Life 2(1):100053. https://doi.org/10.59717/j.xinn-life.2024.100053
118. Lian LM, Xie MB, Luo ZY et al (2024) Rapid volumetric bioprinting of decellularized extracellular matrix bioinks. Adv Mater 36(34):e2304846. https://doi.org/10.1002/adma.202304846
119. Zhang B, He JK, Lei Q et al (2020) Electrohydrodynamic printing of sub-microscale fibrous architectures with improved cell adhesion capacity. Virt Phys Prototy 15(1):62–74. https://doi.org/10.1080/17452759.2019.1662991
120. He JK, Hao GZ, Meng ZJ et al (2022) Expanding melt-based electrohydrodynamic printing of highly-ordered microfibrous architectures to cm-height via in situ charge neutralization. Adv Mater Technol 7(7):2101197. https://doi.org/10.1002/admt.202101197
121. Mao M, He JK, Li Z et al (2020) Multi-directional cellular alignment in 3D guided by electrohydrodynamically-printed microlattices. Acta Biomater 101:141–151. https://doi.org/10.1016/j.actbio.2019.10.028
122. Han K, He JK, Fu LY et al (2023) Engineering highly-aligned three-dimensional (3D) cardiac constructs for enhanced myocardial infarction repair. Biofabrication 15(1):15003. https://doi.org/10.1088/1758-5090/ac94f9
123. Yao C, Qiu ZN, Li X et al (2023) Electrohydrodynamic printing of microfibrous architectures with cell-scale spacing for improved cellular migration and neurite outgrowth. Small 19(19):e2207331. https://doi.org/10.1002/smll.202207331
124. Qiu ZN, Zhu H, Wang YT et al (2023) Functionalized alginate-based bioinks for microscale electrohydrodynamic bioprinting of living tissue constructs with improved cellular spreading and alignment. Bio-Des Manuf 6(2):136–149. https://doi.org/10.1007/s42242-022-00225-z
125. Li Q, Ma L, Gao ZQ et al (2022) Regulable supporting baths for embedded printing of soft biomaterials with variable stiffness. ACS Appl Mater Interfaces 14(37):41695–41711. https://doi.org/10.1021/acsami.2c09221
126. Li Q, Jiang ZR, Ma L et al (2022) A versatile embedding medium for freeform bioprinting with multi-crosslinking methods. Biofabrication 14(3):35022. https://doi.org/10.1088/1758-5090/ac7909
127. Gao ZQ, Yin J, Liu P et al (2023) Simultaneous multi-material embedded printing for 3D heterogeneous structures. Int J Extrem Manuf 5(3):35001. https://doi.org/10.1088/2631-7990/acd285
128. Wu Y, Yang X, Gupta D et al (2024) Dissecting the interplay mechanism among process parameters toward the biofabrication of high-quality shapes in embedded bioprinting. Adv Funct Mater 34(21):2313088. https://doi.org/10.1002/adfm.202313088
129. Wu Y, Yang X, Yuan TY et al (2024) Development of embedded bioprinting for fabricating zonally stratified articular cartilage. Int J Bioprinting 10(4):3520. https://doi.org/10.36922/ijb.3520
130. Fang YC, Ji MK, Wu BY et al (2023) Engineering highly vascularized bone tissues by 3D bioprinting of granular prevascularized spheroids. ACS Appl Mater Interfaces 15(37):43492–43502. https://doi.org/10.1021/acsami.3c08550
131. Fang YC, Guo YH, Wu BY et al (2023) Expanding embedded 3D bioprinting capability for engineering complex organs with freeform vascular networks. Adv Mater 35(22):e2205082.

https://doi.org/10.1002/adma.202205082
132. Koons GL, Diba M, Mikos AG (2020) Materials design for bone-tissue engineering. Nat Rev Mater 5(8):584–603. https://doi.org/10.1038/s41578-020-0204-2
133. Liu YQ, He K, Chen G et al (2017) Nature-inspired structural materials for flexible electronic devices. Chem Rev 117(20): 12893–12941. https://doi.org/10.1021/acs.chemrev.7b00291
134. Kotikian A, McMahan C, Davidson EC et al (2019) Untethered soft robotic matter with passive control of shape morphing and propulsion. Sci Robot 4(33):eaax7044. https://doi.org/10.1126/scirobotics.aax7044
135. Xing RZ, Yang JY, Zhang DG et al (2023) Metallic gels for conductive 3D and 4D printing. Matter 6(7):2248–2262. https://doi.org/10.1016/j.matt.2023.06.015
136. Qu HW, Fu HY, Han ZY et al (2019) Biomaterials for bone tissue engineering scaffolds: a review. RSC Adv 9(45):26252–26262. https://doi.org/10.1039/C9RA05214C
137. Liu K, Hu N, Yu ZH et al (2023) 3D printing and bioprinting in urology. Int J Bioprinting 9(6):325–342. https://doi.org/10.36922/ijb.0969
138. Qu HW, Han ZY, Chen ZG et al (2021) Fractal design boosts extrusion-based 3D printing of bone-mimicking radial-gradient scaffolds. Research 2021:9892689. https://doi.org/10.34133/2021/9892689
139. Qu HW, Gao CJ, Liu KZ et al (2024) Gradient matters via filament diameter-adjustable 3D printing. Nat Commun 15(1):2930. https://doi.org/10.1038/s41467-024-47360-y
140. Liu WW, Li XK, Jiao YL et al (2020) Biological effects of a three-dimensionally printed Ti6Al4V scaffold coated with piezoelectric $BaTiO_3$ nanoparticles on bone formation. ACS Appl Mater Interfaces 12(46):51885–51903. https://doi.org/10.1021/acsami.0c10957
141. Chen L, Yang JY, Cai ZW et al (2024) Electroactive biomaterials regulate the electrophysiological microenvironment to promote bone and cartilage tissue regeneration. Adv Funct Mater 34(23): 2314079. https://doi.org/10.1002/adfm.202314079
142. Shuai CJ, Liu GF, Yang YW et al (2020) A strawberry-like Ag-decorated barium titanate enhances piezoelectric and antibacterial activities of polymer scaffold. Nano Energy 74:104825. https://doi.org/10.1016/j.nanoen.2020.104825
143. Shuai CJ, Cheng Y, Yang WJ et al (2020) Magnetically actuated bone scaffold: microstructure, cell response and osteogenesis. Compos Part B Eng 192:107986. https://doi.org/10.1016/j.compositesb.2020.107986
144. Shuai CJ, Chen X, He CX et al (2022) Construction of magnetic nanochains to achieve magnetic energy coupling in scaffold. Biomater Res 26(1):38. https://doi.org/10.1186/s40824-022-00278-2
145. Qi FW, Liao RB, Shuai Y et al (2022) A conductive network enhances nerve cell response. Addit Manuf 52:102694. https://doi.org/10.1016/j.addma.2022.102694
146. Qi FW, Liao RB, Wu P et al (2023) An electrical microenvironment constructed based on electromagnetic induction stimulates neural differentiation. Mater Chem Front 7(8):1671–1683. https://doi.org/10.1039/d2qm01193j
147. Silvani G, Basirun C, Wu HJ et al (2021) A 3D-bioprinted vascularized glioblastoma-on-a-chip for studying the impact of simulated microgravity as a novel pre-clinical approach in brain tumor therapy. Adv Ther 4(11):2100106. https://doi.org/10.1002/adtp.202100106
148. Melnik D, Krueger M, Schulz H et al (2021) The cellbox-2 mission to the international space station: thyroid cancer cells in space. Int J Mol Sci 22(16):8777. https://doi.org/10.3390/ijms22168777
149. Mao M, Meng ZJ, Huang XX et al (2024) 3D printing in space: from mechanical structures to living tissues. Int J Extrem Manuf 6(2):23001. https://doi.org/10.1088/2631-7990/ad23ef
150. Parfenov VA, Khesuani YD, Petrov SV et al (2020) Magnetic levitational bioassembly of 3D tissue construct in space. Sci Adv 6(29):eaba4174. https://doi.org/10.1126/sciadv.aba4174
151. Warth N, Berg M, Schumacher L et al (2024) Bioprint FirstAid: a handheld bioprinter for first aid utilization on space exploration missions. Acta Astronaut 215:194–204. https://doi.org/10.1016/j.actaastro.2023.11.033
152. Mo XW, Zhang YM, Wang ZX et al (2023) Satellite-based on-orbit printing of 3D tumor models. Adv Mater 36(34):e2309618. https://doi.org/10.1002/adma.202309618
153. Somasekhar L (2021) Bioink Optimization and Effects of Microgravity on 3D Bioprinted Cell Laden Constructs. PhD Thesis, Florida Institute of Technology, USA. https://repository.fit.edu/etd/588
154. Kishore MN, Qian D, Li W (2023) Multi-physics modeling of 3D bioprinting of polycaprolactone scaffolds for in-space additive manufacturing. In: Thermal and Fluids Analysis Workshop Conference. https://www.researchgate.net/publication/377628724_Multiphysics_Modeling_of_3D_Bioprinting_of_Polycaprolactone_Scaffolds_for_in-Space_Additive_Manufacturing [Accessed on July 25, 2024]
155. Windisch J, Reinhardt O, Duin S et al (2023) Bioinks for space missions: the influence of long-term storage of alginate-methylcellulose-based bioinks on printability as well as cell viability and function. Adv Healthc Mater 12(23):e2300436. https://doi.org/10.1002/adhm.202300436
156. Han YL, Zeger L, Tripathi R et al (2021) Molecular genetic analysis of neural stem cells after space flight and simulated microgravity on earth. Biotechol Bioeng 118(10):3832–3846. https://doi.org/10.1002/bit.27858
157. Nie J, Gao Q, Fu JZ et al (2020) Grafting of 3D bioprinting to in vitro drug screening: a review. Adv Healthc Mater 9(7):e1901773. https://doi.org/10.1002/adhm.201901773
158. Nie J, Fu JZ, He Y (2020) Hydrogels: the next generation body materials for microfluidic chips? Small 16(46):2003797. https://doi.org/10.1002/smll.202003797
159. Nie J, Gao Q, Wang YD et al (2018) Vessel-on-a-chip with hydrogel-based microfluidics. Small 14(45):e1802368. https://doi.org/10.1002/smll.201802368
160. Nie J, Gao Q, Xie CQ et al (2020) Construction of multi-scale vascular chips and modelling of the interaction between tumours and blood vessels. Mater Horiz 7(1):82–92. https://doi.org/10.1039/c9mh01283d
161. Nie J, Lou S, Pollet A et al (2024) A cell pre-wrapping seeding technique for hydrogel-based tubular organ-on-a-chip. Adv Sci 11(30):2400970. https://doi.org/10.1002/advs.202400970
162. Lv S, Nie J, Gao Q et al (2020) Micro/nanofabrication of brittle hydrogels using 3D printed soft ultrafine fiber molds for damage-free demolding. Biofabrication 12(2):025015. https://doi.org/10.1088/1758-5090/ab57d8
163. Aazmi A, Zhang D, Mazzaglia C et al (2024) Biofabrication methods for reconstructing extracellular matrix mimetics. Bioact Mater 31:475–496. https://doi.org/10.1016/j.bioactmat.2023.08.018
164. Ma L, Wu YT, Li YT et al (2020) Current advances on

3D-bioprinted liver tissue models. Adv Healthc Mater 9(24): e2001517.
https://doi.org/10.1002/adhm.202001517
165. Ma L, Li YT, Wu YT et al (2020) The construction of in vitro tumor models based on 3D bioprinting. Bio-Des Manuf 3(3): 227–236.
https://doi.org/10.1007/s42242-020-00068-6
166. Ma L, Li YT, Wu YT et al (2020) 3D bioprinted hyaluronic acid-based cell-laden scaffold for brain microenvironment simulation. Bio-Des Manuf 3(3):164–174.
https://doi.org/10.1007/s42242-020-00076-6
167. Lv WK, Zhou HZ, Aazmi A et al (2022) Constructing biomimetic liver models through biomaterials and vasculature engineering. Regener Biomater 9:rbac079.
https://doi.org/10.1093/rb/rbac079
168. Aazmi A, Zhou HZ, Lv WK et al (2022) Vascularizing the brain. iScience 25(4):104110.
https://doi.org/10.1016/j.isci.2022.104110
169. Aazmi A, Zhou HZ, Li YT et al (2022) Engineered vasculature for organ-on-a-chip systems. Engineering 9(2):131–147.
https://doi.org/10.1016/j.eng.2021.06.020
170. Aazmi A, Guo ZX, Yu HR et al (2023) Enhanced mixing efficiency for a novel 3D Tesla micromixer for Newtonian and non-Newtonian fluids. J Zhejiang Univ-Sci A (Appl Phys & Eng) 24(12): 1065–1078.
https://doi.org/10.1631/jzus.A2300589
171. Jian HL, Wang MY, Wang ST et al (2018) 3D bioprinting for cell culture and tissue fabrication. Bio-Des Manuf 1(1):45–61.
https://doi.org/10.1007/s42242-018-0006-1
172. Li X, Jian HL, Han QQ et al (2023) Three-dimensional (3D) bioprinting of medium toughened dipeptide hydrogel scaffolds with Hofmeister effect. J Colloid Interface Sci 639:1–6.
https://doi.org/10.1016/j.jcis.2023.02.033
173. Jian HL, Wang MY, Dong QQ et al (2019) Dipeptide self-assembled hydrogels with tunable mechanical properties and degradability for 3D bioprinting. ACS Appl Mater Interfaces 11(50): 46419–46426.
https://doi.org/10.1021/acsami.9b13905
174. Dong QQ, Su X, Li X et al (2023) In vitro construction of lung cancer organoids by 3D bioprinting for drug evaluation. Colloid Surf A Physicochem Eng Aspect 666:131288.
https://doi.org/10.1016/j.colsurfa.2023.131288
175. Jian HL, Li X, Dong QQ et al (2023) In vitro construction of liver organoids with biomimetic lobule structure by a multicellular 3D bioprinting strategy. Cell Prolif 56(5):e13465.
https://doi.org/10.1111/cpr.13465
176. Birey F, Andersen J, Makinson CD et al (2017) Assembly of functionally integrated human forebrain spheroids. Nature 545(7652): 54–59.
https://doi.org/10.1038/nature22330
177. Pasca SP (2019) Assembling human brain organoids. Science 363(6423):126–127.
https://doi.org/10.1126/science.aau5729
178. Kanton S, Pasca SP (2022) Human assembloids. Development 149(20):dev201120.
https://doi.org/10.1242/dev.201120
179. Liu TK, Zhou C, Ji JY et al (2023) Spheroid on-demand printing and drug screening of endothelialized hepatocellular carcinoma model at different stages. Biofabrication 15(4):44102.
https://doi.org/10.1088/1758-5090/ace3f9
180. Zhang YM, Hu QF, Pei YQ et al (2024) A patient-specific lung cancer assembloid model with heterogeneous tumor microenvironments. Nat Commun 15(1):3382.
https://doi.org/10.1038/s41467-024-47737-z
181. Wei Q, Sun D, Li M et al (2023) Modification of hydroxyapatite (HA) powder by carboxymethyl chitosan (CMCS) for 3D printing bioceramic bone scaffolds. Ceramics International 49(1): 538–547.
https://doi.org/10.1016/j.ceramint.2022.09.021
182. Gillman CE, Jayasuriya AC (2021) FDA-approved bone grafts and bone graft substitute devices in bone regeneration. Mater Sci Eng C 130:112466.
https://doi.org/10.1016/j.msec.2021.112466
183. Li XP, Wang YE, Zhang B et al (2022) The design and evaluation of bionic porous bone scaffolds in fluid flow characteristics and mechanical properties. Comput Meth Prog Biomed 225:107059.
https://doi.org/10.1016/j.cmpb.2022.107059
184. Wei QH, Wang YE, Li XP et al (2016) Study the bonding mechanism of binders on hydroxyapatite surface and mechanical properties for 3DP fabrication bone scaffolds. J Mech Behav Biomed Mater 57:190–200.
https://doi.org/10.1016/j.jmbbm.2015.12.007
185. Wei QH, Wang YE, Chai WH et al (2017) Molecular dynamics simulation and experimental study of the bonding properties of polymer binders in 3D powder printed hydroxyapatite bioceramic bone scaffolds. Ceram Int 43(16):13702–13709.
https://doi.org/10.1016/j.ceramint.2017.07.082
186. Chai WH, Wei QH, Yang MM et al (2020) The printability of three water based polymeric binders and their effects on the properties of 3D printed hydroxyapatite bone scaffold. Ceram Int 46(5): 6663–6671.
https://doi.org/10.1016/j.ceramint.2019.11.154
187. Zhang HJ, Wu CT (2023) 3D printing of biomaterials for vascularized and innervated tissue regeneration. Int J Bioprint 9(3):706.
https://doi.org/10.18063/ijb.706
188. Zhang M, Lin RC, Wang X et al (2020) 3D printing of Haversian bone-mimicking scaffolds for multicellular delivery in bone regeneration. Sci Adv 6(12):eaaz6725.
https://doi.org/10.1126/sciadv.aaz6725
189. Zhang HJ, Zhang M, Zhai D et al (2023) Polyhedron-like biomaterials for innervated and vascularized bone regeneration. Adv Mater 35(42):e2302716.
https://doi.org/10.1002/adma.202302716
190. Feng C, Zhang WJ, Deng CJ et al (2017) 3D printing of lotus root-like biomimetic materials for cell delivery and tissue regeneration. Adv Sci 4(12):1700401.
https://doi.org/10.1002/advs.201700401
191. Zhang WJ, Feng C, Yang GZ et al (2017) 3D-printed scaffolds with synergistic effect of hollow-pipe structure and bioactive ions for vascularized bone regeneration. Biomaterials 135:85–95.
https://doi.org/10.1016/j.biomaterials.2017.05.005
192. Li T, Zhai D, Ma B et al (2019) 3D printing of hot dog-like biomaterials with hierarchical architecture and distinct bioactivity. Adv Sci 6(19):1901146.
https://doi.org/10.1002/advs.201901146
193. Yang ZB, Xue JM, Shi Z et al (2024) Naturally derived flexible bioceramics: biomass recycling approach and advanced function. Matter 7(3):1275–1291.
https://doi.org/10.1016/j.matt.2024.01.016
194. Li MM, Ma HS, Han F et al (2021) Microbially catalyzed biomaterials for bone regeneration. Adv Mater 33(49):e2104829.
https://doi.org/10.1002/adma.202104829
195. Deng CJ, Lin RC, Zhang M et al (2019) Micro/Nanometer-structured scaffolds for regeneration of both cartilage and subchondral bone. Adv Funct Mater 29(4):1806068.
https://doi.org/10.1002/adfm.201806068

196. Yu XP, Wang YF, Zhang M et al (2023) 3D printing of gear-inspired biomaterials: immunomodulation and bone regeneration. Acta Biomater 156:222–233. https://doi.org/10.1016/j.actbio.2022.09.008
197. Qin C, Zhang HJ, Chen L et al (2023) Cell-laden scaffolds for vascular-innervated bone regeneration. Adv Healthc Mater 12(13): e2201923. https://doi.org/10.1002/adhm.202201923
198. Zhang HJ, Qin C, Zhang M et al (2022) Calcium silicate nanowires-containing multicellular bioinks for 3D bioprinting of neural-bone constructs. Nano Today 46:101584. https://doi.org/10.1016/j.nantod.2022.101584
199. Zhang HJ, Qin C, Shi Z et al (2024) Bioprinting of inorganic-biomaterial/neural-stem-cell constructs for multiple tissue regeneration and functional recovery. Natl Sci Rev 11(4):nwae035. https://doi.org/10.1093/nsr/nwae035
200. Du L, Qin C, Zhang HJ et al (2023) Multicellular bioprinting of biomimetic inks for tendon-to-bone regeneration. Adv Sci 10(21): e2301309. https://doi.org/10.1002/advs.202301309
201. Du L, Wu JF, Han YH et al (2024) Immunomodulatory multicellular scaffolds for tendon-to-bone regeneration. Sci Adv 10(10): eadk6610. https://doi.org/10.1126/sciadv.adk6610
202. Qin C, Ma JG, Chen L et al (2021) 3D bioprinting of multicellular scaffolds for osteochondral regeneration. Mater Today 49:68–84. https://doi.org/10.1016/j.mattod.2021.04.016
203. Deng CJ, Qin C, Li ZG et al (2024) Diatomite-incorporated hierarchical scaffolds for osteochondral regeneration. Bioact Mater 38:305–320. https://doi.org/10.1016/j.bioactmat.2024.05.004
204. Gaharwar AK, Singh I, Khademhosseini A (2020) Engineered biomaterials for in situ tissue regeneration. Nat Rev Mater 5(9): 686–705. https://doi.org/10.1038/s41578-020-0209-x
205. He HM, Li D, Lin ZF et al (2020) Temperature-programmable and enzymatically solidifiable gelatin-based bioinks enable facile extrusion bioprinting. Biofabrication 12(4):045003. https://doi.org/10.1088/1758-5090/ab9906
206. Gao CJ, Tang L, Qu HW et al (2023) A small-molecule polycationic crosslinker boosts alginate-based bioinks for extrusion bioprinting. Adv Funct Mater 34(9):2310369. https://doi.org/10.1002/adfm.202310369
207. Zhai XY, Ruan CS, Ma YF et al (2018) 3D-bioprinted osteoblast-laden nanocomposite hydrogel constructs with induced microenvironments promote cell viability, differentiation, and osteogenesis both in vitro and in vivo. Adv Sci 5(3):1700550. https://doi.org/10.1002/advs.201700550
208. Yang JR, Chen ZG, Gao CJ et al (2024) A mechanical-assisted post-bioprinting strategy for challenging bone defects repair. Nat Commun 15(1):3565. https://doi.org/10.1038/s41467-024-48023-8
209. Qin Y, Wen P, Guo H et al (2019) Additive manufacturing of biodegradable metals: current research status and future perspectives. Acta Biomater 98:3–22. https://doi.org/10.1016/j.actbio.2019.04.046
210. Qin Y, Liu JG, Chen YZ et al (2021) Influence of laser energy input and shielding gas flow on evaporation fume during laser powder bed fusion of Zn metal. Materials 14(10):2677. https://doi.org/10.3390/ma14102677
211. Wen P, Voshage M, Jauer L et al (2018) Laser additive manufacturing of Zn metal parts for biodegradable applications: processing, formation quality and mechanical properties. Mater Des 155: 36–45. https://doi.org/10.1016/j.matdes.2018.05.057
212. Wen P, Qin Y, Chen YZ et al (2019) Laser additive manufacturing of Zn porous scaffolds: shielding gas flow, surface quality and densification. J Mater Sci Technol 35(2):368–376. https://doi.org/10.1016/j.jmst.2018.09.065
213. Wang X, Liu AB, Zhang ZB et al (2024) Additively manufactured Zn-2Mg alloy porous scaffolds with customizable biodegradable performance and enhanced osteogenic ability. Adv Sci 11(5):e2307329. https://doi.org/10.1002/advs.202307329
214. Liu JG, Liu BC, Min SY et al (2022) Biodegradable magnesium alloy WE43 porous scaffolds fabricated by laser powder bed fusion for orthopedic applications: process optimization, in vitro and in vivo investigation. Bioact Mater 16:301–319. https://doi.org/10.1016/j.bioactmat.2022.02.020
215. Peng B, Wei Y, Qin Y et al (2023) Machine learning-enabled constrained multi-objective design of architected materials. Nat Commun 14(1):6630. https://doi.org/10.1038/s41467-023-42415-y
216. Liu JE, Yin BZ, Song F et al (2024) Improving corrosion resistance of additively manufactured WE43 magnesium alloy by high temperature oxidation for biodegradable applications. JMA 12(3): 940–953. https://doi.org/10.1016/j.jma.2022.08.009
217. Li S, Yang HT, Qu XH et al (2024) Multiscale architecture design of 3D printed biodegradable Zn-based porous scaffolds for immunomodulatory osteogenesis. Nat Commun 15(1):3131. https://doi.org/10.1038/s41467-024-47189-5
218. Zhang ZB, Liu AB, Fan JD et al (2023) A drug-loaded composite coating to improve osteogenic and antibacterial properties of Zn–1Mg porous scaffolds as biodegradable bone implants. Bioact Mater 27:488–504. https://doi.org/10.1016/j.bioactmat.2023.04.017
219. Yin BZ, Liu JE, Peng B et al (2024) Influence of layer thickness on formation quality, microstructure, mechanical properties, and corrosion resistance of WE43 magnesium alloy fabricated by laser powder bed fusion. JMA 12(4):1367–1385. https://doi.org/10.1016/j.jma.2022.09.016
220. Qin Y, Liu AB, Guo H et al (2022) Additive manufacturing of Zn-Mg alloy porous scaffolds with enhanced osseointegration: in vitro and in vivo studies. Acta Biomater 145:403–415. https://doi.org/10.1016/j.actbio.2022.03.055
221. Wang CX, Liu JE, Min SY et al (2023) The effect of pore size on the mechanical properties, biodegradation and osteogenic effects of additively manufactured magnesium scaffolds after high temperature oxidation: an in vitro and in vivo study. Bioact Mater 28:537–548. https://doi.org/10.1016/j.bioactmat.2023.06.009
222. Liu BC, Liu JE, Wang CX et al (2024) High temperature oxidation treated 3D printed anatomical WE43 alloy scaffolds for repairing periarticular bone defects: in vitro and in vivo studies. Bioact Mater 32:177–189. https://doi.org/10.1016/j.bioactmat.2023.09.016
223. Gao F, Xu ZY, Liang QF et al (2018) Direct 3D printing of high strength biohybrid gradient hydrogel scaffolds for efficient repair of osteochondral defect. Adv Funct Mater 28(13):13. https://doi.org/10.1002/adfm.201706644
224. Gao F, Xu ZY, Liang QF et al (2019) Osteochondral regeneration with 3D-printed biodegradable high-strength supramolecular polymer reinforced-gelatin hydrogel scaffolds. Adv Sci 6(15): 1900867. https://doi.org/10.1002/advs.201900867

225. Liu YZ, Peng LQ, Li LL et al (2021) 3D-bioprinted BMSC-laden biomimetic multiphasic scaffolds for efficient repair of osteochondral defects in an osteoarthritic rat model. Biomaterials 279: 121216. https://doi.org/10.1016/j.biomaterials.2021.121216
226. Zhang YJ, Li D, Liu Y et al (2024) 3D-bioprinted anisotropic bicellular living hydrogels boost osteochondral regeneration via reconstruction of cartilage-bone interface. Innovation 5(1):100542. https://doi.org/10.1016/j.xinn.2023.100542
227. Gui XY, Peng ZY, Song P et al (2023) 3D printing of personalized polylactic acid scaffold laden with GelMA/autologous auricle cartilage to promote ear reconstruction. Bio-Des Manuf 6(4): 451–463. https://doi.org/10.1007/s42242-023-00242-6
228. Tang P, Song P, Peng ZY et al (2021) Chondrocyte-laden GelMA hydrogel combined with 3D printed PLA scaffolds for auricle regeneration. Mater Sci Eng C Mater Biol Appl 130:112423. https://doi.org/10.1016/j.msec.2021.112423
229. Han Y, Jia B, Lian MF et al (2021) High-precision, gelatin-based, hybrid, bilayer scaffolds using melt electro-writing to repair cartilage injury. Bioact Mater 6(7):2173–2186. https://doi.org/10.1016/j.bioactmat.2020.12.018
230. Han Y, Lian MF, Sun BB et al (2020) Preparation of high precision multilayer scaffolds based on melt electro-writing to repair cartilage injury. Theranostics 10(22):10214–10230. https://doi.org/10.7150/thno.47909
231. Han Y, Lian MF, Zhang CY et al (2022) Study on bioactive PEGDA/ECM hybrid bi-layered hydrogel scaffolds fabricated by electro-writing for cartilage regeneration. Appl Mater Today 28: 101547. https://doi.org/10.1016/j.apmt.2022.101547
232. Qiao ZG, Lian MF, Han Y et al (2021) Bioinspired stratified electrowritten fiber-reinforced hydrogel constructs with layer-specific induction capacity for functional osteochondral regeneration. Biomaterials 266:120385. https://doi.org/10.1016/j.biomaterials.2020.120385
233. Ding CM, Qiao ZG, Jiang WB et al (2013) Regeneration of a goat femoral head using a tissue-specific, biphasic scaffold fabricated with CAD/CAM technology. Biomaterials 34(28):6706–6716. https://doi.org/10.1016/j.biomaterials.2013.05.038
234. Sun Y, Zhao J, Wu Q et al (2022) Chondrogenic primed extracellular vesicles activate miR-455/SOX11/FOXO axis for cartilage regeneration and osteoarthritis treatment. npj Regener Med 7(1):53. https://doi.org/10.1038/s41536-022-00250-7
235. Lian MF, Sun BB, Han Y et al (2021) A low-temperature-printed hierarchical porous sponge-like scaffold that promotes cell-material interaction and modulates paracrine activity of MSCs for vascularized bone regeneration. Biomaterials 274:120841. https://doi.org/10.1016/j.biomaterials.2021.120841
236. Cao BJ, Lin JM, Tan J et al (2023) 3D-printed vascularized biofunctional scaffold for bone regeneration. Int J Bioprint 9(3): 185–199. https://doi.org/10.18063/ijb.702
237. Hao YQ, Cao BJ, Deng L et al (2023) The first 3D-bioprinted personalized active bone to repair bone defects: a case report. Int J Bioprint 9(2):70–75. https://doi.org/10.18063/ijb.v9i2.654
238. Xue Y, Li JL, Jiang TH et al (2024) Biomimetic conductive hydrogel scaffolds with anisotropy and electrical stimulation for in vivo skeletal muscle reconstruction. Adv Healthc Mater 13(4): e2302180. https://doi.org/10.1002/adhm.202302180
239. Fan TT, Wang S, Jiang ZM et al (2022) Controllable assembly of skeletal muscle-like bundles through 3D bioprinting. Biofabrication 14(1):15009. https://doi.org/10.1088/1758-5090/ac3aca
240. Wang L, Li T, Wang ZH et al (2022) Injectable remote magnetic nanofiber/hydrogel multiscale scaffold for functional anisotropic skeletal muscle regeneration. Biomaterials 285:121537. https://doi.org/10.1016/j.biomaterials.2022.121537
241. Gao ZQ, Liu X, Zhao H et al (2023) Synthesis of easily-processable collagen bio-inks using ionic liquid for 3D bioprinted liver tissue models with branched vascular networks. Sci China Chem 66(5):1489–1499. https://doi.org/10.1007/s11426-022-1472-6
242. Huang YM, Zhao H, Wang XH et al (2022) Polyurethane-gelatin methacryloyl hybrid ink for 3D printing of biocompatible and tough vascular networks. Chem Commun 58(49):6894–6897. https://doi.org/10.1039/d2cc02176e
243. Guo BJ, Duan YC, Li ZW et al (2023) High-strength cell sheets and vigorous hydrogels from mesenchymal stem cells derived from human embryonic stem cells. ACS Appl Mater Interfaces 15(23):27586–27599. https://doi.org/10.1021/acsami.3c03117
244. Liu X, Wang XH, Zhang LM et al (2021) 3D liver tissue model with branched vascular networks by multimaterial bioprinting. Adv Healthc Mater 10(23):e2101405. https://doi.org/10.1002/adhm.202101405
245. Wang XH, Liu X, Liu WL et al (2023) 3D bioprinting microgels to construct implantable vascular tissue. Cell Prolif 56(5):e13456. https://doi.org/10.1111/cpr.13456
246. Wang HR, Liu X, Gu Q et al (2023) Vascularized organ bioprinting: from strategy to paradigm. Cell Prolif 56(5):e13453. https://doi.org/10.1111/cpr.13453
247. Pimentel CR, Ko SK, Caviglia C et al (2018) Three-dimensional fabrication of thick and densely populated soft constructs with complex and actively perfused channel network. Acta Biomater 65:174–184. https://doi.org/10.1016/j.actbio.2017.10.047
248. Szklanny AA, Machour M, Redenski I et al (2021) 3D bioprinting of engineered tissue flaps with hierarchical vessel networks (VesselNet) for firect host-to-implant perfusion. Adv Mater 33(42): e2102661. https://doi.org/10.1002/adma.202102661
249. Liu X, Wang XH, Zhang LM et al (2021) 3D liver tissue model with branched vascular networks by multimaterial bioprinting. Adv Healthc Mater 10(23):e2101405. https://doi.org/10.1002/adhm.202101405
250. Wang HR, Liu X, Gu Q et al (2023) Vascularized organ bioprinting: from strategy to paradigm. Cell Prolif 56(5):e13453. https://doi.org/10.1111/cpr.13453
251. Gao Q, Liu ZJ, Lin ZW et al (2017) 3D bioprinting of vessel-like structures with multilevel fluidic channels. ACS Biomater Sci Eng 3(3):399–408. https://doi.org/10.1021/acsbiomaterials.6b00643
252. Jin Y, Xie CQ, Gao Q et al (2021) Fabrication of multi-scale and tunable auxetic scaffolds for tissue engineering. Mater Des 197:109277. https://doi.org/10.1016/j.matdes.2020.109277
253. Xie CQ, Gao Q, Wang P et al (2019) Structure-induced cell growth by 3D printing of heterogeneous scaffolds with ultrafine fibers. Mater Des 181:108092. https://doi.org/10.1016/j.matdes.2019.108092
254. Gao Q, He Y, Fu JZ et al (2015) Coaxial nozzle-assisted 3D bioprinting with built-in microchannels for nutrients delivery. Bio-

materials 61:203–215.
https://doi.org/10.1016/j.biomaterials.2015.05.031
255. Shao L, Gao Q, Xie CQ et al (2020) Synchronous 3D bioprinting of large-scale cell-laden constructs with nutrient networks. Adv Healthc Mater 9(15):e1901142.
https://doi.org/10.1002/adhm.201901142
256. Gu ZM, Xie MJ, Lv S et al (2022) Perfusable vessel-on-a-chip for antiangiogenic drug screening with coaxial bioprinting. Int J Bioprint 8(4):619.
https://doi.org/10.18063/ijb.v8i4.619
257. Meng ZJ, He JK, Li JX et al (2020) Melt-based, solvent-free additive manufacturing of biodegradable polymeric scaffolds with designer microstructures for tailored mechanical/biological properties and clinical applications. Virt Phys Prototy 15(4):417–444.
https://doi.org/10.1080/17452759.2020.1808937
258. Meng ZJ, He JK, Cai ZH et al (2020) In-situ re-melting and re-solidification treatment of selective laser sintered polycaprolactone lattice scaffolds for improved filament quality and mechanical properties. Biofabrication 12(3):035012.
https://doi.org/10.1088/1758-5090/ab860e
259. Zeng XB, Meng ZJ, Qiu ZN et al (2023) Melt-based embedded printing for freeform fabrication of overhanging and flexible polycaprolactone scaffolds. Virt Phys Prototy 18(1):e2209778.
https://doi.org/10.1080/17452759.2023.2209778
260. Yao C, Qiu ZN, Li X et al (2023) Electrohydrodynamic printing of microfibrous architectures with cell-scale spacing for improved cellular migration and neurite outgrowth. Small 19(19):e2207331.
https://doi.org/10.1002/smll.202207331
261. Zhang B, He JK, Li X et al (2016) Micro/nanoscale electrohydrodynamic printing: from 2D to 3D. Nanoscale 8(34):15376–15388.
https://doi.org/10.1039/c6nr04106j
262. He JK, Xia P, Li DC (2016) Development of melt electrohydrodynamic 3D printing for complex microscale poly (ε-caprolactone) scaffolds. Biofabrication 8(3):035008.
https://doi.org/10.1088/1758-5090/8/3/035008
263. He JK, Zhang B, Li Z et al (2020) High-resolution electrohydrodynamic bioprinting: a new biofabrication strategy for biomimetic micro/nanoscale architectures and living tissue constructs. Biofabrication 12(4):042002.
https://doi.org/10.1088/1758-5090/aba1fa
264. Meng ZJ, Mu XD, He JK et al (2023) Embedding aligned nanofibrous architectures within 3D-printed polycaprolactone scaffolds for directed cellular infiltration and tissue regeneration. Int J Extrem Manuf 5(2):025001.
https://doi.org/10.1088/2631-7990/acbd6c
265. Hu SG, Meng ZJ, Zhou JP et al (2022) Enhanced attachment and collagen type I deposition of MC3T3-E1 cells via electrohydrodynamic printed sub-microscale fibrous architectures. Int J Bioprint 8(2):514.
https://doi.org/10.18063/ijb.v8i2.514
266. Meng ZJ, He JK, Li DC (2021) Additive manufacturing and large deformation responses of highly-porous polycaprolactone scaffolds with helical architectures for breast tissue engineering. VPP 16(3):291–305.
https://doi.org/10.1080/17452759.2021.1930069
267. Liu WH, Meng ZJ, Zheng KF et al (2021) Development of three-dimensional printed biodegradable external airway splints with native-like shape and mechanical properties for tracheomalacia treatment. Mater Des 210:110105.
https://doi.org/10.1016/j.matdes.2021.110105
268. Meng ZJ, He JK, Cai ZH et al (2020) Design and additive manufacturing of flexible polycaprolactone scaffolds with highly-tunable mechanical properties for soft tissue engineering. Mater Des 189:108508.
https://doi.org/10.1016/j.matdes.2020.108508
269. Liu YJ, Zheng KF, Meng ZJ et al (2023) A cell-free tissue-engineered tracheal substitute with sequential cytokine release maintained airway opening in a rabbit tracheal full circumferential defect model. Biomaterials 300:122208.
https://doi.org/10.1016/j.biomaterials.2023.122208
270. Wang L, Li DC, He JK et al (2018) Research center of biomanufacturing in Xi'an Jiaotong University. Bio-Des Manuf 1(4):280–288.
https://doi.org/10.1007/s42242-018-0026-x
271. Hou L, Yan CJ, Zhang MK et al (2024) A novel 3D-printed scaffold for patient-specific partial breast reconstruction: a prospective, single-arm clinical trial. J Clin Oncol 42(16):e23227.
https://doi.org/10.1200/JCO.2024.42.16_suppl.e23227
272. Huang LJ, Wang L, He JK et al (2016) Tracheal suspension by using 3-dimensional printed personalized scaffold in a patient with tracheomalacia. J Thorac Disease 8(11):3323–3328.
https://doi.org/10.21037/jtd.2016.10.53
273. Yu D, Peng W, Mo XM et al (2022) Personalized 3D-printed bioresorbable airway external splint for tracheomalacia combined with congenital heart disease. Front Bioeng Biotechnol 10:859777.
https://doi.org/10.3389/fbioe.2022.859777
274. Han YH, Yin Q, Wang Y et al (2018) Three-dimensional printed degradable splint in the treatment of pulmonary artery sling associated with severe bilateral bronchus stenosis. Cardiol Young 28(12):1477–1480.
https://doi.org/10.1017/s1047951118001579
275. Wang L, Liu WH, He JK et al (2019) Treatment of bronchomalacia using three-dimensional printed polycaprolactone scaffold in a pediatric patient. J Thorac Cardiovasc Surg 157(5):e287–e290.
https://doi.org/10.1016/j.jtcvs.2018.11.095
276. Zhang F, Zhang M, Liu S et al (2022) Application of hybrid electrically conductive hydrogels promotes peripheral nerve regeneration. Gels 8(1):41.
https://doi.org/10.3390/gels8010041
277. Zhang CY, Gong JX, Zhang JY et al (2023) Three potential elements of developing nerve guidance conduit for peripheral nerve regeneration. Adv Funct Mater 33(40):2302251.
https://doi.org/10.1002/adfm.202302251
278. You DQ, Chen GC, Liu C et al (2021) 4D printing of multi-responsive membrane for accelerated in vivo bone healing via remote regulation of stem cell fate. Adv Funct Mater 31(40): 2103920.
https://doi.org/10.1002/adfm.202103920
279. Sun MY, You DQ, Zhan N et al (2023) 4D oriented dynamic scaffold for promoting peripheral nerve regeneration and functional recovery. Adv Funct Mater 34(2):2305827.
https://doi.org/10.1002/adfm.202305827
280. Qian Y, Gong JX, Lu KJ et al (2023) DLP printed hDPSC-loaded GelMA microsphere regenerates dental pulp and repairs spinal cord. Biomaterials 299:122137.
https://doi.org/10.1016/j.biomaterials.2023.122137
281. Qiu C, Sun Y, Li JY et al (2023) A 3D-printed dual driving forces scaffold with self-promoted cell absorption for spinal cord injury repair. Adv Sci 10(33):e2301639.
https://doi.org/10.1002/advs.202301639
282. Karna S, Lee JE, Kim YS et al (2023) Comprehensive feasibility evaluation of small-diameter 3D templated vascular graft via physical characterizations and in-vivo experiments. Biomed Mater 18(5): 55018.
https://doi.org/10.1088/1748-605X/aceced
283. Atari M, Saroukhani A, Manshaei M et al (2023) Preclinical in vivo assessment of a cell-free multi-layered scaffold prepared

by 3D printing and electrospinning for small-diameter blood vessel tissue engineering in a canine model. Biomater Sci 11(20):6871–6880.
https://doi.org/10.1039/d3bm00642e
284. Zhi DK, Cheng QH, Midgley AC et al (2022) Mechanically reinforced biotubes for arterial replacement and arteriovenous grafting inspired by architectural engineering. Sci Adv 8(11):eabl3888.
https://doi.org/10.1126/sciadv.abl3888
285. Shao L, Gao Q, Xie CQ et al (2020) Directly coaxial 3D bioprinting of large-scale vascularized tissue constructs. Biofabrication 12(3):035014.
https://doi.org/10.1088/1758-5090/ab7e76
286. Gu ZM, Xie MJ, Lv S et al (2022) Perfusable vessel-on-a-chip for antiangiogenic drug screening with coaxial bioprinting. Int J Bioprint 8(4):292–306.
https://doi.org/10.18063/ijb.v8i4.619
287. Pan BC, Shao L, Jiang JH et al (2022) 3D printing sacrificial templates for manufacturing hydrogel constructs with channel networks. Mater Des 222:111012.
https://doi.org/10.1016/j.matdes.2022.111012
288. Zhang SS, Qi C, Zhang W et al (2023) In situ endothelialization of free-form 3D network of interconnected tubular channels via interfacial coacervation by aqueous-in-aqueous embedded bioprinting. Adv Mater 35(7):e2209263.
https://doi.org/10.1002/adma.202209263
289. Song BW, Wang CW, Fan SY et al (2023) Rapid construction of 3D biomimetic capillary networks with complex morphology using dynamic holographic processing. Adv Funct Mater 34(1):2305345.
https://doi.org/10.1002/adfm.202305245
290. Jorgensen AM, Yoo JJ, Atala A (2020) Solid organ bioprinting: strategies to achieve organ function. Chem Rev 120(19):11093–11127.
https://doi.org/10.1021/acs.chemrev.0c00145
291. Gu Z, Guo J, Zhai JL et al (2022) A uterus-inspired niche drives blastocyst development to the early organogenesis. Adv Sci 9(28):e2202282.
https://doi.org/10.1002/advs.202202282
292. Fedorovich NE, Schuurman W, Wijnberg HM et al (2012) Biofabrication of osteochondral tissue equivalents by printing topologically defined, cell-laden hydrogel scaffolds. Tissue Eng Part C Methods 18(1):33–44.
https://doi.org/10.1089/ten.TEC.2011.0060
293. Gu Q, Tomaskovic-Crook E, Lozano R et al (2016) Functional 3D neural mini-tissues from printed gel-based bioink and human neural stem cells. Adv Healthc Mater 5(12):1429–1438.
https://doi.org/10.1002/adhm.201600095
294. Fan TT, Wang S, Jiang ZM et al (2021) Controllable assembly of skeletal muscle-like bundles through 3D bioprinting. Biofabrication 14(1):15009.
https://doi.org/10.1088/1758-5090/ac3aca
295. Ouyang LL, Yao R, Mao SS et al (2015) Three-dimensional bioprinting of embryonic stem cells directs highly uniform embryoid body formation. Biofabrication 7(4):044101.
https://doi.org/10.1088/1758-5090/7/4/044101
296. Gu Q, Tomaskovic-Crook E, Wallace GG et al (2017) 3D bioprinting human induced pluripotent stem cell constructs for in situ cell proliferation and successive multilineage differentiation. Adv Healthc Mater 6(17):1700175.
https://doi.org/10.1002/adhm.201700175
297. Guo J, Li YY, Gao ZL et al (2022) 3D printed controllable microporous scaffolds support embryonic development in vitro. J Cell Physiol 237(8):3408–3420.
https://doi.org/10.1002/jcp.30810
298. Mao M, Meng ZJ, Huang XX et al (2024) 3D printing in space: from mechanical structures to living tissues. Int J Extrem Manuf 6(2):023001.
https://doi.org/10.1088/2631-7990/ad23ef
299. Zhu H, Yao C, Wei BY et al (2023) 3D printing of functional bioengineered constructs for neural regeneration: a review. Int J Extrem Manuf 5(4):042004.
https://doi.org/10.1088/2631-7990/ace56c
300. Mao M, Bei HP, Lam CH et al (2020) Human-on-leaf-chip: a biomimetic vascular system integrated with chamber-specific organs. Small 16(22):e2000546.
https://doi.org/10.1002/smll.202000546
301. Lei Q, He JK, Li DC (2019) Electrohydrodynamic 3D printing of layer-specifically oriented, multiscale conductive scaffolds for cardiac tissue engineering. Nanoscale 11(32):15195–15205.
https://doi.org/10.1039/c9nr04989d
302. Mao M, Qu XL, Zhang YB et al (2023) Leaf-venation-directed cellular alignment for macroscale cardiac constructs with tissue-like functionalities. Nat Commun 14(1):2077.
https://doi.org/10.1038/s41467-023-37716-1
303. Mao M, Meng ZJ, He JK et al (2024) Microphysiological systems inspired by leaf venation. Trends Biotechnol 42(11):1331–1334.
https://doi.org/10.1016/j.tibtech.2024.03.011
304. Wang S, Bai LG, Hu XX et al (2023) 3D bioprinting of neurovascular tissue modeling with collagen-based low-viscosity composites. Adv Healthc Mater 12(25):e2300004.
https://doi.org/10.1002/adhm.202300004
305. Lei D, Yang Y, Liu ZH et al (2019) 3D printing of biomimetic vasculature for tissue regeneration. Mater Horiz 6(6):1197–1206.
https://doi.org/10.1039/c9mh00174c
306. Duan JH, Lei D, Ling C et al (2022) Three-dimensional-printed polycaprolactone scaffolds with interconnected hollow-pipe structures for enhanced bone regeneration. Regen Biomater 9:rbac033.
https://doi.org/10.1093/rb/rbac033
307. Ha YJ, Ma XJ, Li SK et al (2022) Bone microenvironment-mimetic scaffolds with hierarchical microstructure for enhanced vascularization and bone regeneration. Adv Funct Mater 32(20):2200011.
https://doi.org/10.1002/adfm.202200011
308. Huang SX, Lei D, Yang Q et al (2021) A perfusable, multifunctional epicardial device improves cardiac function and tissue repair. Nat Med 27(3):480–490.
https://doi.org/10.1038/s41591-021-01279-9
309. Kong LC, Gao X, Yao XY (2024) Multilevel neurium-mimetic individualized graft via additive manufacturing for efficient tissue repair. Nat Commun 15(1):6428.
https://doi.org/10.1038/s41467-024-49980-w
310. Shamloul R, Ghanem H (2013) Erectile dysfunction. Lancet 381(9861):153–165.
https://doi.org/10.1016/S0140-6736(12)60520-0
311. Ren Y, Yuan J, Xue YG et al (2023) Advanced hydrogels: new expectation for the repair of organic erectile dysfunction. Mater Today Bio 19:100588.
https://doi.org/10.1016/j.mtbio.2023.100588
312. Andrew TW, Kanapathy M, Murugesan L et al (2019) Towards clinical application of tissue engineering for erectile penile regeneration. Nat Rev Urol 16(12):734–744.
https://doi.org/10.1038/s41585-019-0246-7
313. An G, Guo FX, Liu XM et al (2020) Functional reconstruction of injured corpus cavernosa using 3D-printed hydrogel scaffolds seeded with HIF-1α-expressing stem cells. Nat Commun 11(1):2687.
https://doi.org/10.1038/s41467-020-16192-x
314. Chai MY, Zhong WW, Yan ST et al (2024) Diffusion-induced

phase separation 3D printed scaffolds for dynamic tissue repair. BMEMat 2(3):e12108. https://doi.org/10.1002/bmm2.12108
315. Chai MY, Zhai ZC, Liu XM et al (2023) Bionic artificial penile Tunica albuginea. Matter 6(2):626–641. https://doi.org/10.1016/j.matt.2022.11.032
316. Liu XM, Wu K, Gao L et al (2022) Biomaterial strategies for the application of reproductive tissue engineering. Bioact Mater 14:86–96. https://doi.org/10.1016/j.bioactmat.2021.11.023
317. Liu J, Zhou ZT, Zhang M et al (2022) Simple and robust 3D bioprinting of full-thickness human skin tissue. Bioengineered 13(4): 10090–10100. https://doi.org/10.1080/21655979.2022.2063651
318. Zhao M, Wang J, Zhang JX et al (2022) Functionalizing multicomponent bioink with platelet-rich plasma for customized in-situ bilayer bioprinting for wound healing. Mater Today Bio 16:100334. https://doi.org/10.1016/j.mtbio.2022.100334
319. Chen HY, Zhang Y, Zhou DZ et al (2022) Mechanical engineering of hair follicle regeneration by in situ bioprinting. Biomater Adv 142:213127. https://doi.org/10.1016/j.bioadv.2022.213127
320. Yao B, Wang R, Wang YH et al (2020) Biochemical and structural cues of 3D-printed matrix synergistically direct MSC differentiation for functional sweat gland regeneration. Sci Adv 6(10):eaaz1094. https://doi.org/10.1126/sciadv.aaz1094
321. Liu YY, Liu X, Guo HT et al (2024) 3D bioprinting bioglass to construct vascularized full-thickness skin substitutes for wound healing. Mater Today Bio 24:100899. https://doi.org/10.1016/j.mtbio.2023.100899
322. Jin RH, Cui YC, Chen HJ et al (2021) Three-dimensional bioprinting of a full-thickness functional skin model using acellular dermal matrix and gelatin methacrylamide bioink. Acta Biomater 131:248–261. https://doi.org/10.1016/j.actbio.2021.07.012
323. Ma JG, Qin C, Wu JF et al (2021) 3D printing of strontium silicate microcylinder-containing multicellular biomaterial inks for vascularized skin regeneration. Adv Healthc Mater 10(16):e2100523. https://doi.org/10.1002/adhm.202100523
324. Yao B, Zhu DZ, Cui XL et al (2022) Modeling human hypertrophic scars with 3D preformed cellular aggregates bioprinting. Bioact Mater 10:247–254. https://doi.org/10.1016/j.bioactmat.2021.09.004
325. Zhao H, Xu JW, Yuan HT et al (2022) 3D printing of artificial skin patches with bioactive and optically active polymer materials for anti-infection and augmenting wound repair. Mater Horiz 9(1): 342–349. https://doi.org/10.1039/d1mh00508a
326. Sun H, Liu J, Lv FT et al (2021) Selective reaction of conjugated polymers with basic proteins for broad-spectrum antivirulence therapy. NPG Asia Mater 13(1):21. https://doi.org/10.1038/s41427-020-00252-1
327. Zhao WX, Chen HY, Zhang Y et al (2022) Adaptive multi-degree-of-freedom in situ bioprinting robot for hair-follicle-inclusive skin repair: a preliminary study conducted in mice. Bioeng Transl Med 7(3):e10303. https://doi.org/10.1002/btm2.10303
328. Gao Q, Niu XF, Shao L et al (2019) 3D printing of complex GelMA-based scaffolds with nanoclay. Biofabrication 11(3):035006. https://doi.org/10.1088/1758-5090/ab0cf6
329. Phan NV, Rathbun EM, Ouyang YX et al (2023) Biology-driven material design for ischaemic stroke repair. Nat Rev Bioeng 2(1): 44–63. https://doi.org/10.1038/s44222-023-00117-6
330. Camarero-Espinosa S, Beeren I, Liu H et al (2024) 3D niche-inspired scaffolds as a stem cell delivery system for the regeneration of the osteochondral interface. Adv Mater 36(34):e2310258. https://doi.org/10.1002/adma.202310258
331. Hu Y, Cui J, Liu H et al (2022) Single-cell RNA-sequencing analysis reveals the molecular mechanism of subchondral bone cell heterogeneity in the development of osteoarthritis. RMD Open 8(2):e002314. https://doi.org/10.1136/rmdopen-2022-002314
332. Yang Z, Wang B, Liu W et al (2023) In situ self-assembled organoid for osteochondral tissue regeneration with dual functional units. Bioact Mater 27:200–215. https://doi.org/10.1016/j.bioactmat.2023.04.002
333. An JM, Zhang SY, Wu J et al (2024) Assessing bioartificial organ function: the 3P model framework and its validation. Lab Chip 24(6):1586–1601. https://doi.org/10.1039/d3lc01020a

Authors and Affiliations

Chaofan He[1,2] · Jiankang He[3] · Chengtie Wu[4] · Changshun Ruan[5,6] · Qi Gu[7,8] · Yongqiang Hao[9] · Yang Wu[10] · Shuo Bai[11,12] · Xiaoxiao Han[13] · Liliang Ouyang[14,15] · Jun Yin[1] · Hongzhao Zhou[1] · Zhuo Xiong[14] · Maobin Xie[16,17] · Lei Shao[18] · Jing Nie[19] · Liang Ma[1] · Cijun Shuai[20] · Changchun Zhou[21] · Xin Zhao[22] · Xuetao Shi[23] · Mengfei Yu[24,25] · Jiayin Fu[26] · Peng Wen[27] · Huixia Xuan[28,29] · Yuan Pang[14] · Yan'en Wang[30] · Yuan Sun[1,2] · Ziqi Gao[1] · Abdellah Aazmi[1] · Jingbo Zhang[1] · Tianhong Qiao[1,2] · Qixiang Yang[1,2] · Ke Yao[1,2] · Mao Mao[3] · Jianxin Hao[4] · Pinpin Wang[5,6] · Jirong Yang[5,6] · Huawei Qu[5,6] · Xinhuan Wang[7,8] · Xin Liu[7,8] · Shen Ji[7,8] · Shasha Liu[9] · Jingke Fu[9] · Bingxian Lu[10] · Mohan Wu[10] · Feng Chen[13] · Zihao Zheng[16,17] · Boqing Zhang[21] · Muyuan Chai[23] · Chaoying Zhang[24,25] · Mouyuan Sun[24,25] · Bo Peng[27] · Huayong Yang[1] · Yong He[1,2,31]

✉ Huayong Yang
yhy@zju.edu.cn

✉ Yong He
yongqin@zju.edu.cn

1 State Key Laboratory of Fluid Power and Mechatronic Systems, School of Mechanical Engineering, Zhejiang University, Hangzhou 310027, China

2 Key Laboratory of 3D Printing Process and Equipment of Zhejiang Province, School of Mechanical Engineering, Zhejiang University, Hangzhou 310027, China

3 State Key Laboratory for Manufacturing Systems Engineering, Xi'an Jiaotong University, Xi'an 710049, China

4 State Key Laboratory of High Performance Ceramics and Superfine Microstructure, Shanghai Institute of Ceramics, Chinese Academy of Sciences, Shanghai 200050, China

5 Research Center for Human Tissue and Organ Degeneration, Institute of Biomedicine and Biotechnology, Shenzhen Institutes of Advanced Technology, Chinese Academy of Sciences, Shenzhen 518055, China

6 University of Chinese Academy of Sciences, Beijing 100049, China

7 Key Laboratory of Organ Regeneration and Reconstruction, State Key Laboratory of Membrane Biology, Institute of Zoology, Chinese Academy of Sciences, Beijing 100101, China

8 Beijing Institute for Stem Cell and Regenerative Medicine, Beijing 100101, China

9 Shanghai Engineering Research Center of Innovative Orthopaedic Instruments and Personalized Medicine, Clinical and Translational Research Center for 3D Printing Technology, Shanghai 200011, China

10 School of Biomedical Engineering, Harbin Institute of Technology (Shenzhen), Shenzhen 518055, China

11 State Key Laboratory of Biochemical Engineering, Institute of Process Engineering, Chinese Academy of Sciences, Beijing 100190, China

12 Key Laboratory of Biopharmaceutical Preparation and Delivery, Institute of Process Engineering, Chinese Academy of Sciences, Beijing 100190, China

13 National Engineering Research Centre for High Efficiency Grinding, Hunan University, Changsha 410082, China

14 Biomanufacturing Center, Department of Mechanical Engineering, Tsinghua University, Beijing 100084, China

15 State Key Laboratory of Tribology in Advanced Equipment, Tsinghua University, Beijing 100084, China

16 The Fourth Affiliated Hospital of Guangzhou Medical University, Guangzhou 511436, China

17 School of Biomedical Engineering, Guangzhou Medical University, Guangzhou 511436, China

18 Research Institute for Medical and Biological Engineering, Ningbo University, Ningbo 315211, China

19 Department of Biomedical Engineering, Research Center for Nano-biomaterials & Regenerative Medicine, College of Artificial Intelligence, Taiyuan University of Technology, Taiyuan 030024, China

20 State Key Laboratory of High Performance Complex Manufacturing, Central South University, Changsha 410083, China

21 National Engineering Research Center for Biomaterials, Sichuan University, Chengdu 610064, China

22 Department of Applied Biology and Chemical Technology, The Hong Kong Polytechnic University, Hong Kong SAR 999077, China

23 School of Materials Science and Engineering, South China University of Technology, Guangzhou 510640, China

24 Stomatology Hospital, School of Stomatology, Zhejiang University School of Medicine, Hangzhou 310016, China

25 Key Laboratory of Oral Biomedical Research of Zhejiang Province, Hangzhou 310006, China

26 Key Laboratory of Cardiovascular Intervention and Regenerative Medicine of Zhejiang Province, Department of Cardiology, Sir Run Run Shaw Hospital, Zhejiang University, Hangzhou 310016, China

27 State Key Laboratory of Clean and Efficient Turbomachinery Power Equipment, Department of Mechanical Engineering, Tsinghua University, Beijing 100084, China

28 State Key Laboratory for Modification of Chemical Fibers and Polymer Materials, College of Chemistry, Chemical Engineering and Biotechnology, Donghua University, Shanghai 201620, China

29 Institute for Frontier Medical Technology, College of Chemistry and Chemical Engineering, Shanghai University of Engineering Science, Shanghai 201620, China

30 Department of Industry Engineering, School of Mechanical Engineering, Northwestern Polytechnical University, Xi'an 710072, China

31 The Second Affiliated Hospital, Zhejiang University School of Medicine, Hangzhou 310027, China